Mirror Color Symmetry Breaking

in Twin Higgs Model

by

Wei Hu

B.E., Measurement & Control Technology and Instrument, University of Shanghai for Science and Technology, 2004

Ph.D., Optics/Optics Engineering, Fudan University, 2010

Submitted to the Graduate Faculty of

the Kenneth P. Dietrich School of Arts and Sciences

in partial fulfillment

of the requirements for the degree of

Doctor of Philosophy

University of Pittsburgh

2020

UNIVERSITY OF PITTSBURGH

THE KENNETH P. DIETRICH SCHOOL OF ARTS AND SCIENCES

This dissertation was presented

by

Wei Hu

It was defended on

July 29th 2020

and approved by

Brian Batell, Assistant Professor, University of Pittsburgh

Ayres Freitas, Associate Professor, University of Pittsburgh

Michael Wood-Vasey, Associate Professor, University of Pittsburgh

James A Mueller, Professor, University of Pittsburgh

Colin Morningstar, Professor, Carnegie Mellon University

Dissertation Director: Brian Batell, Assistant Professor, University of Pittsburgh

Mirror Color Symmetry Breaking
in Twin Higgs Model

Wei Hu, PhD

University of Pittsburgh, 2020

Many conventional approaches to the hierarchy problem necessitate colored top partners around the TeV scale, in tension with bounds from direct searches. The Mirror Twin Higgs (MTH) model address this by positing top partners that are neutral under the Standard Model (SM) gauge group. The SM Higgs emerges as a pseudo Nambu Goldstone boson (pNGB) from a spontaneously broken accidental global symmetry. A crucial ingredient is a $\mathbb{Z}_2$ mirror symmetry that exchanges SM fields with partner fields with equal couplings, removing the quadratic UV sensitivity. However, an exact mirror symmetry is in conflict with Higgs coupling measurements, the $\mathbb{Z}_2$ must be broken to achieve a viable model.

In this thesis, we describe a new dynamical approach. Starting from an exact $\mathbb{Z}_2$, we introduce an additional colored scalar field in the visible sector along with its twin partner field. Given a suitable potential, the mirror sector color scalar field obtains a vacuum expectation value and spontaneously breaks both the twin color gauge and $\mathbb{Z}_2$ symmetries.

Meanwhile, dramatic differences between the twin and visible sectors occur, in terms of the residual unbroken gauge symmetries, strong confinement scales, and particle spectra. Assuming a single colored scalar of triplet, sextet, or octet we describe five minimal possibilities. In several cases there is a residual color symmetry, either $SU(2)_c$ or $SO(3)_c$, featuring a low confinement scale relative to $\Lambda_{\rm QCD}$. Furthermore, there can be one or more unbroken abelian gauge symmetries. Couplings between the colored scalar and matter are also allowed, providing a new source of twin fermion masses. It implies a fraternal-like scenario by lifting the first and second generation twin fermions. A variety of correlated visible sector effects can be probed through precision measurements and collider searches, coming from baryon and lepton number violation, flavor changing processes, CP-violation, electroweak measurements, Higgs couplings, and direct searches at the LHC. This opens up new possibilities for a viable twin Higgs cosmology with interesting implications for the dark sector physics.

Table of Contents

List of Tables

List of Figures

Preface

Upon the completion of this thesis, I owe greatly to my advisor, Brian Batell, who introduced me to the wonderland of theoretical particle physics more than four years ago. He has kept me busy in the inspirational adventure of research and conveyed excitement in teaching. His understanding of the field, commitment and enthusiasm towards physics has given me continual opportunities to explore new ideas and motivation to learn new knowledge. Without his detailed and seasoned guidance in every steps, the accomplishment of this work is impossible. He has also provided support and advice in other aspects of my life and career.

In the academic journey, the committee and faculty members in the physics department have my gratitude as well, especially Michael Wood-Vasey, who is my previous advisor at Pitt and ushered me into the mystical astrophysical world. Ayres Freitas, who has taught me a lot in physics class and patient in discussing any questions. Ralph Roskies, who gave me the initial encouragement to pursue particle physics. Daniel Boyanovsky, who led me to the introductory course of particle physics and kind in chatting about physics. I also like to thank Professors Eric Swanson, Robert P. Devaty, David Jasnow, Raphael Flauger, Tao Han, Hael Collins, W. Vincent Liu, Andrew R Zentner, David W Snoke, Kaoru Hagiwara, Ira Rothstein, Jeffrey A Newman, Roger Mong, Tae Min Hong, and Adam K Leibovich, as my physics course teachers, Xiao-lun Wu, Jeremy Levy, Russell J. Clark, Paul F Shepard as my TA instructors, and James A Mueller, Colin Morningstar to serve as my committee members.

Special thanks go to my collaborator Christopher B. Verhaaren who is involved in the current project of this thesis, and Satyanarayan Mukhopadhyay, Keping Xie, for the initial or ongoing projects. In the academic environment, many other people have had positive influence on me, I would also thank Ismail Ahmed, Dorival Goncalves, and fellow graduate students Xing Wang, Binbin Tian, Kara Ponder, Rongpu Zhou, Xiaopeng Li, Jerod Caligiuri, Luther Rinehart, Lin Dai, Xiaowu Sun, Yuchi He, Dritan Kodra, Louis Lello, Junmo Chen, Chenxu Liu, Qing Guo, Barmak Shams Es Haghi, Zhuoni Qian, Fernando Salviatto Zago,

to name a few, for their random discussions of general or class physics questions, and the collective creation of the academic ambient at Pitt.

Lastly, I would thank the everlasting spiritual support from my parents and my uncle, to the career I have pursued so far.

1.0 Introduction

The Standard Model (SM) of particle physics provides a remarkably successful description of the basic constituents of matter and their interactions. The spectacular discovery of the Higgs boson in 2012 at the Large Hadron Collider experiments ATLAS and CMS represents a critical milestone in our understanding, completing the menu of elementary particles predicted by the SM and confirming our basic understanding of electroweak symmetry breaking. However, there are a number of outstanding questions in particle physics and cosmology that cannot be answered in the SM. In some cases these include empirical mysteries, such as the origin of the matter-antimatter asymmetry, the dynamics behind neutrino masses, and the composition of dark matter in the universe. Other questions are of a more conceptual nature, from the patterns in the fermion masses and mixings to the smallness of the cosmological constant and the QCD theta parameter.

In the latter category of theoretical puzzles is the so-called hierarchy problem, related to the nature of the Higgs boson and the dynamics of electroweak symmetry breaking. It is this puzzle which motivates the work presented in this thesis. In this introductory chapter we will give a basic description of the hierarchy problem and discuss some of the traditional approaches based on the concept of symmetry related partner states. These traditional solutions have become more constrained as the expansive program of LHC searches for new colored particles have explored the TeV scale. Finally, we introduce the notion of neutral top partners which do not face the same experimental constraints from the LHC. This includes the original Mirror Twin Higgs Model, which is of central importance in this thesis.

1.1 Motivation

The Higgs mechanism [1, 2, 3, 4, 5, 6] explains the dynamical origin of masses of the elementary particles in the SM [7, 8, 9], namely, the quarks, leptons, and massive electroweak gauge bosons. Through this mechanism, elementary particle masses are tied to the vacuum

expectation value (VEV) of the scalar Higgs field, $\langle H \rangle \equiv v = 246$ GeV, which itself is ultimately tied to the Higgs squared mass parameter in the Lagrangian of the theory. The Higgs is the only scalar field in the SM, and according to our current best understanding it is the only known elementary scalar field present in Nature.

However, there is a well-known potential issue with elementary scalar fields. If new degrees of freedom beyond the Standard Model (BSM) are present at a higher energy scale, say $\Lambda \gg v$, it is expected based on general effective field theory reasoning that this physics will give a large contribution to the Higgs squared mass parameter. In particular, the natural expectation is that the Higgs mass squared should be of order Λ^2, rather than its experimentally measured value of order v^2. Moreover, there are plenty of good reasons to expect new physics thresholds in nature, such as those related to inflation, grand unification, and quantum gravity. In particular, the hierarchy problem manifests itself in the vast disparity between the strength of weak force which governs the beta decay and muon decay processes in microscopic world and that of gravity which governs the macroscopic and astrophysical world. The strengths of these two forces are determined by their respective fundamental physical parameters: the Fermi constant $G_F = 1/(\sqrt{2}v^2)$ and Newton's gravitational constant $G_N = 1/M_{\rm Pl}^2$, where $M_{\rm Pl} \sim 10^{19}$ GeV is the Planck mass and v is the electroweak VEV discussed above. Understanding the observed smallness of the electroweak scale relative to new high energy physics scales such as the Planck scale is the essence of the hierarchy problem.

To understand the hierarchy problem more clearly, we will need to examine the Lagrangian that encapsulates the essential dynamics of particles and fields, especially that of Higgs which is crucial for electroweak interaction and its interaction to any other heavy particles. Therefore, we begin in the next section by reviewing the structure of the SM and the Higgs mechanism for the origin of elementary particle masses, before turning to a more careful description of the hierarchy problem.

1.2 The Standard Model and The Higgs Mechanism

The Standard Model is based on the theoretical framework of non-Abelian gauge quantum field theory. It provides the natural generalization of quantum electrodynamics (QED), which is itself a marriage of Maxwell's classical theory based on the Abelian $U(1)_{\rm EM}$ gauge symmetry and quantum mechanics [10, 11, 12]. The SM describes the known non-gravitaitonal forces, which are mediated by non-abelian Yang-Mills gauge vector fields [13] to describe the $SU(2)_L \times U(1)_Y$ electroweak [7, 8, 9] and $SU(3)_c$ strong interactions [14, 15, 16, 17, 18] of fermionic matter particles. The matter fields include the quarks, which carry color charge of the strong interaction and the leptons which only experience the electroweak force. Finally, there is the Higgs field, responsible for spontaneously breaking the electroweak symmetry to the unbroken electromagnetism. Through its gauge and Yukawa interactions, the Higgs endows masses to the electroweak gauge bosons and matter particles.

Field Name	Spin	Label	$SU(3)_c$, $SU(2)_L$, $U(1)_Y$
Hypercharge boson	1	B	$(\mathbf{1}, \mathbf{1}, 0)$
Weak bosons	1	W	$(\mathbf{1}, \mathbf{3}, 0)$
Gluons	1	G	$(\mathbf{8}, \mathbf{1}, 0)$
Quarks	$\frac{1}{2}$	$Q_L = (u_L, d_L)^T$	$(\mathbf{3}, \mathbf{2}, \frac{1}{6})$
	$\frac{1}{2}$	u_R	$(\mathbf{3}, \mathbf{1}, \frac{2}{3})$
	$\frac{1}{2}$	d_R	$(\mathbf{3}, \mathbf{1}, -\frac{1}{3})$
Leptons	$\frac{1}{2}$	$L_L = (\nu_L, e_L)^T$	$(\mathbf{1}, \mathbf{2}, -\frac{1}{2})$
	$\frac{1}{2}$	e_R	$(\mathbf{1}, \mathbf{1}, -1)$
Higgs	0	$H = (H^+, H^0)^T$	$(\mathbf{1}, \mathbf{2}, \frac{1}{2})$

Table 1: Field content of the Standard Model. We indicate the name of the field, its label, its spin, and its quantum numbers under the $SU(3)_c$, $SU(2)_L$, $U(1)_Y$ interactions.

The field content of the SM is shown in Table 1 in the unbroken phase. The spin 1 gauge bosons mediating the basic interactions include the hypercharge boson B, the $SU(2)_L$

weak bosons W, and the gluons G of the strong force. The spin $\frac{1}{2}$ fermion matter fields include $SU(2)_L$ doublet and singlet quark fields, which after electroweak symmetry breaking partition into the up-type quark fields with electric charge 2/3 and the down type fields with electric charge -1/3. There are also the $SU(2)_L$ doublet and singlet lepton fields, leading to the neutrino and charged leptons at low energies. Finally, there is the Higgs field carrying electroweak charge. It contains the physical h fluctuation identified with the Higgs boson and the Nambu-Goldstone bosons eaten by the massive $W^{\pm}$ and Z gauge bosons after symmetry breaking.

The SM is a renormalizable quantum field theory which can in principle be valid to very high energy scales that are far beyond the direct reach of existing or planned high energy accelerator experiments. On the other hand, we know that the SM does not provide a quantum mechanical description of gravity. Furthermore, it does not account for neutrino masses, dark matter, the baryon asymmetry, or inflation. We must therefore consider the SM to be an incomplete theory.

The Higgs boson stands at the center of the SM and may ultimately provide a window into BSM physics. We will start from the Higgs potential and its Lagrangian. The general form of the potential is:

$$V = -\mu^2 H^\dagger H + \lambda (H^\dagger H)^2, \tag{1}$$

where the Higgs field is represented as (see Table 1)

$$H = \begin{pmatrix} H^+ \\ H^0 \end{pmatrix}. \tag{2}$$

We have chosen the parameters $\mu^2 > 0$ and $\lambda > 0$ such that the Higgs develops a VEV at low energies. The VEV can be determined by minimizing the scalar potential and is given by $\langle H \rangle = v/\sqrt{2}$[1], where $v = \sqrt{\mu^2/\lambda}$. Before EWSB, the weak force is transmitted by three massless vector bosons $W^1_\mu, W^2_\mu, W^3_\mu$, while there is also a hypercharge $U(1)_Y$ force carrier B_μ.

[1]In principle this should be an all order result in the low energy effective theory, combining all the know and unknown physics.

After EWSB, in the unitary gauge where the three Nambu-Goldstone bosons are absorbed by the corresponding weak gauge bosons, the Higgs H can be written as:

$$H = \begin{pmatrix} 0 \\ \frac{v+h}{\sqrt{2}} \end{pmatrix}, \tag{3}$$

where $h(x)$ is the radial field fluctuation around the minimum of potential, acting as the physical Higgs boson field which is electrically neutral, and both charge conjugate (C) even and parity (P) even. Inserting Eq. (3) into (4) and expanding to the quadratic order[2] in the fluctuation h, the mass of the Higgs boson is determined to be $m_h = \sqrt{2\,\lambda}\,v = \sqrt{2}\,\mu = 125$ GeV. Fixing the VEV and the Higgs mass to their experimental values, $v = 246$ GeV and $m_h = 125.1$ GeV, the Higgs potential parameters are then determined to be $\lambda \simeq 0.13$, $\mu \simeq 88.4$ GeV [19].

The Lagrangian of Higgs field is:

$$\mathcal{L}_(= (D^\mu H)^\dagger D_\mu H - V, \tag{4}$$

where the covariant derivative is given by $D_\mu = \partial_\mu - igW_\mu - ig'\frac{1}{2}B_\mu$, with $W_\mu = W_\mu^\alpha \tau^\alpha$, $\tau^\alpha = \frac{1}{2}\sigma^\alpha$, $\alpha = 1, 2, 3$ the $SU(2)_L$ generators, and σ^α the Pauli matrices. Furthermore, $g(g')$ are the coupling constant for weak (hypercharge) force.

The kinetic terms for EW gauge bosons before EWSB are[3]:

$$\mathcal{L} \supset -\frac{1}{2}Tr(W_{\mu\nu}W^{\mu\nu}) - \frac{1}{4}B_{\mu\nu}B^{\mu\nu}, \tag{5}$$

where the field strength tensors are $W_{\mu\nu} = W_{\mu\nu}^\alpha \tau^\alpha = D_\mu W_\nu - D_\nu W_\mu$, $W_{\mu\nu}^\alpha = \partial_\mu W_\nu^\alpha - \partial_\nu W_\mu^\alpha + g\epsilon^{\alpha\beta\gamma}W_\mu^\beta W_\nu^\gamma$, $B_{\mu\nu} = \partial_\mu B_\nu - \partial_\nu B_\mu$.

Upon EWSB, the electroweak gauge boson mass terms arise from the Higgs kinetic term, $\mathcal{L} \supset |D_\mu H|^2$. These mass terms can be written as

$$\begin{aligned} \mathcal{L} &\supset \frac{1}{2}\left\{ \frac{g^2 v^2}{4}\left[(W_\mu^1)^2 + (W_\mu^2)^2 + (W_\mu^3)^2\right] + \frac{g'^2 v_B^2}{4}(B_\mu)^2 - \frac{g g' v^2}{2}\, W_\mu^3\, B^\mu \right\}, \\ &= m_W^2\, |W_\mu^+|^2 + \frac{1}{2}m_Z^2 Z^2, \end{aligned} \tag{6}$$

[2]Note that any higher order in the expansion does not contribute.

[3]Throughout this thesis, we use the notation $\mathcal{L} \supset \mathcal{O}$ to indicate that the Lagrangian contains the operator $\mathcal{O}$

where we have defined the physical mass eigenstates W, Z, and photon fields:

$$W_\mu^\pm = \frac{1}{\sqrt{2}}(W_\mu^1 \mp iW_\mu^2), \quad Z_\mu = \cos\theta_W W_\mu^3 - \sin\theta_W B_\mu, \quad A_\mu = \cos\theta_W B_\mu + \sin\theta_W W_\mu^3. \tag{7}$$

The weak mixing angle, θ_W, is defined such that

$$\sin\theta_W \equiv \frac{g'}{\sqrt{g^2+g'^2}}, \qquad \cos\theta_W \equiv \frac{g}{\sqrt{g^2+g'^2}}. \tag{8}$$

The W and Z boson masses can then be written as

$$m_W \equiv \frac{g\,v}{2}, \qquad m_Z \equiv \frac{\sqrt{g^2+g'^2}}{2}v = \frac{m_W}{\cos\theta_W}, \tag{9}$$

while the photon A_μ remains massless after symmetry breaking. The electroweak gauge couplings to fermions stem from the fermion kinetic terms,

$$\mathcal{L} \supset \bar{f}_L i D_{L\mu}\gamma^\mu f_L + \bar{f}_R i D_{R\mu}\gamma^\mu f_R, \tag{10}$$

with

$$\begin{aligned} D_{L\mu} &= \partial_\mu - igW_\mu - Y_L g' B_\mu \qquad (11)\\ &= \partial_\mu - i\frac{g}{\sqrt{2}}(W_\mu^+\sigma^+ + W_\mu^-\sigma^-) - ieQA_\mu - ig_Z(\tau^3 - \sin^2\theta_W Q)Z_\mu, \\ D_{R\mu} &= \partial_\mu - g' Y_R B_\mu \qquad (12)\\ &= \partial_\mu - ieQA_\mu + ig_Z \sin^2\theta_W Q Z_\mu, \end{aligned}$$

where $Y_{L,R}$ is the hypercharge for left/right-handed chiral fermions, and $\sigma^\pm = \frac{1}{2}(\sigma^1 \pm i\sigma^2)$. After EWSB the gauge interactions are reorganized into charged and neutral currents with respective charge parameters related to the mixing angle. The $U(1)_{EM}$ electric charge generator is $Q = Y + \tau^3$, with the EM gauge coupling given as $e = g\sin\theta_W = g'\cos\theta_W$, and $g_Z = g/\cos\theta_W$.

The Yukawa interactions of Higgs field to fermions are:

$$\mathcal{L} \supset -y_d \bar{Q}_L H d_R - y_u \bar{Q}_L \tilde{H} u_R - y_l \bar{L}_L H e_R + \text{H.c.} \tag{13}$$

where $\tilde{H} = i\sigma_2 H^*$ (see also Table 1 for field definitions). Additionally, y_d, y_u, y_l are Yukawa coupling constants for down, up quarks and leptons, which are in general given by 3×3 complex matrices in the generation space. Following electroweak symmetry breaking, the fermion mass matrices, $M = y\frac{v}{\sqrt{2}}$, can be diagonalized through bi-unitary rotations of the fermion fields, i.e., $u_R = T^u u'_R$, $d_R = T^d d'_R$, $e_R = T^l e'_R$, $u_L = S^u u'_L$, $d_L = S^d d'_L$, $l = S^l l'$, where primed states are mass eigenstates, and $T^{u,d,l}$, $S^{u,d,l}$ the unitary rotation matrices for right and left states. In the quark sector, the rotations lead to physical effects determined by Cabibbo–Kobayashi–Maskawa (CKM) matrix, $V_{\rm CKM} = S^{u\dagger} S^d$, which describes quark flavor changing charged current interactions [20, 21]. Similarly, with additional dynamics beyond the SM generating neutrino masses, rotations in the lepton sector lead to the Pontecorvo–Maki–Nakagawa–Sakata (PMNS) matrix [22, 23]. There are no tree level flavor changing neutral currents (FCNC) in the SM.

Thus, we conclude that the masses of the heavy electroweak gauge bosons and fermions are dynamically generated through the Higgs mechanism and spontaneous electroweak symmetry breaking. In the minimal SM with one elementary Higgs scalar field there is a single physical Higgs scalar field fluctuation, the existence of which has been spectacularly confirmed at the LHC experiments. Next we discuss the experimental status of the Higgs boson.

1.2.1 Higgs Discovery and Experimental Status

The 2012 discovery of the Higgs boson by the ATLAS [25] and CMS [26] experiments at the LHC is an important milestone in the journey to understand the properties of elementary particles, putting into place the last particle predicted in the SM. The discovery was the culmination of a decades long hunt for the Higgs particle, which surveyed a wide mass range using a variety of experiments [27].

Since the discovery, the primary effort of the LHC experiments has focused on the investigation of the basic properties of the Higgs boson, including its spin and CP quantum numbers and its couplings to other known elementary particles. With the large integrated luminosity close to 140 fb^{-1} collected during Run 2 of the LHC at center of mass $\sqrt{s} = 13$

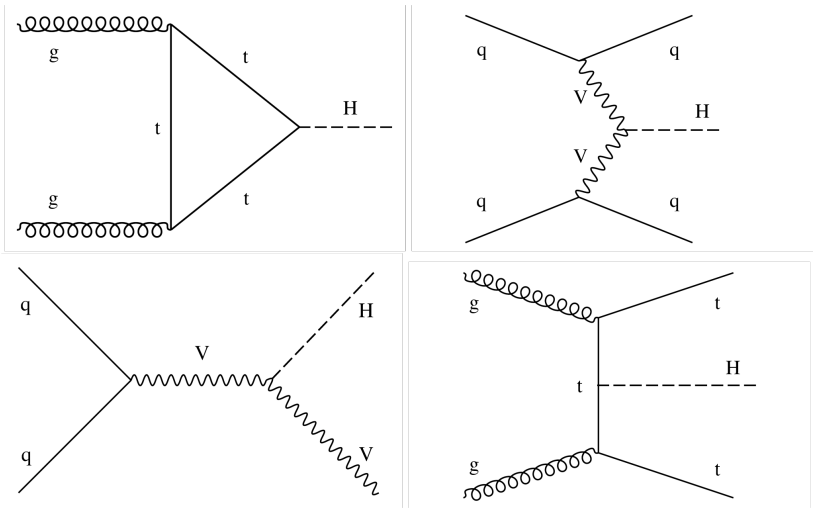

Figure 1: Feynman diagrams showing the main Higgs production channels at the LHC: gluon fusion (upper left), vector boson fusion (upper right), production in association with a vector boson (lower left) and production in association with a $t\bar{t}$ pair (lower right). The diagrams are taken from Ref. [24].

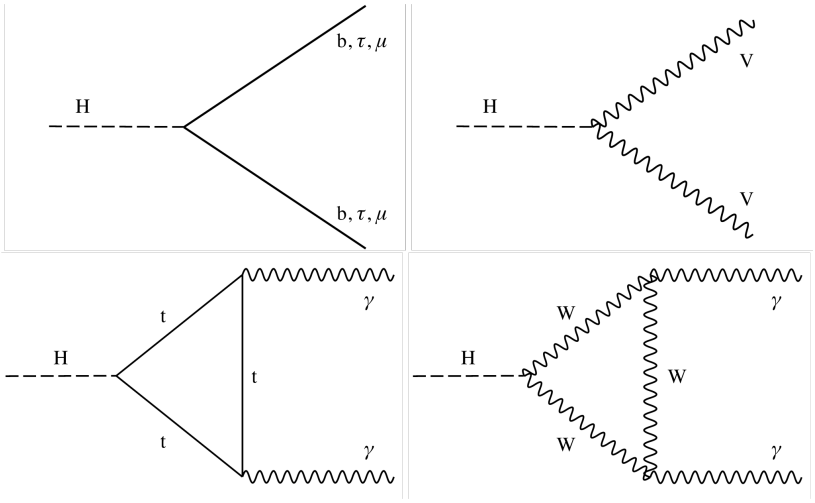

Figure 2: Feynman diagrams for the main Higgs decay channels at the LHC : decay to fermion pairs (upper left), decay to vector boson pairs (upper right), and decays to photons (lower left and right). The diagrams are taken from Ref. [24].

TeV, significant progress has been made in this endeavor.

Figures 1 and 2 show the most important Higgs production and decay channels relevant for proton-proton collisions at the LHC. The importance of these particular processes can be understood by noting the Higgs particle couples more strongly to heavy particles than to light particles, which explains the appearance of the heavy fermions (top, bottom, tau) and heavy vector boson (W, Z) in Figures 1 and 2. The Higgs is produced via gluon fusion (ggF), weak vector-boson fusion (VBF), Higgs associated with a weak boson (VH), associated with a pair of tops (ttH). For the 125 GeV Higgs, the predicted production cross sections at $\sqrt{s} = 13$ TeV are listed in Table 2, with a total of 55.1 pb [28]. The dominant production channel is gluon fusion, $gg \to h$, mediated at one loop through a triangle diagram involving the top quark, a result of the large Higgs-top Yukawa coupling. The next important property of the Higgs particle is how it decays after it is produced. At the LHC there are nine decay channels with noticeable branching ratios for a 125 GeV Higgs [29, 30]: $H \to b\bar{b}$, W^+W^-, gg, $\tau^+\tau^-$, $c\bar{c}$, ZZ, $\gamma\gamma$, $Z\gamma$, $\mu^+\mu^-$. The Higgs decays primarily to bottom quark pairs, then to WW^* which decay further to leptons or quarks.

Production channels	Cross section σ_i(pb)	Decay channels	Branching ratio B_i
ggF	48.6	$b\bar{b}$	5.82×10^{-1}
VBF	3.77	W^+W^-	2.14×10^{-1}
WH	1.36	gg	8.18×10^{-2}
ZH	0.83	$\tau^+\tau^-$	6.27×10^{-2}
$t\bar{t}H$	0.5	$c\bar{c}$	2.89×10^{-2}
...	...	ZZ	2.62×10^{-2}
total	55.1	$\gamma\gamma$	2.26×10^{-3}
		$Z\gamma$	1.53×10^{-3}
		$\mu^+\mu^-$	2.18×10^{-4}

Table 2: Predicted production cross sections at $\sqrt{s} = 13$ TeV, and decay branching ratios of Higgs. [28, 29, 30]

The variety of Higgs production mechanisms and decay channels affords the opportunity to study various couplings of the Higgs to SM particles. One way the experiments characterize these measurements is in terms of the signal strength modifiers, μ_i, for a given production or decay channel labeled i. The signal strength tells us the ratio of the experimentally measured rate and the predicted rate for the particular process under consideration. A signal strength equal to one within the experimental and theoretical uncertainties tells us that the measurements are in accord with the theoretical prediction. In Figure 3 we show the Higgs signal strength parameters for the various production and decay channels measured by the ATLAS [31] and CMS experiments [24]. We see that all measurements are within 1-2 standard deviations of unity, suggesting that the couplings of the 125 GeV boson to other SM particles are in good agreement with the predictions of the SM. Currently, the precision in the rate measurements is of order 20% in the most important channels, suggesting a corresponding precision in the determination of the corresponding Higgs couplings at the

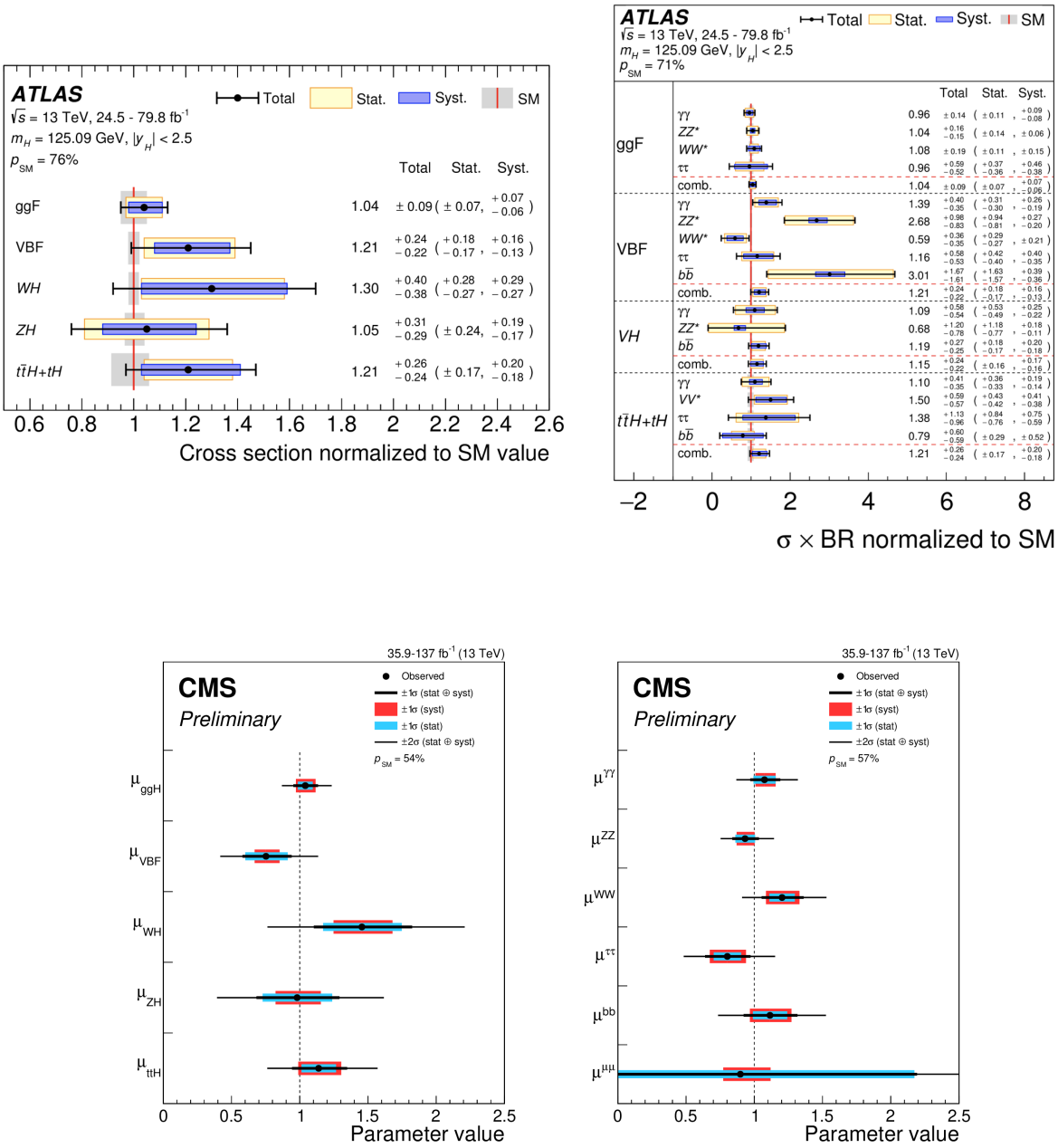

Figure 3: Signal strength modifiers for Higgs production (left) and decay (right) channels as measured by ATLAS (top) [31] and CMS (bottom) [24].

level of 10%. Ultimately, the high luminosity run of the LHC (HL-LHC) with a dataset of 3 inverse attobarn (ab^{-1}) will be able to measure these couplings down to the few % level [32]. Furthermore, the high energy physics community is exploring options for future lepton and hadron colliders which will allow for improvements in the Higgs couplings, possibly down to the percent level [33, 34, 35, 36, 37, 38]. Obviously, it is extremely important to measure the properties of the Higgs as precisely as possible, as any deviation would provide a clear sign of BSM physics.

One of the important properties of Higgs boson is its spin and CP quantum numbers. In the SM, the Higgs is a spin 0 scalar with charge and parity even, $J^{PC} = 0^{++}$. The discovery of Higgs was based on two decay channels: diphoton $H \to \gamma\gamma$ and four leptons $H \to ZZ \to 4l$ (where l means light leptons e, μ). The diphoton signal indicates that this particle is C even, assuming C conservation in the process[29], and it cannot be a spin 1 vector boson based on the Landau-Yang theorem[39], leaving the possibilities of 0 and 2. Depending on the parity and spin of the new particle $0^{++}, 0^{+-}, 2^{++}, 2^{+-}$, there are a variety of ways for its coupling to SM particles. Based on the helicity amplitude, the di-photon signal can be used to differentiate the spin values, as only the spin 0 scalar is polar-angular independent. The second channel $H \to ZZ^*$ can be used to differentiate either the parity of scalar according to its azimuthal angular distribution, or the spin value according to its threshold behavior. The study of the CMS experiment using the $H \to ZZ, Z\gamma^*, \gamma^*\gamma^* \to 4l$, $H \to WW^* \to l\nu l\nu$, and $H \to \gamma\gamma$ decays has eliminated a wide range of alternative spin and parity models at a 99% level or higher [40] in favor of the SM Higgs boson hypothesis. The study of ATLAS experiment using the $H \to ZZ^* \to 4l$, $H \to WW^* \to e\nu\mu\nu$ and $H \to \gamma\gamma$ decays has eliminated all the tested alternative spin and parity models in favor of the SM Higgs boson at more than 99.9% CL [41]. Additionally, the scenario with a mixed CP odd scalar boson and the SM Higgs boson has also been tested [42], and also in favor of the SM.

1.3 The Hierarchy Problem

The squared mass term of the Higgs is a relevant operator of mass dimension two. Without further symmetries to forbid this term, it will unavoidably receive additive quantum corrections from all the other fields coupling to the Higgs. In the SM, the leading radiative correction to the Higgs squared mass comes from a one loop top quark exchange. Using a momentum cutoff Λ to regularize the loop integral, the correction to the Higgs squared mass parameter is

$$\delta\mu^2 = \frac{3}{8\pi^2} y_t^2 \, \Lambda^2. \tag{14}$$

We see the well-known quadratic divergence, $\delta\mu^2 \sim \Lambda^2$, that is often discussed in connection with the hierarchy problem. One can view Λ as the scale where the SM fails to be a valid description and new physics enters. For example, we might expect that new physics is present at the Planck scale associated with quantum gravity, in which case we should take $\Lambda = M_{\rm Pl}$. Interpreted in this way, we conclude that the correction to the Higgs squared mass coming from the top loop (14) is much larger than the experimentally measured value of order $(100\,\text{GeV})^2$. To obtain consistency with experiment, the bare Higgs mass parameter must be precisely fine-tuned to nearly cancel this large correction. This is one way to phrase the hierarchy problem. On the other hand, one can take the perspective that the quadratic divergence is an artifact of the momentum cutoff regulator and does not have a physical interpretation. For instance, using dimensional regularization the quadratic divergences do not appear.

A sharper statement of the issue can be made in extensions of the SM. As a simple toy example that is representative of many realistic theories, we can consider the addition of a heavy scalar field ϕ to the SM with a coupling to the Higgs field,

$$V \supset M^2 \phi^\dagger \phi + \kappa \, \phi^\dagger \phi \, H^\dagger H + \ldots, \tag{15}$$

where M^2 is the squared scalar mass parameter, and κ describes the interaction between ϕ and the Higgs. We will consider the situation $|M| \gg v$, i.e., the scalar is much heavier than the weak scale and the known SM particles. For instance, very similar interactions

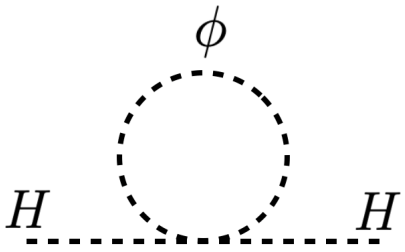

Figure 4: Higgs self energy diagram in the scalar toy model of Eq. (15).

are present in supersymmetric extensions of the SM and in Grand Unified Theories [43, 44]. These new interactions lead to a one loop correction to the Higgs mass term in Eq. (4), as shown in Figure 4. Regardless of how the loop integral is regularized, we find a correction is parametrically given by

$$\delta\mu^2 \sim \frac{\kappa}{16\pi^2} M^2. \tag{16}$$

We see that the correction is quadratically sensitive to the heavy scalar mass, and for order one values of the coupling κ the correction can be much larger than the observed value. To fit the observed electroweak VEV and Higgs boson mass, the bare Higgs mass parameter must cancel the large contribution coming from Eq. (16) to a very high precision. This fine tuning of parameters is unsettling and calls out for a deeper explanation.

While here we discussed an example of a one loop contribution to the Higgs mass, the hierarchy problem can also manifest at the classical level. For example, if $M^2 < 0$ in the scalar theory described by Eq. (16), then we would expect ϕ to also obtain a VEV, $\langle\phi\rangle = v_\phi$, which is expected to be of order M on dimensional grounds. Substituting the ϕ VEV back into the Lagrangian (15), we find an effective contribution to the Higgs squared mass parameter $\delta\mu^2 \sim v_\phi^2 \sim M^2 \gg v$.

We now discuss one of the classic approaches to the hierarchy problem, which will bring focus to the central importance of the top quark and the hypothesis of symmetry related partner states.

1.4 Supersymmetry and Colored Top Partners

The hierarchy problem has been with us for several decades, and over time a number of proposals have been put forth to address the issue. These include supersymmetry (SUSY) [43], strong dynamics (including models in which the Higgs is composite) [45, 46], extra spatial dimensions [47, 48], and even anthropic selection [49]. While all of these ideas are novel and worthy of investigation, here we will briefly review the SUSY solution as it will provide a foundation as well as a motivation for our later work on the Twin Higgs.

SUSY is an extension of the Poincare group of space-time symmetries. At the level of quantum fields, it can be described as a symmetry between bosons and fermions. In the Minimal Supersymmetric Standard Model (MSSM), which is the simplest supersymmetric extension of the SM, each SM field has associated to it a superpartner field. For instance, the top quark of the SM will have a supersymmetric top partner, dubbed the top squark or "stop" for short. Of course, since superpartners have not yet been observed in experiment, it must be that SUSY is spontaneously broken, much in the same way that the electroweak symmetry is broken by the Higgs field VEV. A primary consequence of SUSY breaking is to give the superpartner fields a "soft" mass term, making these states heavy in comparison to the SM fields. However, if SUSY is to play a role in addressing the hierarchy problem, the superpartner mass spectrum should not be far above the electroweak scale.

The top and stop play a particularly important role in the context of the hierarchy problem. Since these states have the strongest interaction with the Higgs field, governed by the top quark Yukawa coupling y_t, they in turn give largest contribution to the Higgs squared mass parameter. The particular interactions needed to understand this point are given below:

$$\begin{aligned} -\mathcal{L} \supset & \left(y_t\, \bar{t}_R\, Q_L H_u + \text{H.c.}\right) + y_t^2 \left(|\widetilde{Q} H_u|^2 + |\,\widetilde{t}\,|^2 |H_u|^2\right) \\ & + m_{\widetilde{Q}}^2\, |\widetilde{Q}|^2 + m_{\widetilde{t}}^2\, |\,\widetilde{t}\,|^2 + \left(y_t A_t\, \widetilde{t}^*\widetilde{Q}\, H_u + \text{H.c.}\right), \end{aligned} \tag{17}$$

where H_u denotes the Higgs field [4], Q (t) are the $SU(2)$ doublet (singlet) fermionic quark fields associated with the top sector, while $\widetilde{Q}$ ($\widetilde{t}$) denote their scalar superpartners. Further-

[4] In contrast to the SM, two Higgs doublet fields are required in the MSSM by gauge anomaly cancellation, and here H_u is the doublet that couples to up-type quarks.

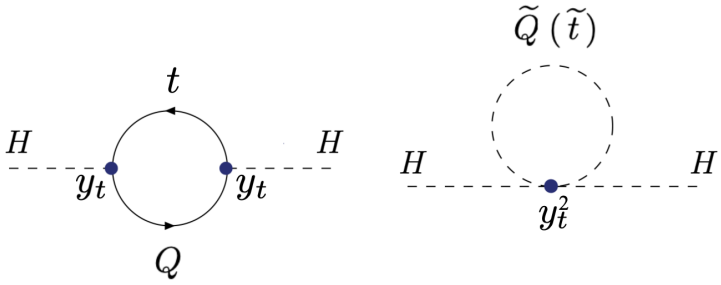

Figure 5: Subset of Higgs self energy correction from one-loop top quark and top squark exchange in the MSSM.

more, in the second line of Eq. (17) we have written soft SUSY breaking terms, including the scalar masses and the A term interaction. A crucial consequence of SUSY is evident in the first line of Eq. (17), namely the relation (or "equality") between the top and stop couplings to the Higgs field, which are both governed by the top Yukawa coupling y_t. These interactions generate one loop contributions to the Higgs squared mass, some of which are shown in Figure. 5. Regulating the momentum integrals with a cutoff, one finds that the quadratic divergences arising from the top loop are precisely canceled by those from the stop loop, which is a direct consequence of SUSY relating the top fields with the stop fields and the strength of the interactions in the first line of Eq. 17. There are however corrections to the Higgs squared mass that depend on the soft SUSY breaking terms [43, 50][5]

$$\delta m_{H_u}^2 = +\frac{3}{8\pi^2} y_t^2 (m_{\tilde{Q}}^2 + m_{\tilde{t}}^2 + |A_t^2|) \log\left(\frac{\Lambda_{\rm med}}{\rm TeV}\right), \tag{18}$$

where $\Lambda_{\rm med}$ is the scale at which SUSY breaking effects are communicated to the supersymmetric SM. We observe that the correction to the Higgs squared mass is governed by the soft SUSY parameters of the stop sector, which also control the physical stop mass spectrum. Thus, in order to keep the correction $\delta m_{H_u}^2$ small in comparison to the electroweak scale and have a satisfactory solution to the hierarchy problem, the stops should not be too heavy.

[5]TeV scale is what we are considering.

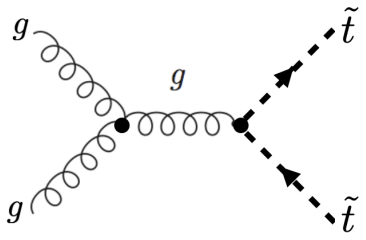

Figure 6: Representative Feynman diagram for stop pair production at the LHC.

We can of course always make the stops heavier, but only at the expense of fine tuning the Higgs sector soft parameters to balance the contribution in Eq. (18).

The SUSY solution to the hierarchy problem is quite attractive from a theoretical viewpoint, although thus far the LHC has not observed any signs of superpartners. In particular, because the stops are charged under the $SU(3)_c$ strong interaction, they should be abundantly produced at the LHC if they are in the mass range naively suggested by the naturalness arguments above, as shown in the digram in Figure 6. The current bounds suggest stop masses should be above 500 GeV - 1 TeV depending on the assumed decay mode [51, 52, 53, 54]. These and other bounds on superpartners put the SUSY solution to the hierarchy problem in some tension.

It should be emphasized that it is in principle possible that the stop and other superpartners are somewhat heavier than our naive expectations, putting them out of direct reach of the LHC experiments. For instance, if the superpartners are 10 TeV range, they would still address most of the 'big' hierarchy problem by protecting the Higgs from corrections between the SUSY soft mass scale and the Planck scale. However, there would remain a 'little' hierarchy problem between the weak scale and the SUSY soft mass scale [55], which would still seem to require some fine tuning. It is possible to take this as a hint for some additional mechanism that stabilizes the little hierarchy, and this motivates the idea of neutral top partners.

1.5 Neutral Top Partners

A creative way to tackle the little hierarchy problem is to suppose the top partners that cancel the quadratic divergences are neutral under the SM charges, or at least under the $SU(3)_c$ strong interaction. This general idea is referred to as the *neutral naturalness* [56]. The production cross section at the LHC for color neutral top partners is much reduced in comparison to colored top partners such as the stops in the MSSM discussed above, and therefore the potential LHC bounds are evaded in a trivial manner. The first example in this class of models is Mirror Twin Higgs model [57, 58, 59], which features completely neutral color top partners. There have been a variety of other models proposed within the neutral naturalness paradigm, including Folded SUSY [60], the Quirky Little Higgs [61], the Dark Top[62], and the Orbifold Higgs [56], among others [63, 64, 65, 66, 67, 68, 69, 70, 71]. In many ways, the original Mirror Twin Higgs model [58, 59] stands out from the others in terms of its elegance and structural simplicity, and motivates the work discussed in this thesis.

2.0 The Mirror Twin Higgs

The Mirror Twin Higgs (MTH) [57] and other 'Neutral Naturalness' scenarios [59, 58, 60, 62, 61, 56, 63, 64, 65, 66, 67, 68, 69, 70, 71] feature color-neutral symmetry-partner states which stabilize the electroweak scale, thereby reconciling a natural Higgs with the increasingly stringent direct constraints on colored states from LHC. The MTH offers an elegant solution to the little hierarchy problem, and a variety of UV completions based on SUSY, compositeness, or extra dimensions have been proposed [72, 73, 74, 75, 76, 77, 78, 79, 80]. In this chapter we review the theoretical structure and basic phenomenology of the MTH. We also discuss some of the outstanding questions in the MTH, which will set the stage for our investigations on the spontaneous breaking of twin color and $\mathbb{Z}_2$.

2.1 Model Construction and Cancellation Mechanism

The original Mirror Twin Higgs (MTH) [57] provides the first and perhaps structurally simplest Neutral Naturalness model with neutral top partners. The model hypothesizes an exact copy of the complete Standard Model (SM), which we will refer to as the mirror sector or twin sector, along with a discrete symmetry that exchanges each SM field with its corresponding partner in the mirror sector. We will label fields in the visible sector (mirror sector) as A (B). The $\mathbb{Z}_2$ symmetry also requires the coupling constants to be the same between two sectors, and thus plays an analogous role to SUSY in the MSSM, as discussed in Chapter 1.4.

Assuming the existence of the mirror sector, let us now narrow our focus on the Higgs bosons in each sector. An additional important assumption in the model is that the Higgs sector enjoys an approximate $SU(4)$ global symmetry. Grouping the A and B sector Higgs doublets into a $SU(4)$ 4-plet,

$$H = \begin{pmatrix} H_A \\ H_B \end{pmatrix}, \tag{19}$$

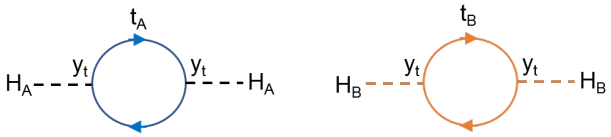

Figure 7: Two-point function of Higgs in sectors A and B, from loops of top and twin top.

the scalar potential can be written in the first approximation as

$$V = -\mu^2 H^\dagger H + \lambda (H^\dagger H)^2 \tag{20}$$

We assume that the Higgs 4-plet obtains a VEV, $\langle H \rangle = (0,\ 0,\ 0,\ f_H)^T$. This spontaneously breaks the global symmetry from $SU(4)$ down to $SU(3)$, leading to the appearance of 7 Nambu-Goldstone bosons. Three of these will be eaten by the twin sector $W_B^\pm$ and Z_B gauge bosons, while the remaining four will serve as the SM Higgs doublet H_A. There is an important question of obtaining the correct vacuum alignment, which will require a source of $\mathbb{Z}_2$ breaking, and we will return to this question shortly.

With this basic setup we are now in a position to discuss the twin protection mechanism. Let us consider the most important correction to the Higgs potential originating from the Higgs interactions with the top quark. These interactions can be written as

$$-\mathcal{L} \supset y_t\, \bar{t}_{AR}\, Q_{AL}\, H_A + y_t\, \bar{t}_{BR}\, Q_{BL}\, H_B + \text{H.c.} \tag{21}$$

The one loop correction to the Higgs self energy arises from the diagrams shown in Figure 7. Regulating the loop integrals with a hard momentum cutoff, we find the correction to the Higgs potential

$$\delta V = -\frac{3y_t^2}{8\pi^2}\Lambda^2 (H_A^\dagger H_A + H_B^\dagger H_B) = -\frac{3y_t^2}{8\pi^2}\Lambda^2\, H^\dagger H. \tag{22}$$

Crucially, we see that the correction to the Higgs mass terms is an $SU(4)$ invariant, and thus does not give a contribution to the Nambu-Goldstone boson masses. Therefore, the SM Higgs boson, being a Nambu-Goldstone Boson, will remain massless under this correction. We note again the importance of the $\mathbb{Z}_2$ symmetry in enforcing the equality of the top Yukawa

couplings, which is critical in rendering the correction above invariant under the $SU(4)$ global symmetry. A similar cancellation mechanism operates for the gauge interactions as a result of the $\mathbb{Z}_2$ symmetry.

The Yukawa interactions (21) and gauge interactions, while respecting $\mathbb{Z}_2$, do not respect the global $SU(4)$ symmetry. While the corrections to the mass terms above in Eq. (22) respect $SU(4)$, top and gauge loops will generate a correction to the Higgs quartic interactions which breaks $SU(4)$. Since the $SU(4)$ symmetry is no longer exact, we expect the SM Higgs to be a pseudo-Nambu-Goldstone boson (pNGB) and pick up a small mass. The contributions to the quartic interactions are only logarithmically sensitive to the UV cutoff of the theory, and therefore we can naturally have a light pNGB Higgs boson for cutoffs of order 5-10 TeV. It is in this way that the MTH addresses the little hierarchy problem, and we emphasize the critical role of the mirror sector top partners that are neutral under the SM gauge interactions.

It is also interesting to study the cancellation mechanism in a low energy description of the theory in which the radial mode of the $SU(4)$ Higgs 4-plet is integrated out. To this end, it is convenient to use a nonlinear realization of symmetry, including only the pNGBs in the low energy description. We can write the Higgs 4-plet as [57, 81]:

$$H = e^{i\Pi_H/f_H} H_0, \qquad \Pi_H = \begin{pmatrix} 0 & 0 & 0 & -ih_1 \\ 0 & 0 & 0 & -ih_2 \\ 0 & 0 & 0 & 0 \\ ih_1 & ih_2 & 0 & 0 \end{pmatrix}, \tag{23}$$

where we work in unitary gauge in which the B-sector NGBs are absorbed by $W_B^{\pm}, Z_B$. Denote $\boldsymbol{h} = (h_1, h_2)^T$ as the SM Higgs doublet we can carry out the matrix exponentiation in Eq. (23) [81]:

$$\begin{aligned} H_A &= \boldsymbol{h} \frac{f_H}{\sqrt{|\boldsymbol{h}|^2}} \sin\left(\frac{\sqrt{|\boldsymbol{h}|^2}}{f_H}\right) \simeq \boldsymbol{h}, \\ H_B &= \begin{pmatrix} 0 \\ f_H \cos\left(\frac{\sqrt{|\boldsymbol{h}|^2}}{f_H}\right) \end{pmatrix} \simeq \begin{pmatrix} 0 \\ f_H - \frac{|\boldsymbol{h}|^2}{2f_H} \end{pmatrix}. \end{aligned} \tag{24}$$

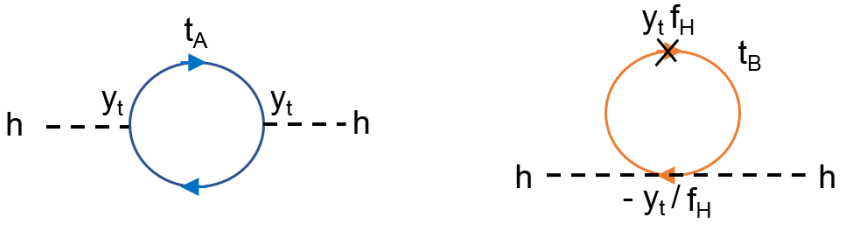

Figure 8: Two-point function of the SM Higgs boson h from loops of top and its twin .

where $|\boldsymbol{h}|^2 \equiv \boldsymbol{h}^\dagger \boldsymbol{h}$. Using the expansion above the top Yukawa couplings in Eq. (21) can be written as

$$-\mathcal{L} \supset y_t\, \bar{t}_{AR}\, \boldsymbol{h}\, Q_{AL} + y_t \left(f_H - \frac{\boldsymbol{h}^\dagger \boldsymbol{h}}{2 f_H} \right) \bar{t}_{BR}\, Q_{BL} + \text{H.c.} \tag{25}$$

Thus, we see that the SM Higgs doublet picks up a coupling to the twin top quarks. The interactions in Eq. (25) give rise to Higgs self energy corrections, shown by the diagrams in Figure 8, and the quadratic divergence coming from the top quark loop is precisely canceled by that from the twin top loop.

On the other hand as mentioned, the quartic contributions are only logarithmically sensitive to the UV cutoff of the theory, and we can end up with a light Higgs boson for cutoffs below 10 TeV. For example, the top quark Yukawa interactions lead to a one loop contribution to the quartic, $\delta V \sim \delta_H(|H_A|^4 + |H_B|^4)$, with $\delta_H \sim (y_t^4/16\pi^2)\log(\Lambda/y_t f_H)$. Using Eq. (24), we find a contribution to the pNGB SM Higgs squared mass of order $\delta_H f_H^2$, which is of order $(100\,\text{GeV})^2$ for f_H of order TeV and Λ of order 5 TeV.

Through the twin protection mechanism discussed above, we see that the little hierarchy problem can be solved by the MTH, along with the mirror top partners that are neutral. We now return to the important issue of vacuum alignment. Consider first the most general $\mathbb{Z}_2$ symmetric potential,

$$V = -\mu^2 H^\dagger H + \lambda (H^\dagger H)^2 + \delta_H(|H_A|^4 + |H_B|^4). \tag{26}$$

The first two terms are manifestly $SU(4)$ symmetric, while the final quartic terms respects $\mathbb{Z}_2$ but not $SU(4)$, and we expect $\delta_H \ll \lambda$. Extremizing the potential (26), we find that the

minimum occurs when both Higgs fields have equal VEVs, $\langle H_A \rangle = \langle H_B \rangle = f_H$. However, this vacuum is not phenomenologically viable as it results in dramatic distortions in the couplings of the Higgs boson to SM fields. Instead, we require a mild hierarchy in the VEVs, such that $\langle H_A \rangle \sim v$, $\langle H_B \rangle \sim f_H$, with $v/f_H \ll 1$. In this case, the Higgs couplings are close to their SM values, with deviations of order v^2/f_H^2. Current data from LHC Higgs coupling and precision electroweak measurements require $v/f_H \lesssim 1/3$. To obtain the correct vacuum alignment, we must introduce a small source of $\mathbb{Z}_2$ breaking into the potential. The simplest option is to add a soft $\mathbb{Z}_2$ breaking mass term [57], though other possibilities have been discussed in the literature and we will come back to these below. We note that aligning the vacuum in this way, such that $v/f \lesssim 1/3$, corresponds to a mild tuning of parameters at the order 20-30% level.

2.2 Phenomenology

The phenomenology associated with the MTH model is quite distinct in comparison to other models addressing the hierarchy problem. First, the twin sector fields are completely neutral under the SM gauge groups, and the only mediator between the two sectors is the Higgs boson itself. Thus, the direct production rates of mirror sector particles at the LHC, including the neutral top partners, would be very low. This is true even if the top partners are relatively light, with masses in the 500 GeV range. In this way, the constraints posed by direct searches for new colored top partners at the LHC is trivially evaded in the MTH model.

One of the most important probes of this model arises from the pNGB nature of the Higgs boson and the modifications to its couplings from their SM predictions. We can see this by again considering the nonlinearly realization following [81]; see Eq. (23). Working in the unitary gauge of the visible sector, $h_1 = 0,\ h_2 = (v_H + h)/\sqrt{2}$, we have

$$H_A = \begin{pmatrix} 0 \\ f_H \sin\left(\frac{v_H+h}{\sqrt{2}f_H}\right) \end{pmatrix}, \qquad H_B = \begin{pmatrix} 0 \\ f_H \cos\left(\frac{v_H+h}{\sqrt{2}f_H}\right) \end{pmatrix}. \tag{27}$$

It is natural to define as [82]:

$$v_A \equiv \sqrt{2} f_H \sin\vartheta, \qquad v_B \equiv \sqrt{2} f_H \cos\vartheta, \tag{28}$$

where we have defined $\vartheta = \frac{v_H}{\sqrt{2} f_H}$, and $v_{\rm EW} \equiv v_A = 246$ GeV is the electroweak VEV. The fermion masses in the two sectors are thus related as $m_B = m_A \cot\vartheta$. From the covariant derivative $|D^A_\mu H_A|^2$ and its twin part, we have:

$$m^2_{WA} = \frac{v_A^2 g^2}{4}, \quad m^2_{WB} = \frac{v_B^2 g^2}{4}. \tag{29}$$

As mentioned in the previous section, if the $\mathbb{Z}_2$ symmetry is exact, than the two VEVs would be equal, the physical Higgs h would be comprised of an equal mixture of visible and twin sector scalars resulting in an order one modification of the couplings to SM particles and a large invisible branching ratio to twin sector states. Such a scenario is incompatible with our current experimental knowledge of the Higgs boson. To avoid this, we need to align the vacuum such that $\tan\vartheta \lesssim 1/3$ such that $v_A \ll v_B \simeq f_H$. This can be easily achieved by introducing to the potential a soft explicit breaking term at the cutoff [82]:

$$V_{\not{\mathbb{Z}}_2} = m^2(|H_A|^2 - |H_B|^2). \tag{30}$$

Substituting Eq. 27 into the potential Eqs. (26,30) with the $SU(4)$ breaking quartic and soft $\mathbb{Z}_2$ breaking mass terms, we obtain the potential for pNGB Higgs (dropping constant terms):

$$V = -\frac{\delta_H f_H^4}{2} \sin^2\left[\frac{\sqrt{2}(v_H + h)}{f_H}\right] - m^2 f_H^2 \cos\left[\frac{\sqrt{2}(v_H + h)}{f_H}\right]. \tag{31}$$

Minimizing the potential, we obtain the condition determining the vacuum angle ϑ:

$$\cos(2\vartheta) = \frac{m^2}{\delta_H f_H^2}. \tag{32}$$

A mild tuning in the scalar potential parameters is required to obtain $\vartheta \lesssim 1/3$.

The physical couplings of the pNGB Higgs to gauge bosons and fermions can be obtained by replacing $v_H \to v_H + h$ and expanding about the vacuum. For the gauge boson couplings we obtain

$$\mathcal{L} \supset \frac{2h}{v_{\rm EW}} \left\{ \cos\vartheta \left[m_{W_A}^2 |W_{A\mu}|^2 + \frac{m_{Z_A}^2}{2} Z_{A\mu}^2 \right] - \tan\vartheta \sin\vartheta \left[m_{W_B}^2 |W_{B\mu}|^2 + \frac{m_{Z_B}^2}{2} Z_{B\mu}^2 \right] \right\}. \tag{33}$$

For the top Yukawa coupling we have:

$$\mathcal{L} \supset -\frac{y_t}{\sqrt{2}} h \left(\cos\vartheta\, \bar{t}_{AR} t_{AL} - \sin\vartheta\, \bar{t}_{BR} t_{BL} \right) + \text{H.c.} \tag{34}$$

In general, the couplings of Higgs to the SM sector are modified by a factor of $\cos\vartheta$ relative to their SM values. This causes a reduction in the Higgs production cross sections and decay branching ratios to SM particles by a factor of $\cos^2\vartheta$. In addition, the Higgs also obtains couplings to the B sector particles that are suppressed by the small vacuum angle. Through these couplings the Higgs can have subdominant decay to mirror sector states leading to an invisible Higgs decay signature at the LHC. Therefore, in summary we expect the Higgs event rates in SM final states to be suppressed by a factor of $\cos^2\vartheta$, along with a small but potentially observable invisible Higgs width.

The measurement precision for the ZZ, WW, and $\gamma\gamma$ couplings to the Higgs is currently around 10%, and can eventually be probed to the few percent level at the HL-LHC [32]. For the Higgs invisible decay, an observed(expected) upper limit of 0.19(0.15) at 95% CL was obtained by CMS experiment [83], while both observed and expected upper limits of 0.13 is set at 95% CL by the ATLAS experiment [84], and can be further constrained down to few percent level at the HL-LHC [32]. Therefore $\vartheta \lesssim 1/3$ is currently allowed but the HL-LHC may be able to constrain this further; see Ref [81] for a detailed investigation.

2.3 Open Questions In The Mirror Twin Higgs

Several open issues exist in this basic framework. First, the $\mathbb{Z}_2$ symmetry must be broken to achieve a phenomenologically viable vacuum, featuring a hierarchy between the global $SU(4)$ breaking scale and the electroweak scale. From a bottom up perspective a suitable source of $\mathbb{Z}_2$ breaking can be implemented 'by hand' in a variety of ways, including a 'soft' breaking mass term in the scalar potential [57] (see previous section for a discussion) or a 'hard' breaking through the removal of a subset of states in the twin sector, as in the Fraternal Twin Higgs [85]. However, it would be appealing to have a dynamical origin for the required $\mathbb{Z}_2$ breaking source. One possibility is that the $\mathbb{Z}_2$ is an exact symmetry of the theory but is spontaneously broken [86, 87, 88, 89, 90].

A second issue is about the cosmology. Given the large number of states in the mirror sector which were presumably in equilibrium with the SM radiation bath at early times, a standard thermal cosmology would predict too many relativistic degrees of freedom at late times. A detailed study leads to the prediction for the predicted effective neutrino number $\Delta N_{\text{eff}} \approx 5.6$ [91]. This prediction clashes with observations of primordial element abundances and the microwave background radiation, which requires $\Delta N_{eff} < 0.6$ at 2σ level [92]. To address this question, one could remove the lightest first and second generation twin fermions, which are not strictly required by naturalness considerations. This provides a simple way to evade this ΔN_{eff} problem [85, 93, 94] and is also connected with how the $\mathbb{Z}_2$ symmetry is ultamately broken. Other mechanisms have also been proposed that lead to a viable cosmology [95, 96, 91, 97, 98, 99]. Following these successes many other cosmological topics can be addressed, including the nature of dark matter [100, 93, 101, 95, 102, 103, 97, 104, 105, 106, 107, 108, 109], the order of the electroweak phase transition [110], baryogenesis [103, 111], and large and small scale structure [112, 113].

3.0 Motivation for Mirror Color Symmetry Breaking

A spontaneous breaking of the $\mathbb{Z}_2$ symmetry can address the vacuum alignment question and, potentially, lead to a viable thermal cosmology. Furthermore, such $\mathbb{Z}_2$ breaking is an inevitable consequence of a pattern of gauge symmetry breaking in the mirror sector that differs from the SM's electroweak symmetry breaking pattern. Interestingly, such spontaneous mirror gauge symmetry breaking can dynamically generate effective soft $\mathbb{Z}_2$ breaking mass terms in the scalar potential required for vacuum alignment. They can also produce new twin fermion and gauge boson mass terms, which mimic the hard breaking of the Fraternal Twin Higgs scenario [85] by raising the light twin sector states. Due to the exact $\mathbb{Z}_2$ symmetry, this scenario generically leads to a variety of new phenomena in the visible sector that can be probed through precision tests of baryon and lepton number violation, quark and lepton flavor violation, CP violation, the electroweak and Higgs sectors, and directly at high energy colliders such as the LHC.[1]

This approach was advocated recently in Ref. [82, 116], which explored the simultaneous spontaneous breakdown of mirror hypercharge gauge symmetry and $\mathbb{Z}_2$ symmetry. In this work we examine the spontaneous breakdown of the twin color symmetry. Beginning from a MTH model, with an exact $\mathbb{Z}_2$ symmetry, we add a new scalar field charged under $SU(3)_c$ and its twin counterpart. A suitable scalar potential causes the twin colored scalar to develop a vacuum expectation value (VEV), spontaneously breaking both twin color and $\mathbb{Z}_2$. Depending on the scalar representation and potential, a variety of symmetry breaking patterns can be realized with distinct consequences. There are several possible residual color gauge symmetries of the twin sector which may or may not confine, and when they do at vastly different scales. The possible couplings of the scalar to fermions may also produce new twin fermion mass terms. All of these possibilities lead to very different twin phenomenology and the rich variation that can spring from an initially mirror $\mathbb{Z}_2$ set up.

While the complete breakdown of twin color was explored in Ref. [116], the aim was a

[1] Other connections between Twin Higgs models and SM flavor structure have been explored in [104, 114, 115].

particular cosmology and employed two scalars that acquired VEVs. We focus on a different part of the vast span of possibilities that is in some sense a minimal set of color breaking patterns. These follow from the introduction of a single new colored multiplet (in each sector) which may transform in the triplet, sextet, or octet representation. This scalar field is assumed to be a singlet under the weak gauge group, though it may carry hypercharge.

The remainder of this thesis explores these possibilities in detail[2] and consists of four chapters organized as follows. First a detailed analysis of minimal possibilities of models is presented in Chapter 4. In the next Chapter 5 we summarize the five models and discuss their gauge sector dynamics, with four of them featuring interesting low twin sector confinement scales. In Chapter 6 the couplings of the colored scalars to fermions are investigated and shown to dynamically generate new twin fermion mass terms, providing a possible way to realize a fraternal-like twin fermion spectrum. The correlated effects of these couplings in the visible sector through a variety of precision tests are discussed in Chapter 7. The new colored scalars can also be directly probed at the LHC and future high energy colliders, and we detail the current limits and prospects for these searches in Chapter 8. Finally, we conclude with some perspectives on future studies in Chapter 9.

[2] A short version of this work can be found in [117]

4.0 Spontaneous Breakdown of Twin Color

We begin with a basic description of our setup. We consider the Mirror Twin Higgs (MTH) model, which contains an exact copy of the SM called the twin sector. In all that follows the label A (B) denotes visible (twin) sector fields and the exact $\mathbb{Z}_2$ exchange symmetry interchanges A and B fields. This symmetry provides the foundation for the Higgs mass protection mechanism, as it implies the equality of gauge and Yukawa couplings in the two sectors. To this base we add the scalar fields, Φ_A and Φ_B, that are respectively charged under SM and twin $SU(3)_c$ gauge symmetries. We will consider the following complex triplet, complex sextet, and real octet representations for the scalar fields:

$$(\mathbf{3}, \mathbf{1}, Y_\Phi), \quad (\mathbf{6}, \mathbf{1}, Y_\Phi), \quad (\mathbf{8}, \mathbf{1}, 0). \tag{35}$$

We will not consider modifications to the $SU(2)_L$ weak symmetry breaking pattern, so we have chosen singlet representations under that group in Eq. (35). Later we will investigate several specific values of the scalar hypercharge Y_Φ, which allow different scalar coupling to fermions. Given an appropriate scalar potential, Φ_B obtains a VEV and spontaneously breaking twin color and $\mathbb{Z}_2$. As we will see, this will allow sufficient freedom to align the vacuum in a phenomenologically viable direction. Later, in Chapter 6 we will also see that this symmetry breaking can also generate new twin fermion mass terms.

We pause briefly to make a couple of general remarks about our scenario. First, the phenomenologically desirable vacuum will always have the property that Φ_B obtains a VEV, while Φ_A does not. We note that in each case analyzed below, as a consequence of the exact $\mathbb{Z}_2$ symmetry of the models, there is always another vacuum of equal depth for which the VEV lies entirely in the A sector, i.e., $\langle \Phi_A \rangle \neq 0$ and $\langle \Phi_B \rangle = 0$. This vacuum is clearly unacceptable from a phenomenological perspective as it breaks $[SU(3)_c]_A$, and our universe must therefore correspond to the other vacuum, $\langle \Phi_A \rangle = 0$ and $\langle \Phi_B \rangle \neq 0$. Second, the spontaneous breaking of the discrete $\mathbb{Z}_2$ symmetry raises potential concerns of a domain wall problem. However, this problem can be circumvented if, for instance, there is a low Hubble scale during inflation, or if there are additional small explicit sources of $\mathbb{Z}_2$ breaking in the

theory. See Ref. [82] for further related discussion in scenarios where mirror hypercharge and $\mathbb{Z}_2$ are spontaneously broken.

One may also wonder if a new tuning must be introduced when the mirror color is spontaneously broken. Indeed, the Fraternal Twin Higgs [85] emphasizes the importance of twin color in preventing new large two-loop contributions to the Higgs mass due to the difference in the running of the SM and twin top Yukawa couplings. Because our models begin from an exact mirror symmetric set up, however, the Yukawa couplings are identical at the UV cutoff, significantly reducing the estimated tuning compared to Ref. [85]. Furthermore, the difference in Yukawa running only occurs below the scale of twin color breaking, which can be well below the UV cutoff, further mitigating the tuning, or fully alleviating the tuning. Finally, in every case we examine some fraction of the twin gluons remain massless, causing the twin top Yukawa to run more like its SM counterpart, again reducing the tuning. Therefore, taken together we expect the two-loop contributions to the Higgs mass to be unimportant relative to the leading v/f tuning required by the Twin Higgs, and most pNGB constructions.

4.1 Warmup: Colored Scalar Potential Analysis

To gain some footing, in this subsection we will first analyze the symmetry breaking dynamics of the colored scalar sector in isolation. This will enable us to highlight some of the differences in the symmetry breaking for the triplet, sextet and octet cases in Eq. (35). Following this analysis, we will investigate the full electroweak and color gauge symmetry breaking by studying the full scalar potential including the Higgs fields and their interactions.

Throughout we use the standard definitions for the $SU(3)$ generators, $T^a = \frac{1}{2}\lambda^a$ with λ^a the Gell-Mann matrices and $a = 1, 2, \ldots 8$. The $SU(3)$ structure constants are given by

$$f^{123} = 1, \qquad f^{147} = -f^{156} = f^{246} = f^{257} = f^{345} = -f^{367} = \frac{1}{2}, \qquad f^{458} = f^{678} = \frac{\sqrt{3}}{2}. \quad (36)$$

4.1.1 Color Triplet Scalar

The first example we consider involves a color triplet scalar. We extend the Mirror Twin Higgs model with scalar $\Phi_A \sim (\mathbf{3}, \mathbf{1}, Y_\Phi)$ in the visible sector along with its $\mathbb{Z}_2$ counterpart Φ_B in the mirror sector. These scalars can be represented as a complex vector, i.e, $(\Phi_A)_i$, with color index $i = 1, 2, 3$ and similarly for Φ_B. The $\mathbb{Z}_2$ symmetric scalar potential for Φ_A and Φ_B is:

$$V_\Phi = -\mu^2 \left(|\Phi_A|^2 + |\Phi_B|^2\right) + \lambda \left(|\Phi_A|^2 + |\Phi_B|^2\right)^2 + \delta \left(|\Phi_A|^4 + |\Phi_B|^4\right). \tag{37}$$

The terms involving μ^2 and λ respect a large $U(6)$ global symmetry while the δ term preserves a smaller $U(3)_A \times U(3)_B \times \mathbb{Z}_2$ symmetry. Note that δ is radiatively generated by the $SU(3)_c$ interactions with characteristic size $\delta \sim \alpha_s^2 \sim 10^{-2}$. We are often interested in the parameter regime $\delta \ll \lambda$. In this case, a vacuum that spontaneously breaks $\mathbb{Z}_2$ is obtained for $\delta < 0$ [59]. The desired vacuum is given by

$$\langle \Phi_{Ai} \rangle = 0, \qquad \langle \Phi_B \rangle = \begin{pmatrix} 0 \\ 0 \\ f_\Phi \end{pmatrix}, \qquad f_\Phi = \frac{\mu}{\sqrt{2(\lambda + \delta)}}. \tag{38}$$

We parameterize the fluctuations around the vacuum as

$$\Phi_A = \phi_A, \qquad \Phi_B = \begin{pmatrix} \eta_B^{(2)} \\ f_\Phi + \frac{1}{\sqrt{2}}(\varphi_B + i\eta_B) \end{pmatrix}. \tag{39}$$

with ϕ_A being a triplet under $[SU(3)_c]_A$, $\eta_B^{(2)}$ a doublet under $[SU(2)_c]_B$, and φ_B and η_B being singlets. Expanding the potential Eq. (37) about the minimum, the scalar masses are found to be

$$m_{\phi_A}^2 = -2\delta f_\Phi^2, \qquad m_{\varphi_B}^2 = 4(\lambda + \delta) f_\Phi^2, \qquad m_{\eta_B^{(2)}}^2 = 0, \qquad m_{\eta_B}^2 = 0. \tag{40}$$

In the limit $|\delta| \ll \lambda$ the global symmetry breaking pattern is $U(6) \to U(5)$, yielding 11 Nambu-Goldstone bosons (complex $[SU(3)_c]_A$ triplet ϕ_A, complex $[SU(2)_c]_B$ doublet $\eta_B^{(2)}$, and real singlet η_B). The field ϕ_A obtains a mass proportional to the $U(6)$ breaking coupling δ and can be considered to be a pNGB in this limit. The fields $\eta_B^{(2)}$, η_B are exact NGBs and

are eaten by the five massive twin gluons, which obtain masses of order $m_{G_B} \sim g_S f_\Phi$. Since the triplet scalar is also assumed to carry hypercharge Y_Φ, it will also contribute a mass term to the twin hypercharge boson. We will examine this shortly when we include the Higgs fields in the scalar potential. Finally, there is a massive radial mode φ_B with mass of order $\sqrt{\lambda} f_\Phi$.

4.1.2 Color Sextet Scalar

We next consider the case of color sextet scalars, with $\Phi_A \sim (\mathbf{6}, \mathbf{1}, Y_\Phi)$ in the visible sector and its $\mathbb{Z}_2$ partner Φ_B in the mirror sector. These scalars can be represented as complex symmetric tensor fields, i.e, $(\Phi_A)_{ij}$, with $i, j = 1, 2, 3$ and similarly for Φ_B. We start by considering first the colored scalar sector in isolation, writing the most general $\mathbb{Z}_2$ symmetric potential as

$$\begin{aligned} V_\Phi = &-\mu^2 \left(\mathrm{Tr}\, \Phi_A^\dagger \Phi_A + \mathrm{Tr}\, \Phi_B^\dagger \Phi_B \right) + \lambda \left(\mathrm{Tr}\, \Phi_A^\dagger \Phi_A + \mathrm{Tr}\, \Phi_B^\dagger \Phi_B \right)^2 \\ &+ \delta_1 \left[(\mathrm{Tr}\, \Phi_A^\dagger \Phi_A)^2 + (\mathrm{Tr}\, \Phi_B^\dagger \Phi_B)^2 \right] + \delta_2 \left[(\mathrm{Tr}\, \Phi_A^\dagger \Phi_A \Phi_A^\dagger \Phi_A) + (\mathrm{Tr}\, \Phi_B^\dagger \Phi_B \Phi_B^\dagger \Phi_B) \right], \end{aligned} \tag{41}$$

The terms in the first line of Eq. (41) above respect a larger $U(12)$ global symmetry. The terms in the second line explicitly break $U(12)$, with δ_1 preserving $U(6)_A \times U(6)_B \times \mathbb{Z}_2$ and δ_2 preserving $U(3)_A \times U(3)_B \times \mathbb{Z}_2$. We will focus on the regime $\delta_{1,2} \ll \lambda$. The vacuum structure can be analyzed following the techniques of Ref. [118], and is governed by the values δ_1 and δ_2. There are two spontaneous $\mathbb{Z}_2$ breaking vacuua of interest, which we now discuss.

The first relevant vacuum for the sextet leads to the gauge symmetry breaking pattern $[SU(3)_c \to SU(2)_c]_B$. The orientation of this vacuum is

$$\langle \Phi_{A\,ij} \rangle = 0, \qquad \langle \Phi_B \rangle = f_\Phi \begin{pmatrix} 0 & 0 & 0 \\ 0 & 0 & 0 \\ 0 & 0 & 1 \end{pmatrix}, \qquad f_\Phi = \frac{\mu}{\sqrt{2(\lambda + \delta_1 + \delta_2)}}. \tag{42}$$

Assuming $|\delta_{1,2}| \ll \lambda$, this vacuum is a global minimum for the parameter regions $\delta_2 < 0$ and $\delta_1 < -\delta_2$. The fluctuations around the vacuum can be parameterized as

$$\Phi_A = \phi_A, \qquad \Phi_B = \left(\begin{array}{c|c} -i\sigma^2 \phi_B & \frac{1}{\sqrt{2}} \eta_B^{(2)} \\ \hline \frac{1}{\sqrt{2}} \eta_B^{(2)\,T} & f_\Phi + \frac{1}{\sqrt{2}} (\varphi_B + i \eta_B) \end{array} \right), \tag{43}$$

with ϕ_A being a sextet under $[SU(3)_c]_A$, $\phi_B = \phi_B^\alpha \tau^\alpha$ a complex triplet under $[SU(2)_c]_B$, $\eta_B^{(2)}$ a doublet under $[SU(2)_c]_B$, and φ_B and η_B singlets. Inserting (43) into the potential (41), the masses of the scalar fluctuations are found to be

$$m^2_{\phi_A} = -2(\delta_1+\delta_2)f_\Phi^2, \qquad m^2_{\varphi_B} = 4(\lambda+\delta_1+\delta_2)f_\Phi^2,$$
$$m^2_{\phi_B} = -2\,\delta_2\, f_\Phi^2, \qquad m^2_{\eta_B^{(2)}} = 0, \qquad m^2_{\eta_B} = 0. \tag{44}$$

In the small δ_1, δ_2 regime the symmetry breaking pattern is $U(12) \to U(11)$, supplying 23 Nambu-Goldstone bosons (complex $[SU(3)_c]_A$ sextet ϕ_A, complex $[SU(2)_c]_B$ triplet ϕ_B, $[SU(2)_c]_B$ doublet $\eta_B^{(2)}$, and real singlet η_B). The field ϕ_A is a pNGB and obtains a mass proportional to the $U(12)$ breaking couplings δ_1, δ_2. Furthermore, since δ_1 respects a $U(6)_B$ symmetry, which is spontaneously broken to $U(5)_B$, it does not generate a contribution to the ϕ_B mass. However, the coupling δ_2 explicitly breaks $U(6)_B$ to $U(3)_B$, and therefore generates a mass for ϕ_B, which is therefore also a pNGB. The fields $\eta_B^{(2)}$ and η_B are exact NGBs, and are eaten to generate mass terms for the heavy gluons. There is also the massive radial model φ_B with its mass proportional to $\sqrt{\lambda} f_\Phi$.

The second vacuum for the sextet is described by the gauge symmetry breaking pattern $[SU(3)_c \to SO(3)_c]_B$. The orientation of this vacuum is

$$\langle \Phi_A \rangle = 0, \qquad \langle \Phi_B \rangle = \frac{f_\Phi}{\sqrt{3}} \begin{pmatrix} 1 & 0 & 0 \\ 0 & 1 & 0 \\ 0 & 0 & 1 \end{pmatrix}, \qquad f_\Phi = \frac{\mu}{\sqrt{2(\lambda+\delta_1+\delta_2/3)}}. \tag{45}$$

Assuming $|\delta_{1,2}| \ll \lambda$, this vacuum is a global minimum for the parameter regions $\delta_2 > 0$ and $\delta_1 < -\delta_2/3$. The fluctuations around the vacuum can be parameterized as

$$\Phi_A = \phi_A, \qquad \Phi_B = \frac{1}{\sqrt{3}}\left[f_\Phi + \frac{1}{\sqrt{2}}(\varphi_B + i\eta_B)\right] \times \begin{pmatrix} 1 & 0 & 0 \\ 0 & 1 & 0 \\ 0 & 0 & 1 \end{pmatrix} + \phi_B + i\eta_B^{(5)}, \tag{46}$$

where we have defined the real $[SO(3)_c]_B$ quintuplets $\phi_B = \phi_B^{\bar{a}} T^{\bar{a}}$ and $\eta_B^{(5)} = \eta_B^{\bar{a}} T^{\bar{a}}$, with barred index referring to the broken $SU(3)$ generators, $\bar{a} = 1, 3, 4, 6, 8$. Inserting (46) into the potential (41), the masses of the scalar fluctuations are found to be

$$m_{\phi_A}^2 = -2\left(\delta_1 + \frac{\delta_2}{3}\right) f_\Phi^2, \qquad m_{\varphi_B}^2 = 4\left(\lambda + \delta_1 + \frac{\delta_2}{3}\right) f_\Phi^2,$$
$$m_{\phi_B}^2 = \frac{4}{3}\delta_2 f_\Phi^2, \qquad m_{\eta_B^{(5)}}^2 = 0, \qquad m_{\eta_B}^2 = 0. \tag{47}$$

In the limit $|\delta_{1,2}| \ll \lambda$ the symmetry breaking pattern is again $U(12) \to U(11)$, yielding 23 Nambu-Goldstone bosons (complex $[SU(3)_c]_A$ sextet ϕ_A, two real $[SO(3)_c]_B$ quintuplets ϕ_B and $\eta_B^{(5)}$, and real singlet η_B). The field ϕ_A obtains a mass proportional to the $U(12)$ breaking couplings δ_1, δ_2, and is thus a pNGB. For the δ_1 term, since it respects a $U(6)_B$ symmetry, which is spontaneously broken to $U(5)_B$, it does not generate a contribution to the ϕ_B mass. However, the coupling δ_2 explicitly breaks $U(6)_B$ to $U(3)_B$, and therefore generates a mass for ϕ_B, which is therefore also a pNGB. The fields $\eta_B^{(5)}$ and η_B are exact NGBs at this level, are eaten by the 5 heavy gluons and the hypercharge gauge boson. Finally, there is the massive radial mode φ_B with its mass proportional to $\sqrt{\lambda} f_\Phi$.

4.1.3 Color Octet Scalar

The final case we will consider is a real octet scalar, $\Phi_A \sim (\mathbf{8}, \mathbf{1}, 0)$ in the visible sector and the analogue field in the twin sector. The octet scalar can be written in matrix notation as $(\Phi_A)_i^j = \Phi_A^a (T^a)_i^j$ and similarly for Φ_B. A $\mathbb{Z}_2$ symmetric potential involving the colored scalars is given by

$$V_\Phi = -\mu^2 \left(\mathrm{Tr}\,\Phi_A^2 + \mathrm{Tr}\,\Phi_B^2\right) + \lambda \left(\mathrm{Tr}\,\Phi_A^2 + \mathrm{Tr}\,\Phi_B^2\right)^2$$
$$+ \delta \left[(\mathrm{Tr}\,\Phi_A^2)^2 + (\mathrm{Tr}\,\Phi_B^2)^2\right] + V_3 + V_6. \tag{48}$$

The terms in the first line of Eq. (48) above respect a larger $O(16)$ global symmetry. The terms in the second line explicitly break $O(16)$, with δ preserving $O(8)_A \times O(8)_B \times \mathbb{Z}_2$. The potential V_3 contains a cubic coupling, $\mathrm{Tr}\,\Phi_A^3 + \mathrm{Tr}\,\Phi_B^3$, which preserves $SU(3)_A \times SU(3)_B \times \mathbb{Z}_2$. Additionally, we have included a term V_6 containing dimension six operators, which will be discussed below.

Again following the methods of Ref. [118], we can work out the vacuum structure of the theory. We first consider the case with V_3 and V_6 set to zero. The cubic coupling in V_3 can be forbidden by a parity symmetry, $\Phi_{A,B} \to -\Phi_{A,B}$, while the high dimensional terms in V_6 are generally expected to be subleading. For $\delta < 0$ the vacuum spontaneously breaks the $\mathbb{Z}_2$ symmetry, and can be parameterized as

$$\langle \Phi_A \rangle = 0, \qquad \langle \Phi_B \rangle = \sqrt{2}\, f_\Phi \,(\sin\beta\, T^3 + \cos\beta\, T^8), \qquad f_\Phi = \frac{\mu}{\sqrt{2\,(\lambda+\delta)}}. \tag{49}$$

The vacuum angle β does not appear in the potential at this level, and thus corresponds to a flat direction. We now examine several possible dynamical effects which explicitly break the large $O(8)_A \times O(8)_B$ symmetry, lifting the flat direction and generating a unique ground state. These include tree level contributions to V_3 and V_6 as well as radiative contributions to the potential.

a. Cubic term

Let us first consider the effect of the cubic coupling,

$$V_3 = A\,(\mathrm{Tr}\,\Phi_A^3 + \mathrm{Tr}\,\Phi_B^3). \tag{50}$$

The coupling A is taken to be real and positive without loss of generality, and we consider the regime $A/\mu \ll 1$. For $\delta < 0$ the vacuum spontaneously breaks the $\mathbb{Z}_2$ symmetry and is described by the configuration

$$\langle \Phi_A \rangle = 0, \qquad \langle \Phi_B \rangle = \sqrt{2}\, f_\Phi \; T^8, \qquad f_\Phi \simeq \frac{\mu}{\sqrt{2(\lambda+\delta)}} + \frac{\sqrt{3}A}{8\sqrt{2}(\lambda+\delta)}. \tag{51}$$

The twin color gauge symmetry is broken from $[SU(3)_c]_B$ down to $[SU(2)_c \times U(1)_c]_B$. The scalar fluctuations are parameterized as

$$\Phi_A = \phi_A, \qquad \Phi_B = (\sqrt{2}\, f_\Phi + \varphi_B)\, T^8 + \left(\begin{array}{c|c} \phi_B & \frac{1}{\sqrt{2}}\eta_B^{(2)} \\ \hline \frac{1}{\sqrt{2}}\eta_B^{(2)\,\dagger} & 0 \end{array}\right), \tag{52}$$

where ϕ_A is a real octet under $[SU(3)_c]_A$, $\phi_B = \phi_B^\alpha \tau^\alpha$ is a real $[SU(2)_c]_B$ triplet, $\eta_B^{(2)}$ is a $[SU(2)_c]_B$ doublet, and φ_B is a singlet. Inserting (52) into the potential (48) and expanding about the vacuum, the scalar masses are found to be

$$m_{\phi_A}^2 = \left(-2\,\delta + \sqrt{\frac{3}{8}}\frac{A}{f_\Phi}\right) f_\Phi^2, \qquad m_{\phi_B}^2 = \sqrt{\frac{27}{8}}\,A\,f_\Phi, \tag{53}$$

$$m_{\eta_B^{(2)}}^2 = 0, \qquad m_{\varphi_B}^2 = \left(4\lambda + 4\delta - \sqrt{\frac{3}{8}}\frac{A}{f_\Phi}\right) f_\Phi^2.$$

In the small $\delta, A/\mu$ regime the symmetry breaking pattern is $O(16) \to O(15)$, generating 15 Nambu-Goldstone bosons (real $[SU(3)_c]_A$ octet ϕ_A, real $[SU(2)_c]_B$ triplet ϕ_B, and $[SU(2)_c]_B$ doublet $\eta_B^{(2)}$). The field ϕ_A is a pNGB and obtains a mass proportional to the $O(16)$ breaking couplings δ and A. Furthermore, since δ respects a $O(8)_B$ symmetry, which is spontaneously broken to $O(7)_B$, it does not generate a contribution to the ϕ_B mass. However, the coupling A explicitly breaks $O(8)_B$ to $SU(3)_B$, and therefore generates a mass for ϕ_B, which is therefore also a pNGB. The field $\eta_B^{(2)}$ is an exact NGB, and is eaten to generate mass terms for four heavy gluons. Finally, φ_B is the massive radial mode with its mass proportional to $\sqrt{\lambda} f_\Phi$.

b. Higher dimension operators

We have seen above that a cubic term in the potential aligns the vacuum in the direction of T^8. Noting Eq. (49) it is interesting to ask if the vacuum can be aligned in the direction of T^3. To this end, we will consider the possible effects of a dimension six operator, which is generally expected to appear given that the Twin Higgs model should have a relatively low UV cutoff. We impose the parity symmetry $\Phi_{A,B} \to -\Phi_{A,B}$, which forbids the cubic term. We consider a simple representative dimension six operator,

$$V_6 = \frac{c}{\Lambda^2}\left(\mathrm{Tr}\,\Phi_A^6 + \mathrm{Tr}\,\Phi_B^6\right), \tag{54}$$

where Λ is the UV cutoff and c is the Wilson coefficient. We will work in the regime $c\mu^2/\Lambda^2 \ll 1$. For $\delta < 0$ and $c > 0$ we find the following $\mathbb{Z}_2$ breaking vacuum orientation:

$$\langle \Phi_A \rangle = 0, \qquad \langle \Phi_B \rangle = \sqrt{2}\,f_\Phi\; T^3, \qquad f_\Phi^2 \simeq \frac{\mu^2}{2(\lambda+\delta)} - \frac{3\,c\,\mu^4}{32\,(\lambda+\delta)^3\,\Lambda^2}. \tag{55}$$

The twin color gauge symmetry is broken from $[SU(3)_c]_B$ down to $[U(1)_c \times U(1)'_c]_B$. The scalar fluctuations are parameterized as

$$\Phi_A = \phi_A, \qquad \Phi_B = (\sqrt{2}\, f_\Phi + \varphi_B)\, T^3 + \phi_B\, T^8 + \begin{pmatrix} 0 & \frac{1}{\sqrt{2}}\eta_B & \frac{1}{\sqrt{2}}\eta'_B \\ \frac{1}{\sqrt{2}}\eta^*_B & 0 & \frac{1}{\sqrt{2}}\eta''_B \\ \frac{1}{\sqrt{2}}\eta'^*_B & \frac{1}{\sqrt{2}}\eta''^*_B & 0 \end{pmatrix}, \tag{56}$$

Inserting (56) into the potential 48 and 54, and expanding about the vacuum, the scalar masses are found to be

$$\begin{aligned} m^2_{\phi_A} &= -\left(2\,\delta + \frac{3}{4}\frac{c f^2_\Phi}{\Lambda^2}\right) f^2_\Phi, \qquad m^2_{\phi_B} = \frac{c f^4_\Phi}{2\Lambda^2}, \\ m^2_{\eta_B} = m^2_{\eta'_B} &= m^2_{\eta''_B} = 0, \qquad m^2_{\varphi_B} = \left(4\,\lambda + 4\,\delta + \frac{3\,c\, f^2_\Phi}{\Lambda^2}\right) f^2_\Phi. \end{aligned} \tag{57}$$

In the small $\delta, c\mu^2/\Lambda^2$ limit the symmetry breaking pattern is $O(16) \to O(15)$, supplying 15 Nambu-Goldstone bosons (real $[SU(3)_c]_A$ octet, a real scalar ϕ_B, three complex scalars $\eta_B, \eta'_B, \eta''_B$). The field ϕ_A is a pNGB and obtains a mass proportional to the $O(16)$ breaking couplings δ and c. Furthermore, since δ respects a $O(8)_B$ symmetry, which is spontaneously broken to $O(7)_B$, it does not generate a contribution to the ϕ_B mass. However, the coupling c explicitly breaks $O(8)_B$ to $SU(3)_B$, and therefore generates a mass for ϕ_B, which is therefore also a pNGB with mass proportional to c. The three complex scalars $\eta_B, \eta'_B, \eta''_B$ are true NGBs, and are eaten by six heavy gluons. Finally, φ_B is the massive radial mode with mass proportional to $\sqrt{\lambda} f_\Phi$.

c. Radiative scalar potential

The final dynamical effect we must consider is the radiative contribution to the scalar potential. Even if the cubic term is not there and dimension six operators are negligible, the $SU(3)_c$ gauge interactions explicitly break the large $O(8)_A \times O(8)_B$ symmetry present in the first line and first two terms in the second line of the tree-level potential (48), leading to a radiatively generated potential for the vacuum angle β in Eq. (49). This can be conveniently studied by computing the one-loop effective potential in $\overline{\rm MS}$ scheme:

$$V_{\Phi,1-\rm loop} = \frac{3 g^4_S f^4_\Phi}{8\pi^2} \sum_{n=0}^{2} \left\{ \sin^4(\beta - n\pi/3) \log\left[\frac{2 g^2_S f^2_\Phi \sin^2(\beta - n\pi/3)}{\hat{\mu}^2}\right] - \frac{5}{6}\right\}. \tag{58}$$

The potential has minima at $\beta = n\pi/3$, which, noting Eq. (49), each lead to the gauge symmetry breaking pattern $[SU(3)_c \to SU(2)_c \times U(1)_c]_B$. Each is simply an $SU(3)_c$ transformation from T^8. Therefore, without loss of generality we consider the vacuum orientation as given by Eq. (49) with $\beta = 0$, i.e.,

$$\langle \Phi_B \rangle = \sqrt{2}\, f_\Phi\, T^8. \tag{59}$$

So, the analysis mimics that of the cubic term, but with the pNGBs mass of order $\alpha_s f_\Phi$.

4.2 Full Scalar Potential and Nonlinear Realization

The analysis carried out above can now be straightforwardly adapted to the realistic case involving both the Higgs and the colored scalar fields in the potential. It will be convenient to use a nonlinear parameterization of the scalar fields, working in unitary gauge and including only the light pNGB degrees of freedom. This will allow for a simple and clear description of the low energy dynamics. Since the technical details of the analyses are similar to each other and to analysis of the hypercharge scalar in Ref. [82], we have chosen to discuss the case of the triplet scalar in detail. Following this, we will provide the results and highlight the differences for the cases of the sextet and octet models.

4.2.1 Color Triplet Scalar

Let us then focus on the case of the triplet scalar (see Section 4.1.1 above), now including the Higgs fields in the description. The $\mathbb{Z}_2$ symmetric scalar potential is given by

$$\begin{aligned} V = &-M_H^2 |H|^2 + \lambda_H |H|^4 - M_\Phi^2 |\Phi|^2 + \lambda_\Phi |\Phi|^4 + \lambda_{H\Phi} |H|^2 |\Phi|^2 \\ &+ \delta_H \left(|H_A|^4 + |H_B|^4 \right) + \delta_\Phi \left(|\Phi_A|^4 + |\Phi_B|^4 \right) + \delta_{H\Phi} \left(|H_A|^2 - |H_B|^2 \right) \left(|\Phi_A|^2 - |\Phi_B|^2 \right), \end{aligned} \tag{60}$$

where we have defined $|H|^2 = H_A^\dagger H_A + H_B^\dagger H_B$ and $|\Phi|^2 = \Phi_A^\dagger \Phi_A + \Phi_B^\dagger \Phi_B$. The terms in the first line of Eq. (60) respect a large $U(4) \times U(6)$ global symmetry, while those in the second line explicitly break this symmetry. We will demand that the symmetry breaking quartic

interactions δ_H and $\delta_{H\Phi}$ are small compared to the symmetry preserving quartics λ_H and $\lambda_{H\Phi}$, to ensure the twin protection mechanism for the light Higgs boson. Though not strictly required, if δ_Φ is small compared to λ_Φ, the radial mode would decouple and the color triplet scalar in the visible sector can naturally be lighter than f_Φ.

In the absence of the colored scalar fields, the choice $\delta_H > 0$ would lead to a vacuum with equal VEVs for H_A and H_B, which is experimentally excluded as it implies order one modifications for the light Higgs boson couplings to SM fields. Including the colored scalar fields helps, we learn from Section 4.1.1 that for negative value of δ_Φ the scalar Φ_B obtains a VEV while Φ_A does not, leading to the spontaneous breaking of the $\mathbb{Z}_2$ symmetry. Crucially, the $\delta_{H\Phi}$ term then generates an effective $\mathbb{Z}_2$ breaking mass term for the Higgs scalars. This allows us to obtain the desired vacuum misalignment, with $\langle H_A \rangle \ll \langle H_B \rangle$.

The nonlinear parameterization for the Higgs fields was given in Eq. 27, while for the colored scalars we have

$$\Phi_A = \phi_A \frac{\sin\left(\sqrt{|\phi_A|^2}/f_\Phi\right)}{\sqrt{|\phi_A|^2}/f_\Phi}, \qquad \Phi_B = \begin{pmatrix} 0 \\ 0 \\ f_\Phi \cos\left(\sqrt{|\phi_A|^2}/f_\Phi\right) \end{pmatrix}. \tag{61}$$

Here ϕ_A is a triplet of $[SU(3)_c]_A$ and can be represented as a complex vector, $(\phi_A)_i$ with $i = 1, 2, 3$.

Inserting the nonlinear fields in Eq. (27) and Eq. (61) into the scalar potential, Eq. (60), and neglecting the constant terms, we find the scalar potential for the pNGB fields:

$$\begin{aligned} V = &-\frac{\delta_H f_H^4}{2} \sin^2\left[\frac{\sqrt{2}(v_H+h)}{f_H}\right] - \frac{\delta_\Phi f_\Phi^4}{2} \sin^2\left[\frac{2\sqrt{|\phi_A|^2}}{f_\Phi}\right] \\ &+ \delta_{H\Phi} f_H^2 f_\Phi^2 \cos\left[\frac{\sqrt{2}(v_H+h)}{f_H}\right] \cos\left[\frac{2\sqrt{|\phi_A|^2}}{f_\Phi}\right]. \end{aligned} \tag{62}$$

The potential (62) has a minimum with $\langle \phi_A \rangle = 0$, $v_H \neq 0$ which obeys the relation

$$f_\Phi^2\, \delta_{H\Phi} + f_H^2\, \delta_H \cos(2\vartheta) = 0, \tag{63}$$

where we have used the vacuum angle $\vartheta = v_H/(\sqrt{2} f_H)$. Expanding the potential about the minimum and using Eq. (63), we obtain the masses of the physical scalar fields h and ϕ_A:

$$m_h^2 = 2\, f_H^2\, \delta_H\, \sin^2(2\vartheta), \tag{64}$$

$$m_{\phi_A}^2 = 2\left(-\delta_\Phi + \frac{\delta_{H\Phi}^2}{\delta_H}\right) f_\Phi^2. \tag{65}$$

To ensure the Higgs mass in Eq. 64 is positive we must require $\delta_H > 0$, and combining this requirement with the vacuum relation (63) leads to the condition $\delta_{H\Phi} < 0$. We must also demand that $m_{\phi_A}^2 > 0$ in Eq. (65), which restricts the allowed values of δ_Φ once δ_H, $\delta_{H\Phi}$ are specified.

To make contact with the standard definition of the weak gauge boson masses, we defined the electroweak VEV and its twin counterpart as in Eq. 28. Using Eqs. (63,64,65,28) we can trade the parameters $f_H, \delta_H, \delta_\Phi, \delta_{H\Phi}$ for v_A, ϑ, m_h, m_{ϕ_A}. In particular, the quartic couplings may be written as

$$\begin{aligned}
\delta_H &= \frac{m_h^2}{4\, v_A^2 \cos^2\vartheta}, \\
\delta_{H\Phi} &= -\frac{m_h^2}{f_\Phi^2}\, \frac{\cos(2\vartheta)}{2\sin^2(2\vartheta)}, \\
\delta_\Phi &= -\frac{m_{\phi_A}^2}{2 f_\Phi^2} + \frac{v_A^2\, m_h^2}{f_\Phi^4}\, \frac{\cos^2\vartheta \cos^2 2\vartheta}{\sin^4 2\vartheta}.
\end{aligned} \tag{66}$$

Fixing the vacuum angle to be $\sin\vartheta \lesssim 1/3$ as suggested by Higgs coupling, decay, and precision electroweak measurements, and naturalness considerations, the free parameters of the model can then be chosen as m_{ϕ_A} and f_Φ. It can be estimated that the natural values of these parameters lie in the range of 100 GeV - 10 TeV. This follows from imposing certain restrictions on the symmetry breaking quartics, δ_Φ and $\delta_{H\Phi}$, which are related to m_{ϕ_A} and f_Φ via Eq. (66). Since the gauge and Yukawa interactions break the large $U(4)\times U(6)$ symmetry, these couplings will be generated radiatively and cannot be taken too small without fine tuning. The quartic δ_Φ is generated by the strong interactions at one loop, implying it should have magnitude larger than roughly $\alpha_s^2 \sim 10^{-2}$. On the other hand, the quartic $\delta_{H\Phi}$ will be generated at one loop by hypercharge interactions, or at two loops due to top

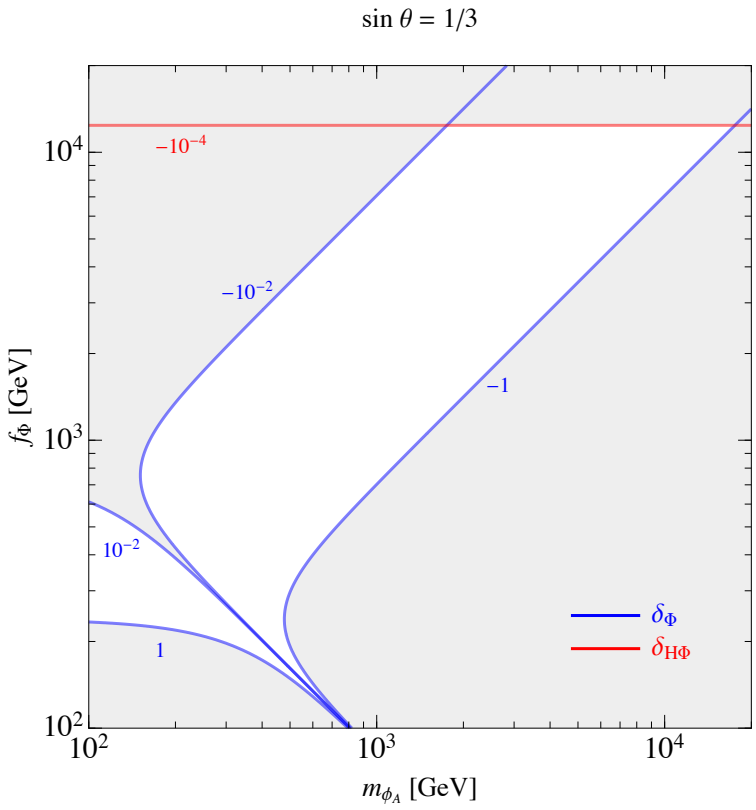

Figure 9: Natural region of parameter space (white region) in the $m_{\phi_A} - f_\Phi$ plane. We have imposed $10^{-2} < |\delta_\Phi| < 1$ (blue contour) and $10^{-4} < |\delta_{H\Phi|} < 1$ (red contour).

quark Yukawa and strong interactions, and suggesting it should be larger in magnitude than about 10^{-4}. We also take these couplings to be smaller than the $U(4) \times U(6)$ preserving quartics and thus require $|\delta_{\Phi,H\Phi}| \lesssim 1$ for strongly coupled UV completions. Collectively, these conditions suggest the range 100 GeV - 10 TeV for the parameter m_{ϕ_A} and f_Φ. Direct constraints from the LHC will also generally lead to stronger bounds on m_{ϕ_A} of order 1 TeV, as we will discuss later. We show a sketch of the natural parameter space for the triplet model in Figure. 9.

We will also be interested in the cubic scalar couplings, $V \supset A_{hhh} h^3 + A_{h\phi_A^\dagger \phi_A} h\,|\phi_A|^2$, which we collect here:

$$A_{hhh} = \frac{m_h^2}{v_A} \frac{\cos(2\vartheta)}{2\cos\vartheta}, \qquad A_{h\phi_A^\dagger\phi_A} = -\frac{m_h^2\, v_A}{f_\Phi^2} \frac{\cot(2\vartheta)}{\sin\vartheta}. \tag{67}$$

The latter Higgs scalar coupling leads to modifications of the Higgs couplings to gluons and photons, and are discussed in Sec. 8.

A similar analysis can be carried out for color sextet or octet. One important difference in those models is the presence of additional pNGB scalar degrees of freedom ϕ_B in the twin sector, as was already apparent in Secs. 4.1.2 and 4.1.3. Otherwise, the analyses of the sextet and octet are very similar to that of the triplet. By a proper normalization, minimizing the potentials of those pNGB fields leads to the same condition defining the vacuum angle as was found for the triplet scalar, Eq. (63), as well as the same expression for the physical Higgs boson mass, Eq. (64). In particular, the trilinear coupling involving the visible sector Higgs boson and colored scalar are always given by Eq. (67).

4.2.2 Color Sextet

We now discuss the nonlinear parameterization for the color sextet models. Including the Higgs fields, the full scalar potential including all terms up to dimension 4 is given by

$$\begin{aligned} V = &-M_H^2\,|H|^2 + \lambda_H\,|H|^4 - M_\Phi^2\,|\Phi|^2 + \lambda_\Phi\,|\Phi|^4 + \lambda_{H\Phi}\,|H|^2\,|\Phi|^2 \\ &+ \delta_H\,\left(|H_A|^4 + |H_B|^4\right) + \delta_{\Phi 1}\left[(\mathrm{Tr}\,\Phi_A^\dagger\Phi_A)^2 + (\mathrm{Tr}\,\Phi_B^\dagger\Phi_B)^2\right] \\ &+ \delta_{\Phi 2}\left(\mathrm{Tr}\,\Phi_A^\dagger\Phi_A\Phi_A^\dagger\Phi_A + \mathrm{Tr}\,\Phi_B^\dagger\Phi_B\Phi_B^\dagger\Phi_B\right) + \delta_{H\Phi}\,\left(|H_A|^2 - |H_B|^2\right)\left(\mathrm{Tr}\,\Phi_A^\dagger\Phi_A - \mathrm{Tr}\,\Phi_B^\dagger\Phi_B\right). \end{aligned} \tag{68}$$

Here we have defined $|H|^2 = H_A^\dagger H_A + H_B^\dagger H_B$ and $|\Phi|^2 = \mathrm{Tr}\,\Phi_A^\dagger \Phi_A + \mathrm{Tr}\,\Phi_B^\dagger \Phi_B$. As shown in Sec. 4.1.2 there are two symmetry breaking patterns to consider:

4.2.2.1 $[SU(3)_c \to SU(2)_c]_B$

We can parameterize the colored scalar fields in unitary gauge as

$$\Phi_A = \phi_A \frac{\sin\left(\hat{\phi}/f_\Phi\right)}{\hat{\phi}/f_\Phi}, \qquad \Phi_B = \left(\begin{array}{c|c} -i\sigma^2\phi_B \dfrac{\sin\left(\hat{\phi}/f_\Phi\right)}{\hat{\phi}/f_\Phi} & 0 \\ \hline 0 & f_\Phi \cos\left(\hat{\phi}/f_\Phi\right) \end{array}\right), \tag{69}$$

where ϕ_A is a complex sextet of $[SU(3)_c]_A$, ϕ_B is a complex triplet under $[SU(2)_c]_B$, and $\hat{\phi}^2 \equiv \mathrm{Tr}\,\phi_A^\dagger \phi_A + \mathrm{Tr}\,\phi_B^\dagger \phi_B$. The sextet is represented as a symmetric tensor, $(\phi_A)_{ij}$ with $i,j = 1,2,3$, and the complex triplet can be represented as $\phi_B = \phi_B^\alpha \tau^\alpha$, with complex components ϕ_B^α, $\alpha = 1,2,3$.

Inserting Eqs. (27) and Eq. (69) into the scalar potential, Eq. (68), and neglecting the constant terms, we obtain the potential for the pNGB fields:

$$\begin{aligned} V = &-\frac{\delta_H f_H^4}{2}\sin^2\left[\frac{\sqrt{2}(v_H+h)}{f_H}\right] \\ &+ \delta_{H\Phi} f_H^2 f_\Phi^2 \cos\left[\frac{\sqrt{2}(v_H+h)}{f_H}\right]\left[\cos^2(\hat{\phi}/f_\Phi) - \frac{\sin^2(\hat{\phi}/f_\Phi)}{\hat{\phi}^2}\left(\mathrm{Tr}\,\phi_A^\dagger\phi_A - \mathrm{Tr}\,\phi_B^\dagger\phi_B\right)\right] \\ &+ \delta_{\Phi 1} f_\Phi^4 \left\{\cos^4(\hat{\phi}/f_\Phi) + \frac{2\cos^2(\hat{\phi}/f_\Phi)\sin^2(\hat{\phi}/f_\Phi)}{\hat{\phi}^2}\mathrm{Tr}\,\phi_B^\dagger\phi_B + \frac{\sin^4(\hat{\phi}/f_\Phi)}{\hat{\phi}^4}\left[(\mathrm{Tr}\,\phi_A^\dagger\phi_A)^2 + (\mathrm{Tr}\,\phi_B^\dagger\phi_B)^2\right]\right\} \\ &+ \delta_{\Phi 2} f_\Phi^4 \left\{\cos^4(\hat{\phi}/f_\Phi) + \frac{\sin^4(\hat{\phi}/f_\Phi)}{\hat{\phi}^4}\left[\mathrm{Tr}\,\phi_A^\dagger\phi_A\phi_A^\dagger\phi_A + \mathrm{Tr}\,\phi_B^\dagger\phi_B\phi_B^\dagger\phi_B\right]\right\}. \end{aligned} \tag{70}$$

As mentioned, we found the same condition for the vacuum angle as Eq. (63), and the same physical Higgs boson mass, Eq. (64). Furthermore, we find the following expressions for the masses of the physical colored scalar fields:

$$m_{\phi_A}^2 = 2\left(-\delta_{\Phi 1} - \delta_{\Phi 2} + \frac{\delta_{H\Phi}^2}{\delta_H}\right) f_\Phi^2, \tag{71}$$

$$m_{\phi_B}^2 = -2\,\delta_{\Phi 2}\, f_\Phi^2, \tag{72}$$

With the same definition of the electroweak VEV and its twin counterpart Eq. (28), using Eqs. (63, 64, 71, 72, 28) we can trade the parameters $f_H, \delta_H, \delta_{\Phi 1}, \delta_{\Phi 2}, \delta_{H\Phi}$ for v_A, ϑ, m_h, m_{ϕ_A}, and m_{ϕ_B}. In particular, the quartic couplings may be written as

$$\begin{aligned} \delta_{\Phi 1} &= -\frac{m_{\phi_A}^2}{2f_\Phi^2} + \frac{m_{\phi_B}^2}{2f_\Phi^2} + \frac{v_A^2\, m_h^2}{f_\Phi^4}\,\frac{\cos^2\vartheta\cos^2 2\vartheta}{\sin^4 2\vartheta}, \\ \delta_{\Phi 2} &= -\frac{m_{\phi_B}^2}{2f_\Phi^2}, \end{aligned} \tag{73}$$

where δ_H and $\delta_{H\Phi}$ are the same as the triplet case Eq. (66).

The similar expression for the cubic scalar coupling $V \supset A_{hhh}h^3 + A_{h\phi_A^\dagger\phi_A} h\,\mathrm{Tr}\,\phi_A^\dagger\phi_A$, and same coefficients as in Eq. (67), are also obtained.

4.2.2.2 $SU(3) \to SO(3)$

In this case, we can parameterize the fields in unitary gauge as

$$\Phi_A = \phi_A \frac{\sin(\hat{\phi}/f_\Phi)}{\hat{\phi}/f_\Phi}, \qquad \Phi_B = \frac{f_\Phi}{\sqrt{3}}\cos(\hat{\phi}/f_\Phi)\begin{pmatrix} 1 & 0 & 0 \\ 0 & 1 & 0 \\ 0 & 0 & 1 \end{pmatrix} + \phi_B \frac{\sin(\hat{\phi}/f_\Phi)}{\hat{\phi}/f_\Phi}, \tag{74}$$

where ϕ_A is a complex sextet of $[SU(3)_c]_A$ and ϕ_B is a real quintuplet under $[SO(3)_c]_B$ where $\hat{\phi}^2 \equiv \mathrm{Tr}\,\phi_A^\dagger\phi_A + \mathrm{Tr}\,\phi_B^2$. In particular, we represent the sextet as a symmetric tensor, $(\phi_A)_{ij}$ with $i,j = 1,2,3$, and the real quintuplet as $\phi_B = \phi_B^{\bar{a}} T^{\bar{a}}$, with real components $\phi_B^{\bar{a}}$ and index $\bar{a} = 1,3,4,6,8$ running over the broken generators.

Inserting Eqs. (27) and Eq. (74) into the scalar potential, Eq. (68), and neglecting the constant terms, we obtain the potential for the pNGB fields:

$$\begin{aligned} V = &-\frac{\delta_H f_H^4}{2}\sin^2\left[\frac{\sqrt{2}(v_H+h)}{f_H}\right] + \delta_{H\Phi} f_H^2 f_\Phi^2 \cos\left[\frac{\sqrt{2}(v_H+h)}{f_H}\right]\left[\cos^2(\hat{\phi}/f_\Phi) - \frac{\sin^2(\hat{\phi}/f_\Phi)}{\hat{\phi}^2}\left(\mathrm{Tr}\,\phi_A^\dagger\phi_A - \mathrm{Tr}\,\phi_B^2\right)\right] \\ &+ \delta_{\Phi 1} f_\Phi^4 \left\{\cos^4(\hat{\phi}/f_\Phi) + \frac{2\cos^2(\hat{\phi}/f_\Phi)\sin^2(\hat{\phi}/f_\Phi)}{\hat{\phi}^2}\mathrm{Tr}\,\phi_B^2 + \frac{\sin^4(\hat{\phi}/f_\Phi)}{\hat{\phi}^4}\left[(\mathrm{Tr}\,\phi_A^\dagger\phi_A)^2 + (\mathrm{Tr}\,\phi_B^2)^2\right]\right\} \\ &+ \frac{1}{3}\delta_{\Phi 2} f_\Phi^4 \left\{\cos^4(\hat{\phi}/f_\Phi) + \frac{6\cos^2(\hat{\phi}/f_\Phi)\sin^2(\hat{\phi}/f_\Phi)}{\hat{\phi}^2}\mathrm{Tr}\,\phi_B^2\right. \\ &\left. + \frac{4\sqrt{3}\cos(\hat{\phi}/f_\Phi)\sin^3(\hat{\phi}/f_\Phi)}{\hat{\phi}^3}\mathrm{Tr}\,\phi_B^3 + \frac{3\sin^4(\hat{\phi}/f_\Phi)}{\hat{\phi}^4}\left[\mathrm{Tr}\,\phi_A^\dagger\phi_A\phi_A^\dagger\phi_A + \frac{1}{2}(\mathrm{Tr}\,\phi_B^2)^2\right]\right\}. \end{aligned} \tag{75}$$

Minimizing this potential leads to the same vacuum condition Eq. (63) and Higgs mass Eq. (64). Furthermore, we find the following expressions for the masses of the physical colored scalar fields:

$$m_{\phi_A}^2 = 2\left(-\delta_{\Phi 1} - \frac{\delta_{\Phi 2}}{3} + \frac{\delta_{H\Phi}^2}{\delta_H}\right) f_\Phi^2, \tag{76}$$

$$m_{\phi_B}^2 = \frac{4}{3}\,\delta_{\Phi 2}\, f_\Phi^2. \tag{77}$$

Using Eqs. (63,64,76,77,28) we can trade the parameters $f_H, \delta_H, \delta_{\Phi 1}, \delta_{\Phi 2}, \delta_{H\Phi}$ for v_A, ϑ, m_h, m_{ϕ_A}, and m_{ϕ_B}. In particular, the quartic couplings may be written as

$$\begin{aligned} \delta_{\Phi 1} &= -\frac{m_{\phi_A}^2}{2f_\Phi^2} - \frac{m_{\phi_B}^2}{4f_\Phi^2} + \frac{v_A^2\, m_h^2}{f_\Phi^4}\,\frac{\cos^2\vartheta\cos^2 2\vartheta}{\sin^4 2\vartheta}, \\ \delta_{\Phi 2} &= \frac{3m_{\phi_B}^2}{4f_\Phi^2}, \end{aligned} \tag{78}$$

where δ_H and $\delta_{H\Phi}$ are the same as the triplet case Eq. (66).

We again obtain the similar expression with the same coefficients for the cubic scalar coupling $V \supset A_{hhh}h^3 + A_{h\phi_A^\dagger\phi_A} h\,\mathrm{Tr}\,\phi_A^\dagger\phi_A$, as in Eq. (67). For completeness we note that a cubic coupling $\mathrm{Tr}\phi_B^3$ is present in this case.

4.2.3 Color Octet

Including the Higgs fields, we will consider the following $\mathbb{Z}_2$ symmetric scalar potential:

$$\begin{aligned} V = &-M_H^2\,|H|^2 + \lambda_H\,|H|^4 - M_\Phi^2\,|\Phi|^2 + \lambda_\Phi\,|\Phi|^4 + \lambda_{H\Phi}\,|H|^2\,|\Phi|^2 \\ &+ \delta_H\left(|H_A|^4 + |H_B|^4\right) + \delta_\Phi\left[(\mathrm{Tr}\,\Phi_A^2)^2 + (\mathrm{Tr}\,\Phi_B^2)^2\right] \\ &+ \delta_{H\Phi}\left(|H_A|^2 - |H_B|^2\right)\left(\mathrm{Tr}\,\Phi_A^2 - \mathrm{Tr}\,\Phi_B^2\right) + V_3 + V_6. \end{aligned} \tag{79}$$

Here we have defined $|H|^2 = H_A^\dagger H_A + H_B^\dagger H_B$ and $|\Phi|^2 = \mathrm{Tr}\,\Phi_A^2 + \mathrm{Tr}\,\Phi_B^2$. We have included the possibility of a cubic interaction and higher dimension operators,

$$V_3 = A\,(\mathrm{Tr}\,\Phi_A^3 + \mathrm{Tr}\,\Phi_B^3), \tag{80}$$

$$V_6 = \frac{c}{\Lambda^2}\,(\mathrm{Tr}\,\Phi_A^6 + \mathrm{Tr}\,\Phi_B^6). \tag{81}$$

As discussed in Section 4.1.3, the inclusion of such terms leads to a unique ground state in which the residual unbroken twin color gauge symmetry is either $[SU(2)_c \times U(1)_c]_B$ or $[U(1)_c \times U(1)'_c]_B$. We now discuss each case in turn:

4.2.3.1 $[\boldsymbol{SU(3)_c \to SU(2)_c \times U(1)_c}]_{\boldsymbol{B}}$

In this case, the color octet can be parameterized in unitary gauge as

$$\Phi_A = \phi_A \frac{\sin(\hat{\phi}/f_\Phi)}{\hat{\phi}/f_\Phi}, \qquad \Phi_B = \sqrt{2}\, f_\Phi \cos(\hat{\phi}/f_\Phi) T^8 + \left(\begin{array}{c|c} \phi_B \dfrac{\sin(\hat{\phi}/f_\Phi)}{\hat{\phi}/f_\Phi} & 0 \\ \hline 0 & 0 \end{array}\right), \tag{82}$$

where ϕ_A is a real octet of $[SU(3)_c]_A$, ϕ_B is a real triplet under $[SU(2)_c]_B$, and $\hat{\phi}^2 \equiv \mathrm{Tr}\,\phi_A^2 + \mathrm{Tr}\,\phi_B^2$. We represent the octet as $\phi_A = \phi_A^a T^a$ with $a = 1, 2, \ldots 8$ and the triplet as $\phi_B = \phi_B^\alpha \tau^\alpha$ with $\alpha = 1, 2, 3$. All components ϕ_A^a, ϕ_B^b are real scalars.

Inserting Eqs. (27) and (82) into the scalar potential, Eq. (79) including the cubic term V_3 (80), we obtain the potential for the pNGB fields:

$$\begin{aligned} V = &-\frac{\delta_H f_H^4}{2} \sin^2\left[\frac{\sqrt{2}(v_H+h)}{f_H}\right] + \delta_{H\Phi} f_H^2 f_\Phi^2 \cos\left[\frac{\sqrt{2}(v_H+h)}{f_H}\right]\left[\cos^2(\hat{\phi}/f_\Phi) - \frac{\sin^2(\hat{\phi}/f_\Phi)}{\hat{\phi}^2}\left(\mathrm{Tr}\,\phi_A^2 - \mathrm{Tr}\,\phi_B^2\right)\right] \\ &+ \delta_\Phi f_\Phi^4 \left\{\cos^4(\hat{\phi}/f_\Phi) + \frac{2\cos^2(\hat{\phi}/f_\Phi)\sin^2(\hat{\phi}/f_\Phi)}{\hat{\phi}^2}\mathrm{Tr}\,\phi_B^2 + \frac{\sin^4(\hat{\phi}/f_\Phi)}{\hat{\phi}^4}\left[(\mathrm{Tr}\,\phi_A^2)^2 + (\mathrm{Tr}\,\phi_B^2)^2\right]\right\} \\ &+ A f_\Phi^3 \left\{-\frac{\cos^3(\hat{\phi}/f_\Phi)}{\sqrt{6}} + \frac{\sqrt{3}\,\cos(\hat{\phi}/f_\Phi)\sin^2(\hat{\phi}/f_\Phi)}{\sqrt{2}\,\hat{\phi}^2}\mathrm{Tr}\,\phi_B^2 + \frac{\sin^3(\hat{\phi}/f_\Phi)}{\hat{\phi}^3}\mathrm{Tr}\,\phi_A^3\right\}. \end{aligned} \tag{83}$$

The vacuum condition and the Higgs mass are the same as Eq. (63) and Eq. (64). Furthermore, we find the following expressions for the masses of the physical colored scalar fields:

$$m_{\phi_A}^2 = \left(-2\,\delta_\Phi + \sqrt{\frac{3}{8}}\frac{A}{f_\Phi} + \frac{2\,\delta_{H\Phi}^2}{\delta_H}\right) f_\Phi^2, \tag{84}$$

$$m_{\phi_B}^2 = \sqrt{\frac{27}{8}} A\, f_\Phi. \tag{85}$$

Using Eqs. (63,64,84,85,28) we can trade the parameters $f_H, \delta_H, \delta_\Phi, \delta_{H\Phi}$, A for v_A, ϑ, m_h, m_{ϕ_A}, and m_{ϕ_B}. In particular, the quartic couplings may be written as

$$\begin{aligned} \delta_\Phi &= -\frac{m_{\phi_A}^2}{2\,f_\Phi^2} + \frac{m_{\phi_B}^2}{6 f_\Phi^2} + \frac{v_A^2\, m_h^2}{f_\Phi^4}\,\frac{\cos^2\vartheta\cos^2 2\vartheta}{\sin^4 2\vartheta}, \\ A &= \sqrt{\frac{8}{27}}\frac{m_{\phi_B}^2}{f_\Phi}, \end{aligned} \tag{86}$$

where δ_H and $\delta_{H\Phi}$ are the same as the triplet case Eq. (66).

We also obtain the similar expression with the same coefficients for the cubic scalar coupling $V \supset A_{hhh}h^3 + A_{h\phi_A^\dagger\phi_A} h\,\mathrm{Tr}\,\phi_A^\dagger\phi_A$, as in Eq. (67). For completeness we note that a cubic coupling $\mathrm{Tr}\,\phi_A^3$ is present in this case, with coupling constant equal to A.

4.2.3.2 $[SU(3)_c \to U(1)_c \times U(1)'_c]_B$

We can parameterize the fields as

$$\Phi_A = \phi_A \frac{\sin\left(\hat{\phi}/f_\Phi\right)}{\hat{\phi}/f_\Phi}, \qquad \Phi_B = \sqrt{2}\,f_\Phi \cos\left(\hat{\phi}/f_\Phi\right) T^3 + \phi_B \frac{\sin\left(\hat{\phi}/f_\Phi\right)}{\hat{\phi}/f_\Phi}\,T^8, \tag{87}$$

where ϕ_A is a real octet of $[SU(3)_c]_A$, ϕ_B is a real singlet scalar, and $\hat{\phi}^2 \equiv \mathrm{Tr}\,\phi_A^2 + \frac{1}{2}\phi_B^2$.

Inserting Eqs. (27) and (87) into the scalar potential, Eq. (79) including the dimension-six operator V_6 (81), we obtain the potential for the pNGB fields:

$$\begin{aligned} V = &-\frac{\delta_H f_H^4}{2}\sin^2\left[\frac{\sqrt{2}(v_H+h)}{f_H}\right] + \delta_{H\Phi} f_H^2 f_\Phi^2 \cos\left[\frac{\sqrt{2}(v_H+h)}{f_H}\right]\left[\cos^2(\hat{\phi}/f_\Phi) - \frac{\sin^2(\hat{\phi}/f_\Phi)}{\hat{\phi}^2}\left(\mathrm{Tr}\,\phi_A^2 - \frac{1}{2}\phi_B^2\right)\right] \\ &+ \delta_\Phi f_\Phi^4\left\{\cos^4(\hat{\phi}/f_\Phi) + \frac{\cos^2(\hat{\phi}/f_\Phi)\sin^2(\hat{\phi}/f_\Phi)}{\hat{\phi}^2}\phi_B^2 + \frac{\sin^4(\hat{\phi}/f_\Phi)}{\hat{\phi}^4}\left[(\mathrm{Tr}\,\phi_A^2)^2 + \frac{1}{4}\phi_B^4\right]\right\} \\ &+ \frac{c}{\Lambda^2} f_\Phi^6\left\{\frac{1}{4}\cos^6(\hat{\phi}/f_\Phi) + \frac{5\cos^4(\hat{\phi}/f_\Phi)\sin^2(\hat{\phi}/f_\Phi)}{8\,\hat{\phi}^2}\phi_B^2 + \frac{5\cos^2(\hat{\phi}/f_\Phi)\sin^4(\hat{\phi}/f_\Phi)}{48\,\hat{\phi}^4}\phi_B^4\right. \\ &\qquad \left. + \frac{\sin^6(\hat{\phi}/f_\Phi)}{\hat{\phi}^6}\left[\mathrm{Tr}\,\phi_A^6 + \frac{11}{288}\phi_B^6\right]\right\}. \end{aligned} \tag{88}$$

The vacuum condition and the Higgs mass are the same as Eq. (63) and Eq. (64). Furthermore, we find the following expressions for the masses of the physical colored scalar fields:

$$m_{\phi_A}^2 = \left(-2\,\delta_\Phi - \frac{3}{4}\frac{c\,f_\Phi^2}{\Lambda^2} + \frac{2\,\delta_{H\Phi}^2}{\delta_H}\right) f_\Phi^2, \tag{89}$$

$$m_{\phi_B}^2 = \frac{c\,f_\Phi^4}{2\,\Lambda^2}. \tag{90}$$

Using Eqs. (63,64,89,90,28) we can trade the parameters $f_H, \delta_H, \delta_\Phi, \delta_{H\Phi}$, c for v_A, ϑ, m_h, m_{ϕ_A}, and m_{ϕ_B}. In particular, the quartic couplings may be written as

$$\begin{aligned} \delta_\Phi &= -\frac{m_{\phi_A}^2}{2f_\Phi^2} - \frac{3m_{\phi_B}^2}{4f_\Phi^2} + \frac{v_A^2\,m_h^2}{f_\Phi^4}\,\frac{\cos^2\vartheta\cos^2 2\vartheta}{\sin^4 2\vartheta}, \\ \frac{c}{\Lambda^2} &= \frac{2\,m_{\phi_B}^2}{f_\Phi^4}, \end{aligned} \tag{91}$$

where δ_H and $\delta_{H\Phi}$ are the same as the triplet case Eq. (66).

We again obtain the similar expression with the same coefficients for the cubic scalar coupling $V \supset A_{hhh}h^3 + A_{h\phi_A^\dagger\phi_A}h\,\mathrm{Tr}\,\phi_A^\dagger\phi_A$, as in Eq. (67).

In the next chapter, we will sum essential features of those five symmetry breaking patterns in the context of the twin gauge sector.

5.0 Twin Gauge Sector

In this chapter we investigate certain features of the gauge sector, including the gauge boson masses and mixings, their couplings to fermions, the nature of the unbroken non-abelian and $U(1)$ gauge symmetries and confinement in the twin sector.

As seen above, several twin color breaking patterns are possible depending on the representation of the colored scalar and form of the scalar potential. By accounting for both twin color and electroweak symmetry breaking, we found five distinct patterns of gauge symmetry breaking:

$$\begin{aligned}
\mathbf{I}: &\quad (\mathbf{3},\mathbf{1},Y_\Phi) &&[SU(3)_c\times SU(2)_L\times U(1)_Y \to SU(2)_c\times U(1)'_{\rm EM}]_B &(92)\\
\mathbf{II}: &\quad (\mathbf{6},\mathbf{1},Y_\Phi) &&[SU(3)_c\times SU(2)_L\times U(1)_Y \to SU(2)_c\times U(1)'_{\rm EM}]_B &(93)\\
\mathbf{III}: &\quad (\mathbf{6},\mathbf{1},Y_\Phi) &&[SU(3)_c\times SU(2)_L\times U(1)_Y \to SO(3)_c]_B &(94)\\
\mathbf{IV}: &\quad (\mathbf{8},\mathbf{1},0) &&[SU(3)_c\times SU(2)_L\times U(1)_Y \to SU(2)_c\times U(1)_c\times U(1)_{\rm EM}]_B &(95)\\
\mathbf{V}: &\quad (\mathbf{8},\mathbf{1},0) &&[SU(3)_c\times SU(2)_L\times U(1)_Y \to U(1)_c\times U(1)'_c\times U(1)_{\rm EM}]_B &(96)
\end{aligned}$$

Of these, cases **I**–**IV** feature a residual non-Abelian color gauge symmetry and confinement at a low scale. In cases **I**, **II**, and **IV**, this non-Abelian group is $SU(2)_c$, while in case **III** it is $SO(3)_c$. All models except **III**, where the twin photon picks up a mass from the color sextet VEV, have one or more unbroken abelian gauge symmetries. At least one of these $U(1)$s is similar to the usual electromagnetic (EM) gauge symmetry, with the massless gauge boson an admixture of weak, hypercharge, and, in cases **I** and **II**, color gauge bosons. In the color octet models there are also color $U(1)$ gauge symmetries which are remnants of $[SU(3)_c]_B$.

In MTH models with unbroken color gauge symmetry the confinement scale is similar to the ordinary QCD confinement scale, $\Lambda_A \sim 1$ GeV. In models **I**–**IV** confinement naturally occurs at a much lower scale, because the number of massless gluonic degrees of freedom contributing to the running below the TeV scale is much smaller. The one-loop beta function can be written as $d\alpha_s^{-1}/d\ln Q = b/2\pi$, with

$$b = \frac{11}{3}C_{\rm Ad} - \frac{2}{3}\sum_f c_f T_f - \frac{1}{6}\sum_s c_s T_s, \tag{97}$$

where $C_{\rm Ad}$ is the quadratic Casimir for the adjoint representation and T_f (T_s) is the Dynkin index for fermions (scalars) charged under the strong gauge group. The factors $c_f = 1(2)$ for Majorana (Dirac) fermions, and $c_s = 1(2)$ for real (complex) scalars. The fermions in both the SM and twin sectors all have masses below the TeV scale and transform in the fundamental representation of the given gauge group, with index $T_f = \frac{1}{2}$. In estimating the evolution of the strong coupling constant we make the mild assumption that the twin fermions are married (grouped) into Dirac states, similar to SM fermions. In the simplest case the twin fermion masses are given by $m_{f_B} = m_{f_A} \cot\vartheta \approx$ few $\times\, m_{f_A}$. In the visible sector, we have $C_{\rm Ad} = 3$ for $[SU(3)_c]_A$ at all energy scales, while for the twin sector below f_Φ we have $C_{\rm Ad} = 2$ for $[SU(2)_c]_B$ and $C_{\rm Ad} = \frac{1}{2}$ for $[SO(3)_c]_B$. There may be additional colored pNGBs in both sectors with TeV masses; the number and particular index T_s are model dependent.

Before estimating the confinement scale for these models, we note that additional dynamical $\mathbb{Z}_2$ breaking effects, such as new twin fermion mass terms or a shift in the strong gauge coupling at the UV scale, $\alpha_s^B(f_\Phi) = \alpha_s^A(f_\Phi) + \delta\alpha_s$, may raise or lower this scale by several orders of magnitude. Nevertheless, the general expectation is that the twin confinement scale is much lower than that in the visible sector, in contrast to MTH models with unbroken $[SU(3)_c]_B$.

5.1 Gauge Interactions In the Twin Sector

5.1.1 Twin Higgs Sector

We will first note some aspects of electroweak symmetry breaking in the twin Higgs sector, which is independent of the colored scalar sector and common among all models. The dynamics is entirely analogous to those of the visible sector. The twin Higgs H_B obtains a VEV given by

$$\langle H_B \rangle = \begin{pmatrix} 0 \\ \dfrac{v_B}{\sqrt{2}} \end{pmatrix}. \tag{98}$$

Upon symmetry breaking electroweak gauge boson mass terms arise from the twin Higgs kinetic term, $\mathcal{L} \supset |D_\mu H_B|^2$, with covariant derivative $D_\mu H_B = (\partial_\mu - igW^\alpha_{B\mu}\tau^\alpha - ig'\frac{1}{2}B_{B\mu})H_B$. These mass terms can be written as

$$\begin{aligned}\mathcal{L} &\supset \frac{1}{2}\left\{\frac{g^2 v_B^2}{4}\left[(W^1_{B\mu})^2 + (W^2_{B\mu})^2 + (W^3_{B\mu})^2\right] + \frac{g'^2 v_B^2}{4}(B_{B\mu})^2 - \frac{g g' v_B^2}{2} W^3_{B\mu} B^\mu_B\right\}, \\ &= a^2 |W^+_{B\mu}|^2 + \frac{1}{2}\left[a^2 (W^3_{B\mu})^2 + b^2 (B_{B\mu})^2 - 2\,a\,b\,W^3_{B\mu} B^\mu_B\right], \end{aligned} \tag{99}$$

where we have defined for later convenience

$$a \equiv \frac{g\, v_B}{2}, \qquad b \equiv \frac{g' v_B}{2}. \tag{100}$$

We again emphasize that these are simply the twin analogues of the usual electroweak gauge boson mass terms Eq. 6. We have not diagonalized the neutral gauge boson sector at this stage as there can in some models be additional contributions to the mass terms from the colored scalar sector. We now turn our focus to the colored scalar sector.

5.1.2 Color Triplet Scalar: Case I

We consider here the color triplet scalar with quantum numbers $\Phi \sim (\mathbf{3}, \mathbf{1}, Y_\Phi)$. The B sector scalar obtains a VEV,

$$\Phi_B = \begin{pmatrix} 0 \\ 0 \\ f_\Phi \end{pmatrix}, \tag{101}$$

leading to the spontaneous symmetry breaking pattern $[SU(3)_c \to SU(2)_c]_B$. Twin gluon and hypercharge mass terms arise from the kinetic term $\mathcal{L} \supset |D_\mu \Phi_B|^2$, where $D_\mu \Phi_B = (\partial_\mu - ig_s\, G^a_{B\mu} T^a - ig'\, Y_\Phi B_{B\mu})\Phi_B$. These mass terms can be written as

$$\begin{aligned}\mathcal{L} &\supset \frac{1}{2}\Bigg\{\frac{g_s^2 f_\Phi^2}{2}\left[(G^4_{B\mu})^2 + (G^5_{B\mu})^2 + (G^6_{B\mu})^2 + (G^7_{B\mu})^2 + \frac{4}{3}(G^8_{B\mu})^2\right] \\ &\quad + 2g'^2 Y_\Phi^2 f_\Phi^2 (B_{B\mu})^2 - \frac{4 g_s g' Y_\Phi f_\Phi^2}{\sqrt{3}} G^8_{B\mu} B^\mu_B\Bigg\}, \\ &= m_G^2 |G_{B\mu}|^2 + \frac{1}{2}\left[c^2 (B_{B\mu})^2 + d^2 (G^8_{B\mu})^2 - 2\,c\,d\,G^8_{B\mu} B^\mu_B\right]. \end{aligned} \tag{102}$$

Here we have defined the vector doublet $G_{B\mu}$ under the unbroken $[SU(2)_c]_B$ gauge symmetry,

$$G_{B\mu} = \begin{bmatrix} \frac{1}{\sqrt{2}}(G^4_{B\mu} - iG^5_{B\mu}) \\ \frac{1}{\sqrt{2}}(G^6_{B\mu} - iG^7_{B\mu}) \end{bmatrix}, \tag{103}$$

with mass $m_G \equiv g_s f_\Phi/\sqrt{2}$. Furthermore, we have defined

$$c \equiv \sqrt{2}\, g'\, Y_\Phi\, f_\Phi, \qquad d \equiv \sqrt{\frac{2}{3}}\, g_s\, f_\Phi, \tag{104}$$

in Eq. (102).

Noting Eqs. (99,102), the mass mixing in the neutral gauge boson sector between $W^3_{B\mu}$, $B_{B\mu}$, and $G^8_{B\mu}$ can be written as

$$\mathcal{L} \supset \frac{1}{2}\, \hat{X}^T_\mu \mathcal{M}^2_X\, \hat{X}_\mu, \tag{105}$$

where we have defined $\hat{X}^T_\mu = (W^3_{B\mu}, B_{B\mu}, G^8_{B\mu})$ and the neutral gauge boson mass matrix,

$$\mathcal{M}^2_X = \begin{pmatrix} a^2 & -ab & 0 \\ -ab & b^2 + c^2 & -cd \\ 0 & -cd & d^2 \end{pmatrix}, \tag{106}$$

where a, b, c, d are defined in Eqs. (100,104) The system can be diagonalized with three successive rotations, $\hat{X}_\mu = \mathcal{R} X_\mu \equiv \mathcal{R}_1 \mathcal{R}_2 \mathcal{R}_3 X_\mu$, where $X^T_\mu = (Z_{B\mu}, A_{B\mu}, Z'_{B\mu})$ and

$$\mathcal{R}_1 = \begin{pmatrix} c_1 & s_1 & 0 \\ -s_1 & c_1 & 0 \\ 0 & 0 & 1 \end{pmatrix}, \quad \mathcal{R}_2 = \begin{pmatrix} 1 & 0 & 0 \\ 0 & c_2 & s_2 \\ 0 & -s_2 & c_2 \end{pmatrix}, \quad \mathcal{R}_3 = \begin{pmatrix} c_3 & 0 & s_3 \\ 0 & 1 & 0 \\ -s_3 & 0 & c_3 \end{pmatrix}. \tag{107}$$

Here $c_1 \equiv \cos\theta_1$, etc., and the mixing angles satisfy

$$\tan\theta_1 \equiv \tan\theta_W = \frac{b}{a} = \frac{g'}{g}, \qquad \tan\theta_2 = -c_W \frac{c}{d}, \qquad \tan 2\theta_3 = \frac{2\, c\, s_W\, \sqrt{c^2_W\, c^2 + d^2}}{(a^2 + b^2 - c^2 - d^2) + 2\, c^2\, s^2_W}. \tag{108}$$

Here $\theta_1 = \theta_W$ is just the usual weak mixing angle. The mass eigenvalues are given by

$$m^2_{A_B} = 0,\ m^2_{Z_B, Z'_B} = \frac{1}{2}\left\{ a^2 + b^2 + c^2 + d^2 \mp \sqrt{(a^2 + b^2 + c^2 + d^2)^2 - 4(a^2c^2 + a^2d^2 + b^2d^2)} \right\}. \tag{109}$$

We note the presence of a massless twin photon corresponding to an unbroken $[U(1)_{\rm EM}]_B$ gauge symmetry in the twin sector. Assuming $f_\Phi \gg v_B$ (which, for $g_s \gg g, g'$ implies $d \gg a, b, c$), we can obtain approximate expressions for the eigenvalues and rotation matrix. In particular, the heavy Z_B, Z'_B states have masses

$$m^2_{Z_B} \simeq a^2 + b^2 = \frac{1}{4}(g^2 + g'^2)v_B^2, \qquad m^2_{Z'_B} \simeq c^2 + d^2 = \left(2g'^2 Y_\Phi^2 + \frac{2}{3}g_s^2\right) f_\Phi^2. \tag{110}$$

The rotation matrices become

$$\mathcal{R} = \mathcal{R}_1\mathcal{R}_2\mathcal{R}_3 \simeq \begin{pmatrix} c_W & s_W & 0 \\ -s_W & c_W & -\frac{c}{d} \\ -s_W\frac{c}{d} & c_W\frac{c}{d} & 1 \end{pmatrix}. \tag{111}$$

The gauge boson-fermion couplings arise from fermion kinetic terms, $\mathcal{L} \supset i\,\psi_B^\dagger\,\bar\sigma^\mu\,D_\mu\psi_B$, with covariant derivative $D_\mu = \partial_\mu - ig_s G^a_{B\mu}T^a - igW^\alpha_{B\mu}\tau^\alpha - ig'YB_{B\mu}$. After the twin electroweak and color symmetry are broken it is natural to split the colored fermions into those forming doublets and singlets under the unbroken $[SU(2)_c]_B$ gauge symmetry. We will write

$$Q_{Bi} = \begin{pmatrix} \hat Q_{B\,\hat\imath} \\ \hat Q_{B3} \end{pmatrix} = \begin{pmatrix} \hat u_{B\,\hat\imath} & \hat d_{B\,\hat\imath} \\ \hat u_{B3} & \hat d_{B3} \end{pmatrix}, \qquad \bar u_B^i = \begin{pmatrix} \epsilon^{\hat\imath\hat\jmath}\,\hat{\bar u}_{B\,\hat\jmath} \\ \hat{\bar u}_{B\,3} \end{pmatrix}, \qquad \bar d_B^i = \begin{pmatrix} \epsilon^{\hat\imath\hat\jmath}\,\hat{\bar d}_{B\hat\jmath} \\ \hat{\bar d}_{B\,3} \end{pmatrix}, \tag{112}$$

where hatted fields denote states of definite charge under $[SU(2)_c]_B$, and $\hat\imath = 1, 2$. For example, $\hat{\bar d}_{B\,\hat\imath}$ ($\hat{\bar d}_{B\,3}$) is a doublet (singlet) under $[SU(2)_c]_B$. In particular, the fermion couplings to the massless $[SU(2)_c]_B$ gluons can be written as

$$\mathcal{L} \supset g_s\,G^{\hat a}_{B\mu}\,\hat\psi_B^{\dagger\hat\imath}\,\bar\sigma^\mu(\tau^{\hat a})^{\hat\jmath}_{\hat\imath}\,\hat\psi_{B\hat\jmath} \tag{113}$$

where $\hat a = 1, 2, 3$, $\hat\imath = 1, 2$ denote the $[SU(2)_c]_B$ indices. The coupling to the massless twin photon is

$$\mathcal{L} \supset e_B\,A_{B\mu}\,\hat\psi_B^\dagger\,\bar\sigma^\mu\,Q_B^{\rm EM}\,\hat\psi_B, \tag{114}$$

where we have defined the twin electromagnetic coupling,

$$e_B = e_A c_2 = g s_W c_2, \tag{115}$$

with $e_A = g s_W$ is the ordinary A-sector electromagnetic coupling, and the generator of the $[U(1)_{\rm EM}]_B$ symmetry,

$$Q_B^{\rm EM} = \tau^3 + Y + \sqrt{3}\, Y_\Phi\, T^8. \tag{116}$$

The electric charges of the twin leptons are the same as those in the visible sector, while the twin quarks have the following electric charges:

$$\begin{aligned}
Q_B^{\rm EM}\big[\hat{u}_{B\,\hat{i}}\big] = -Q_B^{\rm EM}\big[\hat{\bar{u}}_B^{\,\hat{i}}\big] &= \frac{2}{3} + \frac{Y_\Phi}{2}, \\
Q_B^{\rm EM}\big[\hat{d}_{B\,\hat{i}}\big] = -Q_B^{\rm EM}\big[\hat{\bar{d}}_B^{\,\hat{i}}\big] &= -\frac{1}{3} + \frac{Y_\Phi}{2}, \\
Q_B^{\rm EM}\big[\hat{u}_{B3}\big] = -Q_B^{\rm EM}\big[\hat{\bar{u}}_B^{\,3}\big] &= \frac{2}{3} - Y_\Phi, \\
Q_B^{\rm EM}\big[\hat{d}_{B3}\big] = -Q_B^{\rm EM}\big[\hat{\bar{d}}_B^{\,3}\big] &= -\frac{1}{3} - Y_\Phi.
\end{aligned} \tag{117}$$

We note that the twin electric charges depend on T^8 of the fermion as well as the choice of scalar hypercharge Y_Φ. In Table 3 we indicate the electric charges of the twin quark fields for several choices of Y_Φ. The reason for the specific choices will be given in Chapter 6.

I $(\mathbf{3}, \mathbf{1}, Y_\Phi)$				
$\hat{\psi}$ \ Y_Φ	5/3	2/3	−1/3	−4/3
$Q_B^{\rm EM}[\hat{u}_{B\,\hat{i}}] = -Q_B^{\rm EM}[\hat{\bar{u}}_B^{\,\hat{i}}]$	3/2	1	1/2	0
$Q_B^{\rm EM}[\hat{d}_{B\,\hat{i}}] = -Q_B^{\rm EM}[\hat{\bar{d}}_B^{\,\hat{i}}]$	1/2	0	−1/2	−1
$Q_B^{\rm EM}[\hat{u}_{B3}] = -Q_B^{\rm EM}[\hat{\bar{u}}_B^{\,3}]$	−1	0	1	2
$Q_B^{\rm EM}[\hat{d}_{B3}] = -Q_B^{\rm EM}[\hat{\bar{d}}_B^{\,3}]$	−2	−1	0	1

Table 3: Twin quark electric charges for different choices of the triplet scalar hypercharge Y_Φ in case **I.**

One may have concern that the massless gluons and photon in the B sector might lead to some trouble, for instance additional relativistic degrees of freedom at the time of Big Bang Nucleosynthesis (BBN), or the problem of kinetic mixing between visible and twin photons. To this end, we can break the residual $SU(2)_c \times U(1)'_{\rm EM}$ symmetries completely, by introducing two more copies of scalars.

5.1.3 Color Sextet Scalar

Next, we examine the gauge sector in models with a color sextet scalar with quantum numbers $\Phi \sim (\mathbf{6}, \mathbf{1}, Y_\Phi)$.

5.1.3.1 case II: $[SU(3)_c \to SU(2)_c]_B$

In this case, the B sector colored scalar obtains a VEV with vacuum orientation

$$\langle \Phi_B \rangle = f_\Phi \begin{pmatrix} 0 & 0 & 0 \\ 0 & 0 & 0 \\ 0 & 0 & 1 \end{pmatrix}, \tag{118}$$

leading to the symmetry breakdown $[SU(3)_c \to SU(2)_c]_B$. Twin gluon and hypercharge mass terms arise from the kinetic term $\mathcal{L} \supset \mathrm{Tr}\,[(D^\mu \Phi_B)^\dagger (D_\mu \Phi_B)]$, where $D_\mu \Phi_B = (\partial_\mu \Phi_B - i g_s\, G^a_{B\mu}(T^a \Phi_B + \Phi_B T^{a\,T}) - i g'\, Y_\Phi B_{B\mu} \Phi_B)$. These mass terms can be written as

$$\begin{aligned} \mathcal{L} \supset & \frac{1}{2}\Bigg\{ g_s^2 f_\Phi^2 \left[(G^4_{B\mu})^2 + (G^5_{B\mu})^2 + (G^6_{B\mu})^2 + (G^7_{B\mu})^2 + \frac{8}{3}(G^8_{B\mu})^2 \right] \\ & + 2 g'^2 Y_\Phi^2 f_\Phi^2 (B_{B\mu})^2 - \frac{8 g_s g' Y_\Phi f_\Phi^2}{\sqrt{3}}\, G^8_{B\mu}\, B^\mu_B \Bigg\}, \\ = & \, m_G^2\, |G_{B\mu}|^2 + \frac{1}{2}\left[c^2\, (B_{B\mu})^2 + d^2\, (G^8_{B\mu})^2 - 2\, c\, d\, G^8_{B\mu}\, B^\mu_B \right]. \end{aligned} \tag{119}$$

From here the analysis closely follows the triplet case examined above with only a few modifications. In particular, in Eq. (119) we have introduced the vector doublet $G_{B\mu}$ under the unbroken $[SU(2)_c]_B$ gauge symmetry, as in Eq. (103), with mass $m_G \equiv g_s f_\Phi$. Furthermore, we have defined

$$c \equiv \sqrt{2}\, g'\, Y_\Phi\, f_\Phi, \qquad d \equiv 2\sqrt{\frac{2}{3}}\, g_s\, f_\Phi, \tag{120}$$

in Eq. (119). We note d is twice as big as in the triplet case. With the definitions (100,120), the neutral gauge boson mass matrix takes the same form as Eq. (106) and can be brought to the mass basis through a series of orthogonal transformations as in Eq. (107). In particular, we find a massless twin photon and two heavy neutral gauge bosons Z_B, Z'_B with approximate masses

$$m^2_{Z_B} \simeq a^2 + b^2 = \frac{1}{4}(g^2 + g'^2) v_B^2, \qquad m^2_{Z'_B} \simeq c^2 + d^2 = \left(2 g'^2 Y_\Phi^2 + \frac{8}{3} g_s^2 \right) f_\Phi^2. \tag{121}$$

The fermion couplings to the massless twin gluons and twin photon have the same form as Eqs. (113,114). The generator of the $[U(1)_{\rm EM}]_B$ symmetry,

$$Q_B^{\rm EM} = \tau^3 + Y + \frac{\sqrt{3}}{2}\, Y_\Phi\, T^8. \tag{122}$$

We note the contribution from the color group is half as in the triplet case. The electric charges of the twin leptons are the same as those in the visible sector, while the twin quarks have the following electric charges:

$$\begin{aligned}
Q_B^{\rm EM}\big[\hat{u}_{B\,\hat{i}}\big] = -Q_B^{\rm EM}\big[\hat{\bar{u}}_B^{\,\hat{i}}\big] &= \frac{2}{3} + \frac{Y_\Phi}{4}, \\
Q_B^{\rm EM}\big[\hat{d}_{B\,\hat{i}}\big] = -Q_B^{\rm EM}\big[\hat{\bar{d}}_B^{\,\hat{i}}\big] &= -\frac{1}{3} + \frac{Y_\Phi}{4}, \\
Q_B^{\rm EM}\big[\hat{u}_{B3}\big] = -Q_B^{\rm EM}\big[\hat{\bar{u}}_B^{\,3}\big] &= \frac{2}{3} - \frac{Y_\Phi}{2}, \\
Q_B^{\rm EM}\big[\hat{d}_{B3}\big] = -Q_B^{\rm EM}\big[\hat{\bar{d}}_B^{\,3}\big] &= -\frac{1}{3} - \frac{Y_\Phi}{2}.
\end{aligned} \tag{123}$$

In Table 4 we indicate the electric charges of the twin quark fields for the several choices of Y_Φ.

II $(\mathbf{6},\mathbf{1},Y_\Phi)$			
$\hat{\psi}$ \ Y_Φ	4/3	1/3	−2/3
$Q_B^{\rm EM}[\hat{u}_{B\,\hat{i}}] = -Q_B^{\rm EM}[\hat{\bar{u}}_B^{\,\hat{i}}]$	1	3/4	1/2
$Q_B^{\rm EM}[\hat{d}_{B\,\hat{i}}] = -Q_B^{\rm EM}[\hat{\bar{d}}_B^{\,\hat{i}}]$	0	−1/4	−1/2
$Q_B^{\rm EM}[\hat{u}_{B3}] = -Q_B^{\rm EM}[\hat{\bar{u}}_B^{\,3}]$	0	1/2	1
$Q_B^{\rm EM}[\hat{d}_{B3}] = -Q_B^{\rm EM}[\hat{\bar{d}}_B^{\,3}]$	−1	−1/2	0

Table 4: Twin quark electric charges for different choices of the sextet scalar hypercharge Y_Φ in case **II.**

5.1.3.2 case III: $[SU(3)_c \to SO(3)_c]_B$

In this case, the B sector colored scalar obtains a VEV with vacuum orientation

$$\langle \Phi_B \rangle = \frac{f_\Phi}{\sqrt{3}} \begin{pmatrix} 1 & 0 & 0 \\ 0 & 1 & 0 \\ 0 & 0 & 1 \end{pmatrix}, \tag{124}$$

leading to the symmetry breakdown $[SU(3)_c \to SO(3)_c]_B$. Twin gluon and hypercharge mass terms arise from the kinetic term $\mathcal{L} \supset \mathrm{Tr}\,[(D^\mu \Phi_B)^\dagger (D_\mu \Phi_B)]$, where $D_\mu \Phi_B = (\partial_\mu \Phi_B - i g_s\, G^a_{B\mu}(T^a \Phi_B + \Phi_B T^{a\,T}) - i g'\, Y_\Phi B_{B\mu} \Phi_B)$. These mass terms can be written as

$$\begin{aligned} \mathcal{L} &\supset \frac{1}{2}\Big\{ \frac{4}{3}\, g_s^2 f_\Phi^2 \, \left[(G^1_{B\mu})^2 + (G^3_{B\mu})^2 + (G^4_{B\mu})^2 + (G^6_{B\mu})^2 + (G^8_{B\mu})^2 \right] + 2\, g'^2 Y_\Phi^2 f_\Phi^2 (B_{B\mu})^2 \Big\}, \\ &= m_{\bar{G}}^2\, \mathrm{Tr}\,[\bar{G}_{B\mu} \bar{G}_B^\mu] + \frac{1}{2} c^2\, (B_{B\mu})^2. \end{aligned} \tag{125}$$

Here we have defined the real quintuplet vector $\bar{G}_{B\mu}$ under the unbroken $[SO(3)_c]_B$ gauge symmetry,

$$\bar{G}_{B\mu} = \bar{G}^{\bar{a}}_{B\mu} T^{\bar{a}}, \quad \bar{a} = 1, 3, 4, 6, 8, \tag{126}$$

with mass $m_G \equiv 2 g_s f_\Phi / \sqrt{3}$. The barred indices (126) denote the broken $[SU(3)_c]_B$ generators. Furthermore, we have defined

$$c \equiv \sqrt{2}\, g'\, Y_\Phi\, f_\Phi, \tag{127}$$

in Eq. (125), as before. Noting Eqs. (99,125), the mass mixing in the neutral gauge boson sector between $W^3_{B\mu}$, $B_{B\mu}$ can be written as

$$\mathcal{L} \;\supset\; \frac{1}{2}\, \hat{X}_\mu^T \mathcal{M}_X^2\, \hat{X}_\mu, \tag{128}$$

where we have defined $\hat{X}_\mu^T = (W^3_{B\mu}, B_{B\mu})$ and the neutral gauge boson mass matrix,

$$\mathcal{M}_X^2 = \begin{pmatrix} a^2 & -ab \\ -ab & b^2 + c^2 \end{pmatrix}, \tag{129}$$

where a, b, c are defined in Eqs. (100,127). The system via the rotations, $\hat{X}_\mu = \mathcal{R} X_\mu$ where $X_\mu^T = (Z_{B\mu}, A_{B\mu})$ and

$$\mathcal{R} = \begin{pmatrix} c_{W_B} & s_{W_B} \\ -s_{W_B} & c_{W_B} \end{pmatrix}. \tag{130}$$

Here $c_{W_B} \equiv \cos\theta_{W_B}$, etc., and the mixing angle satisfies

$$\tan(2\,\theta_{W_B}) = \frac{2\,a\,b}{b^2 + c^2 - a^2}. \tag{131}$$

Here $\theta_{W_B} \neq \theta_W$ is not the same as the usual weak mixing angle. The mass eigenvalues are given by

$$m^2_{Z_B, A_B} = \frac{1}{2}\left\{a^2 + b^2 + c^2 \mp \sqrt{(a^2+b^2+c^2)^2 - 4a^2c^2}\right\}. \tag{132}$$

We observe that the twin photon picks up a mass, and there are no unbroken $U(1)$ gauge symmetries in the low energy effective theory. Assuming $f_\Phi \gg v_B$, which implies $c \gg a, b$, the approximate expressions of the neutral gauge boson masses are

$$m^2_{Z_B} \simeq a^2 = \frac{g^2\,v_B^2}{4}, \qquad m^2_{A_B} \simeq b^2 + c^2 = g'^2\left(2\,Y_\Phi^2\,f_\Phi^2 + \frac{v_B^2}{4}\right). \tag{133}$$

The gauge boson-fermion couplings arise from fermion kinetic terms, $\mathcal{L} \supset\ i\,\psi_B^\dagger\,\bar{\sigma}^\mu\,D_\mu\psi_B$, with covariant derivative $D_\mu = \partial_\mu - ig_s G^a_{B\mu}T^a - igW^\alpha_{B\mu}\tau^\alpha - ig'YB_{B\mu}$. In particular, after spontaneous symmetry breaking, the quarks transform as vectors under the ubroken $[SO(3)_c]_B$ gauge symmetry, with interactions

$$\mathcal{L} \supset g_s\,G^{\hat{a}}_{B\mu}\,\psi_B^{\dagger i}\ \bar{\sigma}^\mu\,(T^{\hat{a}})^j_i\,\psi_{Bj} \tag{134}$$

where $\hat{a} = 2, 5, 7$ denote the unbroken $[SU(3)_c]_B$ generators (equivalently the $[SO(3)_c]_B$ generators) and $i = 1, 2, 3$. This applies to both chiral quarks, as before.

5.1.4 Color Octet Scalar

Finally, we examine the gauge sector in models with a real color octet scalar with quantum numbers $\Phi \sim (\mathbf{8}, \mathbf{1}, 0)$.

5.1.4.1 case IV: $[SU(3)_c \to SU(2)_c \times U(1)_c]_B$

In this case, the B sector colored scalar obtains a VEV with vacuum orientation

$$\langle \Phi_B \rangle = \sqrt{2}\, f_\Phi\, T^8, \tag{135}$$

leading to the symmetry breakdown $[SU(3)_c \to SU(2)_c \times U(1)_c]_B$. Twin gluon mass terms arise from the kinetic term $\mathcal{L} \supset \mathrm{Tr}\,[(D^\mu \Phi_B)(D_\mu \Phi_B)]$, where $D_\mu \Phi_B = (\partial_\mu \Phi_B - i g_s\, G^a_{B\mu}[T^a, \Phi_B])$. These mass terms can be written as

$$\begin{aligned} \mathcal{L} &\supset \frac{3 g_s^2 f_\Phi^2}{4}\, \left[(G^4_{B\mu})^2 + (G^5_{B\mu})^2 + (G^6_{B\mu})^2 + (G^7_{B\mu})^2\right] \\ &= m_G^2\, |G_{B\mu}|^2, \end{aligned} \tag{136}$$

where we have introduced the vector doublet $G_{B\mu}$ under the unbroken $[SU(2)_c]_B$ gauge symmetry, as in Eq. (103), with mass $m_G \equiv \sqrt{\frac{3}{2}}\, g_s f_\Phi$.

The dynamics of the electroweak sector is the same as in the visible sector, leading to massive $W^\pm$, Z boson and a massless photon. There are two unbroken $U(1)$ gauge symmetries. One is just the usual electromagnetism, with generator $Q_B^{\mathrm{EM}} = \tau^3 + Y$ and coupling constant $e_B = g g'/\sqrt{g^2 + g'^2}$. All twin fermions have the usual electric charges. The other unbroken $U(1)$ gauge symmetry is $[U(1)_c]_B$, with generator T^8 and massless gauge boson $G^8_{B\mu}$.

The quarks decompose into doublets and singlets under the unbroken $[SU(2)_c]_B$ gauge symmetry, and can be represented as in Eq. (112). The doublet and singlet quarks have identical electric charges. The $[U(1)_c]_B$ interaction term can be written as

$$\begin{aligned} \mathcal{L} &\supset g_s\, G^8_{B\mu}\, \psi_B^{\dagger i}\, \bar{\sigma}^\mu\, (T^8)^j_i\, \psi_{Bj} \\ &\supset \left(\frac{g_s}{2\sqrt{3}}\right)\, G^8_{B\mu}\, \left[\hat{\psi}_B^{\dagger \hat{i}}\, \bar{\sigma}^\mu\, \psi_{B\hat{i}} - 2\, \hat{\psi}_B^{\dagger 3}\, \bar{\sigma}^\mu\, \psi_{B3}\right]. \end{aligned} \tag{137}$$

Note there is a minus sign for the right chirality Weyl quarks $\hat{\bar{q}}$ for opposite charge under T^8.

5.1.4.2 case V: $[SU(3)_c \to U(1)_c \times U(1)'_c]_B$

In this case, the B sector colored scalar obtains a VEV with vacuum orientation

$$\langle \Phi_B \rangle = \sqrt{2}\, f_\Phi\, T^3, \tag{138}$$

leading to the symmetry breakdown $[SU(3)_c \to U(1)_c \times U(1)'_c]_B$. Twin gluon mass terms arise from the kinetic term $\mathcal{L} \supset \mathrm{Tr}\,[(D^\mu \Phi_B)(D_\mu \Phi_B)]$, where $D_\mu \Phi_B = (\partial_\mu \Phi_B - i g_s\, G^a_{B\mu}[T^a, \Phi_B])$. These mass terms can be written as

$$\mathcal{L} \supset g_s^2 f_\Phi^2\, \left[(G^1_{B\mu})^2 + (G^2_{B\mu})^2\right] + \frac{g_s^2 f_\Phi^2}{4}\, \left[(G^4_{B\mu})^2 + (G^5_{B\mu})^2 + (G^6_{B\mu})^2 + (G^7_{B\mu})^2\right] \tag{139}$$

with $G^3_{B\mu}$ and $G^8_{B\mu}$ remaining massless. The low energy gauge symmetry is

$$[U(1)_{\mathrm{EM}} \times U(1)_c \times U(1)'_c]_B, \tag{140}$$

with respective generators $Q^{\mathrm{EM}}_B = \tau^3 + Y$, T^3, T^8. The massive gluons in Eq. (139) can be grouped into complex vectors which carry charges under the $U(1)_c$ gauge symmetries. In particular, $G^{1,2}_B$ couple to G^3_B but not G^8_B, while $G^{4,5,6,7}_B$ couple to both G^3_B and G^8_B. Similarly, the different colors of quarks couple with different strengths to the massless $U(1)$ color gluons according to the generators T^3, T^8, while their electric charges are the same as those in the visible sector.

5.2 Twin Confinement

In this section we consider aspects of twin confinement for models **I-IV** in which the twin color gauge symmetry $[SU(3)_c]_B$ is spontaneously broken to a nonabelian subgroup, either $[SU(2)_c]_B$ or $[SO(3)_c]_B$. We will restrict ourselves to a one-loop analysis of the running coupling constant, using the one-loop beta function Eq. 97.

We first discuss the UV matching condition for the strong coupling constants of the visible and twin sector. The $\mathbb{Z}_2$ and twin color symmetries are spontaneously broken at a scale f_Φ between 1 TeV and the UV cutoff $\Lambda \sim 5 - 10$ TeV. Above the scale f_Φ the beta functions of the two sectors are identical. Thus, we match the visible and twin sector gauge couplings at $Q = f_\Phi$ according to relation

$$\alpha_s^B(f_\Phi) = \alpha_s^A(f_\Phi) + \delta\alpha_s, \tag{141}$$

where a small nonzero $\delta\alpha_s$ is in general allowed after spontaneous $\mathbb{Z}_2$ symmetry breaking. For instance, such a shift in the coupling in Eq. (141) could arise from $\mathbb{Z}_2$ symmetric dimension six operators, e.g., in the case of the color triplet scalar we may have

$$\mathcal{L} \supset \frac{c_G}{\Lambda^2}|\Phi_A|^2 G_{A\mu\nu}G_A^{\mu\nu} + \frac{c_G}{\Lambda^2}|\Phi_B|^2 G_{B\mu\nu}G_B^{\mu\nu}, \tag{142}$$

and similarly in other cases. When Φ_B obtains a VEV, and following canonical normalization of the twin gluon kinetic term, we obtain a shift in the strong coupling given by

$$\frac{\delta\alpha_s}{\alpha_s^A} \equiv \frac{\alpha_s^B - \alpha_s^A}{\alpha_s^A} \simeq \frac{4c_G f_\Phi^2}{\Lambda^2}. \tag{143}$$

This shift is expected to be of order 10% or smaller, depending on the nature of the UV dynamics generating operators such as Eq. (142).

It is also possible that some of the twin fermions are significantly heavier, which can be realized through spontaneous $\mathbb{Z}_2$ breaking effects.

We will now analyze each of the four cases containing an unbroken non-abelian color group in the twin sector at low energy.

5.2.1 Color Triplet: Case I

For the case of the color triplet scalar we have the symmetry breaking pattern $[SU(3)_c \to SU(2)_c]_B$. The visible sector contains a (complex) color triplet scalar ϕ_A in the effective theory, having index $T_s = \frac{1}{2}$. The beta function coefficients (97) are therefore given by

$$b_A = 11 - \frac{2}{3}n_f^A - \frac{1}{6}n_s^A, \tag{144}$$

$$b_B = \frac{22}{3} - \frac{2}{3}n_f^B, \tag{145}$$

where n_f^A (n_f^B) denotes the number of light Dirac fermions in the A (B) sector, and $n_s^A = 0$ or 1 is the number of light triplet scalars in the A sector.

Integrating the renormalization group equations, the confinement scales of the visible and twin sectors, Λ_A and Λ_B, respectively, can then be related implicitly through Eq. (141):

$$\frac{2\pi}{\log\left\{\left[\prod_{i=1}^{n_H}\left(\frac{m_{q_B}^i}{\Lambda_B}\right)^{2/3}\right]\left(\frac{f_\Phi}{\Lambda_B}\right)^{10/3}\right\}} = \frac{2\pi}{\log\left[\left(\frac{m_{c_A}m_{b_A}m_{t_A}}{\Lambda_A^3}\right)^{2/3}\left(\frac{m_{\phi_A}}{\Lambda_A}\right)^{1/6}\left(\frac{f_\Phi}{\Lambda_A}\right)^{41/6}\right]} + \delta\alpha_s, \tag{146}$$

where the product on the left hand side runs over the n_H heavy quark flavors in the twin sector with masses $m_{q_B}^i > \Lambda_B$. Furthermore, if $\delta\alpha_s$ is negligible we can write Λ_B explicitly as a function of Λ_A and the other mass scales:

$$\Lambda_B = \Lambda_A\left[\left(\frac{\prod_{i=1}^{n_H} m_{q_B}^i}{m_{c_A}m_{b_A}m_{t_A}\Lambda_A^{n_H-3}}\right)^4\left(\frac{\Lambda_A^{22}}{m_{\phi_A}f_\Phi^{21}}\right)\right]^{1/[2(2n_H+10)]}. \tag{147}$$

Fixing $\alpha_s^A(m_Z) = 0.1179$ (corresponding to $\Lambda_A = 140$ MeV), $\delta\alpha_s = 0$, $m_\phi = 1$ TeV, $f_\Phi = 3$ TeV, and assuming the twin quarks are a factor of 3 heavier than the ordinary quarks, we find $\Lambda_B \simeq 1$ MeV, which is below the lightest up-type quark mass in the twin sector.

In Figure 10 we plot the evolution of the strong coupling in the visible and twin sector. We observe that the twin strong coupling diverges near scales of order $\Lambda_B \sim$ MeV, in agreement with the estimate performed above. Allowing for nonzero $\delta\alpha_s$ can cause the twin confinement scale to be larger or smaller, as illustrated in Figure 10.

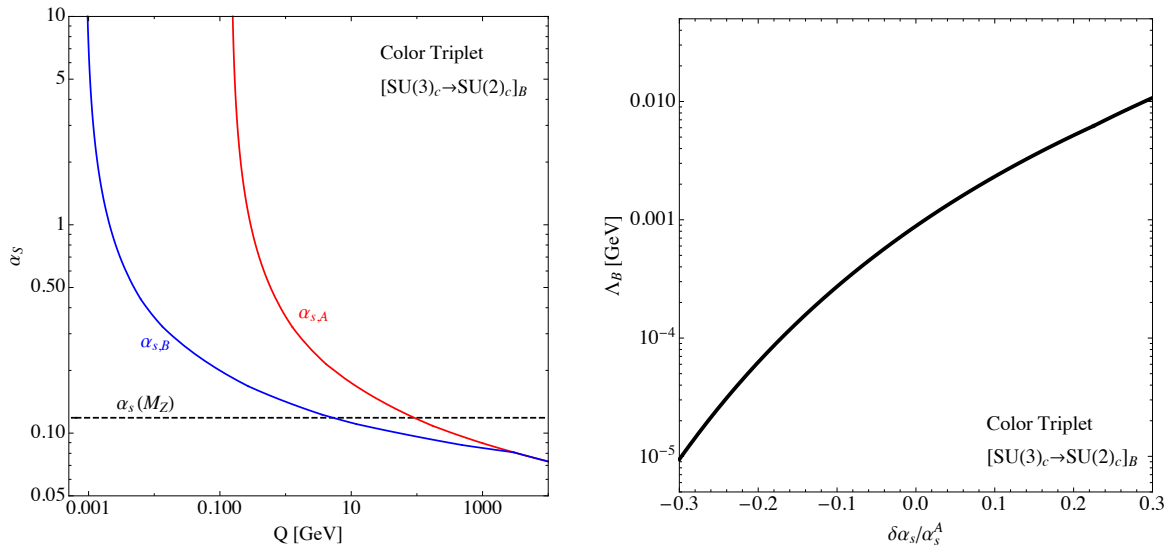

Figure 10: *Left:* Evolution of the strong fine structure constants in the visible sector (red) and twin sector (blue) for the case of the color triplet scalar. The symmetry breaking pattern in this case is $[SU(3)_c \to SU(2)_c]_B$. Here we have fixed $\alpha_s^A(m_Z) = 0.1179$ and $\delta\alpha_s = 0$. *Right:* The twin confinement scale as a function of the UV coupling shift $\delta\alpha_s/\alpha_s^A$. In both plots all twin fermions are assumed to be a factor of 3 heavier than the ordinary fermions (no additional $\mathbb{Z}_2$ breaking effects beyond scalar VEVs). We have also assumed $m_{\phi_A} = 1$ TeV and $f_\Phi = 3$ TeV.

5.2.2 Color Sextet

5.2.2.1 case II: $[SU(3)_c \to SU(2)_c]_B$

For the case of the color sextet scalar with VEV $\langle \Phi_B \rangle \sim \mathrm{diag}(0,0,1)$, the symmetry breaking pattern is $[SU(3)_c \to SU(2)_c]_B$. The visible sector contains a (complex) color sextet scalar ϕ_A in the effective theory, having index $T_s = \frac{5}{2}$. Furthermore, the twin sector contains a complex color triplet scalar ϕ_B in the effective theory, having index $T_s = 2$. The beta function coefficients (97) are therefore given by

$$b_A = 11 - \frac{2}{3} n_f^A - \frac{5}{6} n_s^A, \tag{148}$$

$$b_B = \frac{22}{3} - \frac{2}{3} n_f^B - \frac{2}{3} n_s^B. \tag{149}$$

Integrating the renormalization group equations, the confinement scales of the visible and twin sectors, Λ_A and Λ_B, respectively, can then be related implicitly through Eq. (141):

$$\frac{2\pi}{\log\left\{\left[\prod_{i=1}^{n_H}\left(\frac{m_{q_B}^i}{\Lambda_B}\right)^{2/3}\right]\left(\frac{m_{\phi_B}}{\Lambda_B}\right)^{2/3}\left(\frac{f_\Phi}{\Lambda_B}\right)^{8/3}\right\}} = \frac{2\pi}{\log\left[\left(\frac{m_{c_A} m_{b_A} m_{t_A}}{\Lambda_A^3}\right)^{2/3}\left(\frac{m_{\phi_A}}{\Lambda_A}\right)^{5/6}\left(\frac{f_\Phi}{\Lambda_A}\right)^{37/6}\right]} + \delta\alpha_s, \tag{150}$$

where the product on the left hand side runs over the n_H heavy quark flavors in the twin sector with masses $m_{q_B}^i > \Lambda_B$. Furthermore, if $\delta\alpha_s$ is negligible we can write Λ_B explicitly as a function of Λ_A and the other mass scales:

$$\Lambda_B = \Lambda_A \left[\left(\frac{\prod_{i=1}^{n_H} m_{q_B}^i}{m_{c_A} m_{b_A} m_{t_A} \Lambda_A^{n_H - 3}}\right)^4 \left(\frac{m_{\phi_B}^4 \Lambda_A^{22}}{m_{\phi_A}^5 f_\Phi^{21}}\right)\right]^{1/[2(2n_H+10)]}. \tag{151}$$

The evolution of the strong coupling constants is both qualitatively and quantitatively similar to the case of the color triplet examined above; see Figure 10. Fixing $\alpha_s^A(m_Z) = 0.1179$ ($\Lambda_A = 140$ MeV), $\delta\alpha_s = 0$, $m_{\phi_A} = m_{\phi_B} = 1$ TeV, $f_\Phi = 3$ TeV, and assuming the twin quarks are a factor of 3 heavier than the ordinary quarks, we find $\Lambda_B \simeq 1$ MeV, which is below the lightest up-type quark mass in the twin sector.

5.2.2.2 case III: $[SU(3)_c \to SO(3)_c]_B$

For the case of the color sextet scalar with VEV $\langle \Phi_B \rangle \sim \text{diag}(1,1,1)$, the symmetry breaking pattern is $[SU(3)_c \to SO(3)_c]_B$. The visible sector contains a (complex) color sextet scalar ϕ_A in the effective theory, having index $T_s = \frac{5}{2}$, as before, while the twin sector contains a real quintuplet scalar ϕ_B in the effective theory, having index $T_s = \frac{5}{2}$. The beta function coefficients (97) are therefore given by

$$b_A = 11 - \frac{2}{3} n_f^A - \frac{5}{6} n_s^A, \tag{152}$$

$$b_B = \frac{11}{6} - \frac{2}{3} n_f^B - \frac{5}{12} n_s^B. \tag{153}$$

Integrating the renormalization group equations, the confinement scales of the visible and twin sectors, Λ_A and Λ_B, respectively, can then be related implicitly through Eq. (141):

$$\frac{2\pi}{\log\left\{\left[\prod_{i=1}^{n_H}\left(\frac{m_{q_B}^i}{\Lambda_B}\right)^{2/3}\right]\left(\frac{m_{\phi_B}}{\Lambda_B}\right)^{5/12}\left(\frac{f_\Phi}{\Lambda_B}\right)^{-31/12}\right\}} = \frac{2\pi}{\log\left[\left(\frac{m_{c_A} m_{b_A} m_{t_A}}{\Lambda_A^3}\right)^{2/3}\left(\frac{m_{\phi_A}}{\Lambda_A}\right)^{5/6}\left(\frac{f_\Phi}{\Lambda_A}\right)^{37/6}\right]} + \delta\alpha_s, \tag{154}$$

where the product on the left hand side runs over the n_H heavy quark flavors in the twin sector with masses $m_{q_B}^i > \Lambda_B$. Furthermore, if $\delta\alpha_s$ is negligible we can write Λ_B explicitly as a function of Λ_A and the other mass scales:

$$\Lambda_B = \Lambda_A \left[\left(\frac{\prod_{i=1}^{n_H} m_{q_B}^i}{m_{c_A} m_{b_A} m_{t_A} \Lambda_A^{n_H - 3}}\right)^8 \left(\frac{m_{\phi_B}^5 \Lambda_A^{110}}{m_{\phi_A}^{10} f_\Phi^{105}}\right)\right]^{1/[2(4n_H - 13)]}. \tag{155}$$

Fixing $\alpha_s^A(m_Z) = 0.1179$ ($\Lambda_A = 140$ MeV), $\delta\alpha_s = 0$, $m_{\phi A} = m_{\phi B} = 1$ TeV, $f_\Phi = 3$ TeV, and assuming the twin quarks are a factor of 3 heavier than the ordinary quarks, we find $\Lambda_B \simeq 10^{-23}$ GeV.

In Figure 11 we plot the evolution of the strong coupling in the visible and twin sector. We observe that the twin strong coupling diverges near scales of order $\Lambda_B \sim 10^{-23}$ GeV, in agreement with the estimate performed above. Allowing for nonzero $\delta\alpha_s$ can cause the twin confinement scale to be larger or smaller, as illustrated in Figure 11.

We note that in this case the confinement scale is many orders of magnitude below the QCD confinement scale. This is a consequence of the smaller color charge of the $[SO(3)_c]_B$ gluons, in comparison to the $[SU(2)_c]_B$ case. One observes from Figure 11 that asymptotic

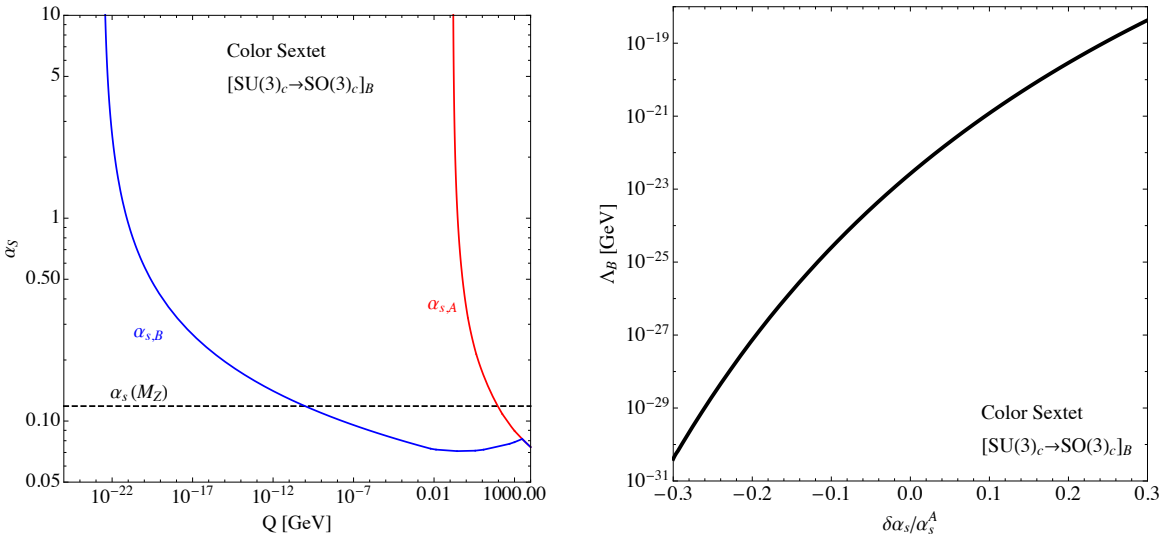

Figure 11: *Left:* Evolution of the strong fine structure constants in the visible sector (red) and twin sector (blue) for the case of the color sextet scalar with symmetry breaking pattern $[SU(3)_c \to SO(3)_c]_B$. Here we have fixed $\alpha_s^A(m_Z) = 0.1179$ and $\delta\alpha_s = 0$. *Right:* The twin confinement scale as a function of the UV coupling shift $\delta\alpha_s/\alpha_s^A$. All twin fermions are assumed to be a factor of 3 heavier than the ordinary fermions (no additional $\mathbb{Z}_2$ breaking effects beyond scalar VEVs). We have assumed $m_{\phi_A} = m_{\phi_B} = 1$ TeV, $f_\Phi = 3$ TeV.

freedom is lost for some range of scales below f_Φ. Even at very low energy scales below the twin quark masses where asymptotic freedom is restored, the beta function, while negative, is comparatively small in magnitude, and thus the coupling runs very slowly.

5.2.3 Color Octet: Case IV

For the case of the color octet scalar with VEV $\langle \Phi_B \rangle \sim T^8$, the symmetry breaking pattern is $[SU(3)_c \to SU(2)_c]_B$. The visible sector contains a (real) color octet scalar ϕ_A in the effective theory, having index $T_s = 3$. Furthermore, the twin sector contains a (real) color triplet scalar ϕ_B in the effective theory, having index $T_s = 2$. The beta function coefficients (97) are therefore given by

$$b_A = 11 - \frac{2}{3} n_f^A - \frac{1}{2} n_s^A, \tag{156}$$

$$b_B = \frac{22}{3} - \frac{2}{3} n_f^B - \frac{1}{3} n_s^B. \tag{157}$$

Integrating the renormalization group equations, the confinement scales of the visible and twin sectors, Λ_A and Λ_B, respectively, can then be related implicitly through Eq. (141):

$$\frac{2\pi}{\log\left\{\left[\prod_{i=1}^{n_H}\left(\frac{m_{q_B}^i}{\Lambda_B}\right)^{2/3}\right]\left(\frac{m_{\phi_B}}{\Lambda_B}\right)^{1/3}\left(\frac{f_\Phi}{\Lambda_B}\right)^3\right\}} = \frac{2\pi}{\log\left[\left(\frac{m_{c_A} m_{b_A} m_{t_A}}{\Lambda_A^3}\right)^{2/3}\left(\frac{m_{\phi_A}}{\Lambda_A}\right)^{1/2}\left(\frac{f_\Phi}{\Lambda_A}\right)^{13/2}\right]} + \delta\alpha_s, \tag{158}$$

where the product on the left hand side runs over the n_H heavy quark flavors in the twin sector with masses $m_{q_B}^i > \Lambda_B$. Furthermore, if $\delta\alpha_s$ is negligible we can write Λ_B explicitly as a function of Λ_A and the other mass scales:

$$\Lambda_B = \Lambda_A \left[\left(\frac{\prod_{i=1}^{n_H} m_{q_B}^i}{m_{c_A} m_{b_A} m_{t_A} \Lambda_A^{n_H - 3}}\right)^4 \left(\frac{m_{\phi_B}^2 \Lambda_A^{22}}{m_{\phi_A}^3 f_\Phi^{21}}\right)\right]^{1/[2(2n_H+10)]}. \tag{159}$$

The evolution of the strong coupling constants is both qualitatively and quantitatively similar to the case of the color triplet examined above; see Figure 10. Taking the same $\alpha_s^A(m_Z) = 0.1179$ ($\Lambda_A \simeq 140$ MeV), $\delta\alpha_s = 0$, $m_{\phi_A} = m_{\phi_B} = 1$ TeV, $f_\Phi = 3$ TeV, and assuming the twin quarks are a factor of 3 heavier than the ordinary quarks, we find $\Lambda_B \simeq 1$ MeV, which is below the lightest up-type quark mass in the twin sector.

5.3 Summary

We can write a general expression of Λ_B in terms of Λ_A and other mass scales, if $\delta\alpha_s$ is negligible:

$$\Lambda_B = \Lambda_A \left(\frac{\left(\prod_{i=1}^{n_H} m_{q_B}^i\right)^{2T_f}}{m_{c_A} m_{b_A} m_{t_A} \Lambda_A^{2T_f n_H - 3}} \right)^{\frac{2}{4T_f n_H + 3b_6}} \left(\frac{m_{\phi_B}^{\frac{c_s^B}{6} T_s^B n_s^B} \Lambda_A^{7-b_6}}{m_{\phi_A}^{\frac{c_s^A}{6} T_s^A n_s^A} f_\Phi^{7-b_6-\frac{c_s^A}{6} T_s^A n_s^A + \frac{c_s^B}{6} T_s^B n_s^B}} \right)^{\frac{3}{4T_f n_H + 3b_6}} \tag{160}$$

where T_s^A is the Dynkin index for scalar representation in the A sector, T_s^B is the Dynkin index in the B sector unbroken group, and $c_s^{A,B} = 1(2)$ for real (complex) scalars in A(B) sector. $n_s^{A,B} \in \{0, 1\}$ the number of active scalars in A(B) sector. $b_6 = \frac{11}{3} C_{\mathrm{A}d} - 4 c_f T_f$ is b_B for all the six active twin quarks below f_Φ without scalars running. For other symbols, refer to Eq. 97.

In summary, cases **I**, **II**, and **IV** have very similar gauge dynamics at low energy owing to the unbroken $[SU(2)_c \times U(1)_{\mathrm{EM}}^{(\prime)}]_B$ color and electromagnetic gauge symmetries. We saw that the twin strong coupling becomes large near scales of order $\Lambda_B \sim$ MeV, as displayed in the left panel of Fig. 10. As mentioned above, this is primarily a consequence of having fewer twin gluonic degrees of freedom and thus a smaller b_B in Eq. (97). The running is essentially identical in those three cases with residual $[SU(2)_c]_B$. The only difference is the contribution of TeV scale colored scalar degrees of freedom, which have essentially no quantitative impact on the results.

The generator of the unbroken electromagnetic symmetry for each case are

$$\mathbf{I}: \qquad (\mathbf{3}, \mathbf{1}, Y_\Phi) \qquad Q_B^{\mathrm{EM}} = \tau^3 + Y + \sqrt{3}\, Y_\Phi\, T^8 \ , \tag{161}$$

$$\mathbf{II}: \qquad (\mathbf{6}, \mathbf{1}, Y_\Phi) \qquad Q_B^{\mathrm{EM}} = \tau^3 + Y + \frac{\sqrt{3}}{2}\, Y_\Phi\, T^8 \ , \tag{162}$$

$$\mathbf{IV}: \qquad (\mathbf{8}, \mathbf{1}, 0) \qquad Q_B^{\mathrm{EM}} = \tau^3 + Y \ . \tag{163}$$

In cases **I** and **II** the twin electric charges depends on a particle's T^8 as well as the colored scalar's hypercharge Y_Φ. This occurs because the triplet and sextet can carry hypercharge, which leads to mass mixing between the neutral hypercharge and color gauge bosons. On the other hand, the octet in case **IV** is real, so the EM generator is identical to the SM.

Since not charged under color, the twin electric charges of the twin leptons are equal to the electric charges of the visible leptons. Following symmetry breaking, the twin quark fields decompose into doublets and singlets under the unbroken $[SU(2)_c]_B$, which carry distinct electric charges. Before symmetry breaking, we denote the quark fields as $Q_B \sim (\mathbf{3}, \mathbf{2}, \frac{1}{6})$, $\bar{u}_B \sim (\overline{\mathbf{3}}, \mathbf{1}, -\frac{2}{3})$, $\bar{d}_B \sim (\overline{\mathbf{3}}, \mathbf{1}, \frac{1}{3})$ using two component Weyl fermions. These fields decompose as in Eq. 112. In Table 3 and Table 4 we indicate the electric charges of the twin quark fields for the several choices of Y_Φ for these cases. These choices of Y_Φ allow Yukawa-type couplings of the colored scalar to pairs of fermions, and their implications are explored in Sec. 6.

We emphasize here the great difference in the twin particle spectrum compared to the basic MTH model. Though much of the dynamics are determined by the $\mathbb{Z}_2$ twin symmetry with the SM fields, we end up with new unconfined quarks, from the part of the field along the VEV direction (3rd color direction), as well as new $SU(2)_c$ bound states. Insights into this bound state spectrum and dynamics of the phase transition can be found in, for example, [119, 120, 121, 122, 123, 124, 125, 126, 127, 128, 129, 130], but a few qualitative items are worth mentioning. First, the lightest quark masses are a few MeV, which is just above the confinement scale so mesons, composed of a quark and an anti-quark, and baryons, composed of two quarks, can likely be simulated as nonrelativisitic bound states. In the absence of additional scalar couplings to matter there is a conserved baryon number that renders the lightest twin baryon stable, which may be interesting from a cosmological perspective. In addition, the mass of the lightest $SU(2)$ glueball is $m_0 \sim 5\,\Lambda_B$ [131, 132] so it is likely that the glueball and meson/baryon spectrum will overlap. However, as the

lightest glueball is a 0^{++} state it will decay rapidly to a pair of twin photons.[1]

In case **III**, with sextet scalar, the unbroken twin color symmetry is $[SO(3)_c]_B$. We found that the twin strong coupling diverges near scales of order $\Lambda_B \sim 10^{-23}$ GeV, many, many orders of magnitude below the QCD confinement scale, as displayed in the left panel of Fig. 11. This is due to smaller color charge of the $[SO(3)_c]_B$ gluons, in comparison to the $[SU(2)_c]_B$ case. Interestingly there are no unbroken $U(1)$ gauge symmetries in this case, as the sextet VEV lifts the twin photon, with mass of order $g' Y_\Phi f_\Phi$. The heavy twin gluons pick up a mass of order $g_s f_\Phi$, and form a quintuplet under the unbroken $[SO(3)_c]_B$ gauge

[1]Here we show how to evaluate the decay rate of glueball.

The effective operator for two gluons and two photons coupling can be found from the box diagram of four photons: the Euler-Heisenberg Lagrangian[133]

$$L = \frac{\alpha^2}{180 m_f^4}\left\{-5((F_{\mu\nu})^2)^2 + 14 F_{\mu\nu}F^{\nu\alpha}F_{\alpha\beta}F^{\beta\mu}\right\}, \tag{164}$$

where m_f is the mass of the fermions running inside the box. Replace two of them by gluons and permutate, we get[134]:

$$\begin{aligned} L_{gg\gamma\gamma} = \tfrac{\alpha_S \alpha Q_f^2}{180 m_f^4}[&-5(F_{\mu\nu})^2 (G^a_{\alpha\beta})^2 - 10(F_{\mu\nu}G^{\mu\nu a})(F_{\alpha\beta}G^{\alpha\beta a}) \\ &+28 F_{\mu\nu}F^{\nu\lambda}G^a_{\lambda\sigma}G^{\sigma\mu a} + 14 F_{\mu\nu}G^{\nu\lambda a}F_{\lambda\sigma}G^{\sigma\mu a}]. \end{aligned} \tag{165}$$

The first term in the bracket is what we need. There is a net correction of $\frac{5}{90} \times (-\frac{3}{10}) = -\frac{1}{60}$ if projecting onto the basis of the eigen operators S, P, T, L[135], to the Naive Dimensional Analysis for glueball-photon coupling operator:

$$L^{\rm NDA}_{gbl\gamma\gamma} = \tfrac{1}{2}\tfrac{(g_3 e Q_f)^2}{16\pi^2 m_f^4}(F_{\mu\nu})^2 (G^a_{\alpha\beta})^2 = \tfrac{\alpha_S \alpha Q_f^2}{2 m_f^4}(F_{\mu\nu})^2 (G^a_{\alpha\beta})^2. \tag{166}$$

From the effective operator, the glueball decay effective vertex can be described by a decay constant[85][136]:

$$< \mathrm{Vac}|(G_{\mu\nu})^2|0^{++}>= f_0, \tag{167}$$

where $4\pi\hat{\alpha}_3 f_0 = 3.06 m_o^3$.
Thus, the decay width of the lightest twin glueball 0^{++} to twin photons is:

$$\Gamma_{0^{++}\to\gamma_B\gamma_B} = \sum_f \frac{(\alpha_s \alpha Q_f^2)^2 f_0^2 m_{0^{++}}^3}{16\pi m_f^8}(\frac{1}{60})^2 \sim \frac{m_{0^{++}}^9}{m_{uB}^8}, \tag{168}$$

where the lightest twin up quark is dominant.

Explicit esitimation of the radiative decay of glueballs, with the twin confinement scale $\Lambda \sim MeV$, gives its lifetime:

$$\tau_{0^{++}} \sim 10^{-10}\ secs. \tag{169}$$

symmetry. The twin quarks on the other hand transform in the fundamental representation of $[SO(3)_c]_B$. This again shows how different the twin and visible sectors can be, even though they are fundamentally related by the $\mathbb{Z}_2$ symmetry. If the twin sector is much colder than the SM, as perhaps motivated by N_{eff} bounds, the quarks would just barely act like quirks[2] [137], but with the width of the color flux tubes connecting them set by $1/\Lambda_B$ the scale of confining forces being about that of a planet. Similarly, the lightest bound states are glueballs with small masses likely a few times Λ_B, and these objects are again roughly Earth-sized. However, we typically expect that the twin quarks and gluons were in equilibrium at some point in the early universe, and the cosmic evolution of this dark sector with such a low confinement scale brings with it many open questions. Such novel dynamics and their cosmological implications is clearly worth further exploration.

In the color octet model of case **V** there is no residual non-Abelian gauge symmetry. There are, however, three unbroken abelian symmetries, $[U(1)_c \times U(1)'_c \times U(1)_{\text{EM}}]_B$, with generators T^3, T^8, and $Q_B^{\text{EM}} = \tau^3 + Y$, respectively. The heavy gluons can be grouped into complex vectors which carry charges under the $U(1)_c^{(\prime)}$ gauge symmetries. Those heavy gluons and fermions of different colors couple with different strengths to the massless $U(1)$ color gluons according to the generators T^3, T^8, while their twin electric charges are the same as the electric charges of their $\mathbb{Z}_2$ partners in the visible sector. We expect in this model that there can be a rich variety of nuclear and atomic states, some of which may have important cosmological applications.

[2]Additional heavy particles charged under a new unbroken non-abelian $SU(N)_c$ gauge group as well as the standard model. The new gauge group gets strong at a scale $\Lambda < m$, and breaking of gauge strings is exponentially suppressed due to its large mass. Quirk production results in strings that are long compared to $1/\Lambda$, leading to exotic phenomena.

6.0 Scalar Couplings to Matter

Thus far we have only considered the dynamics of the scalar potential and gauge sector. We now investigate the consequences of new couplings of the colored scalars to fermions. These couplings have two primary motivations. First, they cause the visible sector colored scalar ϕ_A to decay, explaining in a simple way the absence of stable colored relics. Second, following spontaneous color breaking in the mirror sector, such couplings produce new dynamical twin fermion mass terms. Consequently, the spectrum of twin fermions can be deformed with respect to the mirror symmetric model, which may have important consequences for cosmology and phenomenology. We emphasize, however, that the exact $\mathbb{Z}_2$ symmetry in our setup produces tight correlations between variations in the twin mass spectrum and visible sector phenomenology, including the indirect precision tests (Sec. 7) and collider signals of ϕ_A (Sec. 8).

Given these motivations, we focus mainly on couplings involving a single colored scalar to a pair of fermions. Fermions are written using two component left chirality Weyl spinors. The quantum numbers of the visible sector fields are $Q_A^T = (u_A, d_A)^T \sim (\mathbf{3}, \mathbf{2}, \frac{1}{6})$, $\bar{u}_A \sim (\overline{\mathbf{3}}, \mathbf{1}, -\frac{2}{3})$, $\bar{d}_A \sim (\overline{\mathbf{3}}, \mathbf{1}, \frac{1}{3})$, $L_A^T = (\nu_A, e_A)^T \sim (\mathbf{1}, \mathbf{2}, -\frac{1}{2})$, $\bar{e}_A \sim (\mathbf{1}, \mathbf{1}, 1)$, $H_A \sim (\mathbf{1}, \mathbf{2}, \frac{1}{2})$ and similarly for the mirror sector. In Table 5 we have catalogued all weak $SU(2)_L$ singlet fermion bilinear operators having nontrivial color quantum numbers. The table shows the hypercharge and color quantum numbers of the operator, as well as the possible colored scalar representations that can couple to the operator to form a complete gauge singlet. We note that contraction of $SU(2)_L$ indices is indicated by the parentheses, e.g., $(QH) = \epsilon^{\alpha\beta} Q_\alpha H_\beta$, $(H^\dagger Q) = H^{\dagger\alpha} Q_\alpha$. For the $SU(2)_L$ singlet, color triplet $(\mathbf{3}, \mathbf{1}, Y_\Phi)$, sextet $(\mathbf{6}, \mathbf{1}, Y_\Phi)$, and real octet $(\mathbf{8}, \mathbf{1}, 0)$ scalars considered in this work, we find eight distinct representations that allow such couplings, with quantum numbers

$$\begin{gathered}(\mathbf{3}, \mathbf{1}, \tfrac{2}{3}), \quad (\mathbf{3}, \mathbf{1}, -\tfrac{1}{3}), \quad (\mathbf{3}, \mathbf{1}, -\tfrac{4}{3}), \quad (\mathbf{3}, \mathbf{1}, \tfrac{5}{3}), \\ (\mathbf{6}, \mathbf{1}, \tfrac{1}{3}), \quad (\mathbf{6}, \mathbf{1}, -\tfrac{2}{3}), \quad (\mathbf{6}, \mathbf{1}, \tfrac{4}{3}), \\ (\mathbf{8}, \mathbf{1}, 0), \quad (\mathbf{8}, \mathbf{1}, 1). \end{gathered} \tag{170}$$

These representations are shown in Table 6, along with the complete set of couplings to fermion bilinears which respect the full SM gauge symmetry. The table also indicates the corresponding decays of ϕ_A and the twin fermion mass terms generated by each coupling, which will be discussed in more detail below. We will also make a few brief remarks below regarding possible couplings beyond those in Table 6.

Fermion bilinear	Hypercharge	$SU(3)_c$	Φ
(QQ)	$1/3$	$\bar{\mathbf{3}}+\mathbf{6}$	$(\mathbf{3},\mathbf{1},-\frac{1}{3})$, $(\bar{\mathbf{6}},\mathbf{1},-\frac{1}{3})$
$(H^\dagger Q)(QH)$	$1/3$	$\bar{\mathbf{3}}+\mathbf{6}$	$(\mathbf{3},\mathbf{1},-\frac{1}{3})$, $(\bar{\mathbf{6}},\mathbf{1},-\frac{1}{3})$
$(QH)(QH)$	$4/3$	$\bar{\mathbf{3}}+\mathbf{6}$	$(\mathbf{3},\mathbf{1},-\frac{4}{3})$, $(\bar{\mathbf{6}},\mathbf{1},-\frac{4}{3})$
$(H^\dagger Q)(H^\dagger Q)$	$-2/3$	$\bar{\mathbf{3}}+\mathbf{6}$	$(\mathbf{3},\mathbf{1},\frac{2}{3})$, $(\bar{\mathbf{6}},\mathbf{1},\frac{2}{3})$
$(QH)\,\bar{u}$	0	$\mathbf{1}+\mathbf{8}$	$(\mathbf{8},\mathbf{1},0)$
$(H^\dagger Q)\,\bar{u}$	-1	$\mathbf{1}+\mathbf{8}$	$(\mathbf{8},\mathbf{1},1)$
$(QH)\,\bar{d}$	1	$\mathbf{1}+\mathbf{8}$	$(\mathbf{8},\mathbf{1},-1)$
$(H^\dagger Q)\,\bar{d}$	0	$\mathbf{1}+\mathbf{8}$	$(\mathbf{8},\mathbf{1},0)$
(QL)	$-1/3$	$\mathbf{3}$	$(\bar{\mathbf{3}},\mathbf{1},\frac{1}{3})$
$(H^\dagger Q)(LH)$	$-1/3$	$\mathbf{3}$	$(\bar{\mathbf{3}},\mathbf{1},\frac{1}{3})$
$(QH)(H^\dagger L)$	$-1/3$	$\mathbf{3}$	$(\bar{\mathbf{3}},\mathbf{1},\frac{1}{3})$
$(QH)(LH)$	$2/3$	$\mathbf{3}$	$(\bar{\mathbf{3}},\mathbf{1},-\frac{2}{3})$
$(H^\dagger Q)(H^\dagger L)$	$-4/3$	$\mathbf{3}$	$(\bar{\mathbf{3}},\mathbf{1},\frac{4}{3})$
$(QH)\,\bar{e}$	$5/3$	$\mathbf{3}$	$(\bar{\mathbf{3}},\mathbf{1},-\frac{5}{3})$
$(H^\dagger Q)\,\bar{e}$	$2/3$	$\mathbf{3}$	$(\bar{\mathbf{3}},\mathbf{1},-\frac{2}{3})$
$\bar{u}\,\bar{u}$	$-4/3$	$\mathbf{3}+\bar{\mathbf{6}}$	$(\bar{\mathbf{3}},\mathbf{1},\frac{4}{3})$, $(\mathbf{6},\mathbf{1},\frac{4}{3})$
$\bar{u}\,\bar{d}$	$-1/3$	$\mathbf{3}+\bar{\mathbf{6}}$	$(\bar{\mathbf{3}},\mathbf{1},\frac{1}{3})$, $(\mathbf{6},\mathbf{1},\frac{1}{3})$
$\bar{u}\,(LH)$	$-2/3$	$\bar{\mathbf{3}}$	$(\mathbf{3},\mathbf{1},\frac{2}{3})$
$\bar{u}\,(H^\dagger L)$	$-5/3$	$\bar{\mathbf{3}}$	$(\mathbf{3},\mathbf{1},\frac{5}{3})$
$\bar{u}\,\bar{e}$	$1/3$	$\bar{\mathbf{3}}$	$(\mathbf{3},\mathbf{1},-\frac{1}{3})$
$\bar{d}\,\bar{d}$	$2/3$	$\mathbf{3}+\bar{\mathbf{6}}$	$(\bar{\mathbf{3}},\mathbf{1},-\frac{2}{3})$, $(\mathbf{6},\mathbf{1},-\frac{2}{3})$
$\bar{d}\,(LH)$	$1/3$	$\bar{\mathbf{3}}$	$(\mathbf{3},\mathbf{1},-\frac{1}{3})$
$\bar{d}\,(H^\dagger L)$	$-2/3$	$\bar{\mathbf{3}}$	$(\mathbf{3},\mathbf{1},\frac{2}{3})$
$\bar{d}\,\bar{e}$	$4/3$	$\bar{\mathbf{3}}$	$(\mathbf{3},\mathbf{1},-\frac{4}{3})$

Table 5: $SU(2)_L$ singlet operators with nontrivial color charge containing a fermion bilinear. The final column shows scalar field representations that couple to the operator.

Φ	Coupling to fermion bilinear	ϕ_A decay	Twin fermion mass terms	
			$[SU(2)_c \times U(1)'_{\rm EM}]_B$	
$(\mathbf{3},\mathbf{1},-\frac{1}{3})$	$\Phi\,(Q\,Q)$	$\phi_A \to \bar{u}\,\bar{d}$	$\hat{u}_B\,\hat{d}_B$	
	$\Phi^\dagger\,(Q\,L)$	$\phi_A \to u\,e, d\,\nu$	$\hat{u}_{B3}\,e_B,\ \hat{d}_{B3}\,\nu_B$	
	$\Phi^\dagger\,\bar{u}\,\bar{d}$	$\phi_A \to \bar{u}\,\bar{d}$	$\hat{\bar{u}}_B\,\hat{\bar{d}}_B$	
	$\Phi\,\bar{u}\,\bar{e}$	$\phi_A \to u\,e$	$\hat{\bar{u}}_{B3}\,\bar{e}_B$	
	$\Phi\,\bar{d}\,(L\,H)$	$\phi_A \to d\,\nu$	$\hat{\bar{d}}_{B3}\,\nu_B$	
	$\Phi\,(H^\dagger Q)(Q\,H)$	$\phi_A \to \bar{u}\,\bar{d}$	$\hat{u}_B\hat{d}_B$	
	$\Phi^\dagger\,(H^\dagger Q)(L\,H)$	$\phi_A \to d\nu$	$\hat{d}_{B3}\,\nu_B$	
	$\Phi^\dagger\,(Q\,H)(H^\dagger L)$	$\phi_A \to u\,e$	$\hat{u}_{B3}\,e_B$	
$(\mathbf{3},\mathbf{1},\frac{2}{3})$	$\Phi^\dagger\,\bar{d}\,\bar{d}$	$\phi_A \to \bar{d}\,\bar{d}$	$\hat{\bar{d}}_B\,\hat{\bar{d}}_B$	
	$\Phi\,\bar{u}\,(L\,H)$	$\phi_A \to u\,\nu$	$\hat{\bar{u}}_{B3}\,\nu_B$	
	$\Phi\,\bar{d}\,(H^\dagger L)$	$\phi_A \to d\,\bar{e}$	$\hat{\bar{d}}_{B3}\,e_B$	
	$\Phi^\dagger\,(H^\dagger Q)\,\bar{e}$	$\phi_A \to d\,\bar{e}$	$\hat{d}_{B3}\,\bar{e}_B$	
	$\Phi\,(H^\dagger Q)(H^\dagger Q)$	$\phi_A \to \bar{d}\,\bar{d}$	$\hat{d}_B\,\hat{d}_B$	
	$\Phi^\dagger\,(Q\,H)(L\,H)$	$\phi_A \to u\,\nu$	$\hat{u}_{B3}\,\nu_B$	
$(\mathbf{3},\mathbf{1},-\frac{4}{3})$	$\Phi^\dagger\,\bar{u}\,\bar{u}$	$\phi_A \to \bar{u}\,\bar{u}$	$\hat{\bar{u}}_B\,\hat{\bar{u}}_B$	
	$\Phi\,\bar{d}\,\bar{e}$	$\phi_A \to d\,e$	$\hat{\bar{d}}_{B3}\,\bar{e}_B$	
	$\Phi\,(Q\,H)\,(Q\,H)$	$\phi_A \to \bar{u}\,\bar{u}$	$\hat{u}_B\,\hat{u}_B$	
	$\Phi^\dagger\,(H^\dagger Q)(H^\dagger L)$	$\phi_A \to d\,e$	$\hat{d}_{B3}\,e_B$	
$(\mathbf{3},\mathbf{1},\frac{5}{3})$	$\Phi^\dagger\,(Q\,H)\,\bar{e}$	$\phi_A \to u\,\bar{e}$	$\hat{u}_{B3}\,\bar{e}_B$	
	$\Phi\,\bar{u}\,(H^\dagger L)$	$\phi_A \to u\,\bar{e}$	$\hat{\bar{u}}_{B3}\,e_B$	
			$[SU(2)_c \times U(1)'_{\rm EM}]_B$	$[SO(3)_c]_B$
$(\mathbf{6},\mathbf{1},\frac{1}{3})$	$\Phi^\dagger\,(Q\,Q)$	$\phi_A \to u\,d$	$\hat{u}_{B3}\,\hat{d}_{B3}$	$u_B\,d_B$
	$\Phi\,\bar{u}\,\bar{d}$	$\phi_A \to u\,d$	$\hat{\bar{u}}_{B3}\,\hat{\bar{d}}_{B3}$	$\bar{u}_B\,\bar{d}_B$
	$\Phi^\dagger\,(Q\,H)(H^\dagger Q)$	$\phi_A \to u\,d$	$\hat{u}_{B3}\,\hat{d}_{B3}$	$u_B\,d_B$
$(\mathbf{6},\mathbf{1},-\frac{2}{3})$	$\Phi\,\bar{d}\,\bar{d}$	$\phi_A \to d\,d$	$\hat{\bar{d}}_{B3}\,\hat{\bar{d}}_{B3}$	$\bar{d}_B\,\bar{d}_B$
	$\Phi^\dagger(H^\dagger Q)(H^\dagger Q)$	$\phi_A \to d\,d$	$\hat{d}_{B3}\,\hat{d}_{B3}$	$d_B\,d_B$
$(\mathbf{6},\mathbf{1},\frac{4}{3})$	$\Phi\,\bar{u}\,\bar{u}$	$\phi_A \to u\,u$	$\hat{\bar{u}}_{B3}\,\hat{\bar{u}}_{B3}$	$\bar{u}_B\,\bar{u}_B$
	$\Phi^\dagger(Q\,H)(Q\,H)$	$\phi_A \to u\,u$	$\hat{u}_{B3}\,\hat{u}_{B3}$	$u_B\,u_B$
			$[SU(2)_c \times U(1)_c \times U(1)_{\rm EM}]_B$	$[U(1)_c \times U(1)'_c \times U(1)_{\rm EM}]_B$
$(\mathbf{8},\mathbf{1},0)$	$\Phi\,(Q\,H)\bar{u}$	$\phi_A \to u\,\bar{u}$	$\hat{u}_B\,\hat{\bar{u}}_B - 2\hat{u}_{B3}\,\hat{\bar{u}}_{B3}$	$\hat{u}_{B1}\,\hat{\bar{u}}_{B1} - \hat{u}_{B2}\,\hat{\bar{u}}_{B2}$
	$\Phi\,(H^\dagger Q)\bar{d}$	$\phi_A \to d\,\bar{d}$	$\hat{d}_B\,\hat{\bar{d}}_B - 2\hat{d}_{B3}\,\hat{\bar{d}}_{B3}$	$\hat{d}_{B1}\,\hat{\bar{d}}_{B1} - \hat{d}_{B2}\,\hat{\bar{d}}_{B2}$

Table 6: $SU(2)_L$ singlet scalar representations and allowed couplings to fermion bilinears. Each coupling leads to the indicated decays of ϕ_A to SM fermions, as well as new twin fermion mass terms for the indicated unbroken twin gauge symmetry.

6.1 Lagrangians

We now write the allowed couplings of the colored scalar to fermions for each of the cases listed in Eq. (170)

6.1.1 $\Phi \sim (\mathbf{3}, \mathbf{1}, \frac{2}{3})$

We note that in this case $\Phi^\dagger$ has the same quantum numbers of the $SU(2)_L$ singlet quark $\bar{u}$. The Lagrangian contains the following interactions:

$$\begin{aligned} -\mathcal{L} \supset & \frac{1}{2}\lambda_{\bar{d}\bar{d}}\, \Phi^\dagger \bar{d}\, \bar{d} + \frac{c_{\bar{u}L}}{\Lambda}\, \Phi\, \bar{u}\, (LH) + \frac{c_{\bar{d}L}}{\Lambda}\, \Phi\, \bar{d}\, (H^\dagger L) + \frac{c_{Q\bar{e}}}{\Lambda}\, \Phi^\dagger (H^\dagger Q)\, \bar{e} \\ & + \frac{c_{QQ}}{2\Lambda^2}\, \Phi\, (H^\dagger Q)(H^\dagger Q) + \frac{c_{QL}}{\Lambda^2}\, \Phi^\dagger\, (QH)(LH) + \text{H.c.} \end{aligned} \tag{171}$$

We have suppressed all indices in writing the Lagrangian, but it is straightforward to restore them as needed. A couple of examples are given below:

$$\begin{aligned} \frac{1}{2}\lambda_{\bar{d}\bar{d}}\, \Phi^\dagger \bar{d}\, \bar{d} &= \frac{1}{2}(\lambda_{\bar{d}\bar{d}})_{IJ}\, \epsilon_{ijk}\, \Phi^{\dagger i} \bar{d}^{jI}\, \bar{d}^{kJ}, \\ \frac{c_{\bar{u}L}}{\Lambda}\, \Phi\, \bar{u}\, (LH) &= \frac{(c_{\bar{u}L})^J_I}{\Lambda}\, \Phi_i\, \bar{u}^{iI}\, \epsilon^{\alpha\beta} L_{\alpha J} H_\beta, \end{aligned} \tag{172}$$

where I, J are generation indices, i, j, k are color indices, and a, b are $SU(2)_L$ indices. We note that the couplings $\lambda_{\bar{d}\bar{d}}$, c_{QQ} in Eq. (171) are antisymmetric in the generation space, i.e., $(\lambda_{\bar{d}\bar{d}})_{JI} = -(\lambda_{\bar{d}\bar{d}})_{IJ}$, etc.

6.1.2 $\Phi \sim (\mathbf{3}, \mathbf{1}, -\frac{1}{3})$

We note that in this case $\Phi^\dagger$ has the same quantum numbers of the $SU(2)_L$ singlet quark $\bar{d}$. The Lagrangian contains the following interactions:

$$\begin{aligned} -\mathcal{L} \supset & \frac{1}{2}\lambda_{QQ}\, \Phi (QQ) + \lambda_{QL}\, \Phi^\dagger (QL) + \lambda_{\bar{u}\bar{d}}\, \Phi^\dagger\, \bar{u}\, \bar{d} + \lambda_{\bar{u}\bar{e}}\, \Phi\, \bar{u}\, \bar{e} + \frac{c_{\bar{d}L}}{\Lambda}\, \Phi\, \bar{d}\, (LH) \\ & + \frac{c_{QQ}}{\Lambda^2}\, \Phi\, (QH)\, (H^\dagger Q) + \frac{c_{QL1}}{\Lambda^2}\, \Phi^\dagger\, (H^\dagger Q)(LH) + \frac{c_{QL2}}{\Lambda^2}\, \Phi^\dagger\, (QH)(H^\dagger L) + \text{H.c.} \end{aligned} \tag{173}$$

The coupling λ_{QQ} in Eq. (173) is symmetric in the generation space, $(\lambda_{QQ})^{JI} = (\lambda_{QQ})^{IJ}$.

6.1.3 $\Phi \sim (\mathbf{3}, \mathbf{1}, -\frac{4}{3})$

The Lagrangian contains the following interactions:

$$-\mathcal{L} \supset \frac{1}{2}\lambda_{\bar{u}\bar{u}}\,\Phi^\dagger \bar{u}\,\bar{u} + \lambda_{\bar{d}\bar{e}}\,\Phi\,\bar{d}\,\bar{e} + \frac{c_{QQ}}{2\Lambda^2}\,\Phi\,(QH)(QH) + \frac{c_{QL}}{\Lambda^2}\,\Phi^\dagger\,(H^\dagger Q)(H^\dagger L) + \text{H.c.} \tag{174}$$

The couplings $\lambda_{\bar{u}\bar{u}}$, c_{QQ} in Eq. (174) are antisymmetric in the generation space.

6.1.4 $\Phi \sim (\mathbf{3}, \mathbf{1}, \frac{5}{3})$

The Lagrangian contains the following interactions:

$$-\mathcal{L} \supset \frac{c_{Q\bar{e}}}{\Lambda}\,\Phi^\dagger (QH)\,\bar{e} + \frac{c_{\bar{u}L}}{\Lambda}\,\Phi\,\bar{u}\,(H^\dagger L) + \text{H.c.} \tag{175}$$

6.1.5 $\Phi \sim (\mathbf{6}, \mathbf{1}, \frac{1}{3})$

The Lagrangian contains the following interactions:

$$-\mathcal{L} \supset \frac{1}{2}\lambda_{QQ}\,\Phi^\dagger (QQ) + \lambda_{\bar{u}\bar{d}}\,\Phi\,\bar{u}\,\bar{d} + \frac{c_{QQ}}{\Lambda^2}\,\Phi^\dagger\,(H^\dagger Q)(QH) + \text{H.c.} \tag{176}$$

The couplings λ_{QQ} in Eq. (176) is antisymmetric in the generation space.

6.1.6 $\Phi \sim (\mathbf{6}, \mathbf{1}, -\frac{2}{3})$

The Lagrangian contains the following interactions:

$$-\mathcal{L} \supset \frac{1}{2}\lambda_{\bar{d}\bar{d}}\,\Phi\,\bar{d}\,\bar{d} + \frac{c_{QQ}}{2\Lambda^2}\,\Phi^\dagger\,(H^\dagger Q)(H^\dagger Q) + \text{H.c.} \tag{177}$$

The couplings $\lambda_{\bar{d}\bar{d}}$, c_{QQ} in Eq. (177) are symmetric in the generation space.

6.1.7 $\Phi \sim (\mathbf{6}, \mathbf{1}, \frac{4}{3})$

The Lagrangian contains the following interactions:

$$-\mathcal{L} \supset \frac{1}{2}\lambda_{\bar{u}\bar{u}}\,\Phi\,\bar{u}\,\bar{u} + \frac{c_{QQ}}{2\Lambda^2}\,\Phi^\dagger (QH)(QH) + \text{H.c.} \tag{178}$$

The couplings $\lambda_{\bar{u}\bar{u}}$, c_{QQ} in Eq. (178) are symmetric in the generation space.

6.1.8 $\Phi \sim (\mathbf{8}, \mathbf{1}, 0)$

The Lagrangian contains the following interactions:

$$-\mathcal{L} \supset \frac{c_{Q\bar{u}}}{\Lambda}\,\Phi(QH)\,\bar{u} + \frac{c_{Q\bar{d}}}{\Lambda}\,\Phi(H^\dagger Q)\,\bar{d} + \text{H.c.} \tag{179}$$

6.1.9 $\Phi \sim (\mathbf{8}, \mathbf{1}, 1)$

[1] The Lagrangian contains the following interactions:

$$-\mathcal{L} \supset \frac{c_{Q\bar{u}}}{\Lambda}\,\Phi\,(H^\dagger Q)\,\bar{u} + \frac{c_{Q\bar{d}}}{\Lambda}\,\Phi^\dagger(QH)\,\bar{d} + \text{H.c.} \tag{180}$$

6.2 Decay of ϕ_A

Here we consider the allowed decay modes of the colored scalar to fermions for each of the cases listed in Eq. (170).

6.2.1 $\Phi \sim (\mathbf{3}, \mathbf{1}, \frac{2}{3})$

The Lagrangian contains the following interactions:

$$\begin{aligned}
-\mathcal{L} \supset\ & \frac{1}{2}\lambda_{\bar{d}\bar{d}}\,\Phi_A^\dagger\,\bar{d}_A\,\bar{d}_A + \frac{c_{\bar{u}L}}{\Lambda}\,\Phi_A\,\bar{u}_A\,(L_A H_A) + \frac{c_{\bar{d}L}}{\Lambda}\,\Phi_A\,\bar{d}_A\,(H_A^\dagger L_A) + \frac{c_{Q\bar{e}}}{\Lambda}\,\Phi_A^\dagger(H_A^\dagger Q_A)\,\bar{e}_A \\
& + \frac{c_{QQ}}{2\Lambda^2}\,\Phi_A\,(H_A^\dagger Q_A)(H_A^\dagger Q_A) + \frac{c_{QL}}{\Lambda^2}\,\Phi_A^\dagger\,(Q_A H_A)(L_A H_A) + \text{H.c.} \\
\supset\ & \frac{1}{2}\lambda_{\bar{d}\bar{d}}\,\phi_A^\dagger\,\bar{d}_A\,\bar{d}_A + \frac{c_{\bar{u}L}v_A}{\sqrt{2}\Lambda}\,\phi_A\,\bar{u}_A\,\nu_A\ + \frac{c_{\bar{d}L}v_A}{\sqrt{2}\Lambda}\,\phi_A\,\bar{d}_A\,e_A + \frac{c_{Q\bar{e}}v_A}{\sqrt{2}\Lambda}\,\phi_A^\dagger\,d_A\,\bar{e}_A \\
& + \frac{c_{QQ}v_A^2}{4\Lambda^2}\,\phi_A\,d_A\,d_A + \frac{c_{QL}v_A^2}{2\Lambda^2}\,\phi_A^\dagger\,u_A\,\nu_A + \text{H.c.}
\end{aligned} \tag{181}$$

where in the second line we have used Eqs. (27,61). The interactions in Eq. (181) lead to the following decays of ϕ_A:

$$\begin{aligned}
\phi_A\ &\to \bar{d} + \bar{d} \qquad (\phi_A \to j + j), \\
\phi_A\ &\to u + \nu \qquad (\phi_A \to j + \not{E}_T), \\
\phi_A\ &\to d + \bar{e} \qquad (\phi_A \to j + \ell^+).
\end{aligned} \tag{182}$$

[1] list here for future convenience, though not really considered in our models.

A word on notation here: as an example $\bar{d}$ above (without the subscript A) denotes the outgoing particle state in the decay rather than the field variable in the Lagrangian, in this case anti-down quark. On the other hand, d denotes down quark. Different flavors particle are of course possible in the decays above. Furthermore ν denotes neutrino or anti-neutrino.

6.2.2 $\Phi \sim (\mathbf{3}, \mathbf{1}, -\frac{1}{3})$

The Lagrangian contains the following interactions:

$$\begin{aligned}
-\mathcal{L} \supset\ & \frac{1}{2}\lambda_{QQ}\,\Phi_A(Q_A Q_A) + \lambda_{QL}\,\Phi_A^\dagger(Q_A L_A) + \lambda_{\bar{u}\bar{d}}\,\Phi_A^\dagger\,\bar{u}_A\,\bar{d}_A + \lambda_{\bar{u}\bar{e}}\,\Phi_A\,\bar{u}_A\,\bar{e}_A + \frac{c_{\bar{d}L}}{\Lambda}\,\Phi_A\,\bar{d}_A\,(L_A H_A) \\
& + \frac{c_{QQ}}{\Lambda^2}\,\Phi_A\,(Q_A H_A)\,(H_A^\dagger Q_A) + \frac{c_{QL1}}{\Lambda^2}\,\Phi_A^\dagger\,(H_A^\dagger Q_A)(L_A H_A) + \frac{c_{QL2}}{\Lambda^2}\,\Phi_A^\dagger\,(Q_A H_A)(H_A^\dagger L_A) + \text{H.c.} \\
\supset\ & \lambda_{QQ}\,\phi_A\,u_A\,d_A + \lambda_{QL}\,\phi_A^\dagger\,u_A\,e_A - \lambda_{QL}\,\phi_A^\dagger\,d_A\,\nu_A + \lambda_{\bar{u}\bar{d}}\,\phi_A^\dagger\,\bar{u}_A\,\bar{d}_A + \lambda_{\bar{u}\bar{e}}\,\phi_A\,\bar{u}_A\,\bar{e}_A \\
& + \frac{c_{\bar{d}L} v_A}{\sqrt{2}\Lambda}\,\phi_A\,\bar{d}_A\,\nu_A + \frac{c_{QQ} v_A^2}{2\Lambda^2}\,\phi_A\,u_A\,d_A + \frac{c_{QL1} v_A^2}{2\Lambda^2}\,\phi_A^\dagger\,d_A\,\nu_A + \frac{c_{QL2} v_A^2}{2\Lambda^2}\,\phi_A^\dagger\,u_A\,e_A + \text{H.c.}
\end{aligned} \tag{183}$$

The interactions in Eq. (235) lead to the following decays of ϕ_A:

$$\begin{aligned}
\phi_A &\to \bar{u} + \bar{d} \qquad (\phi_A \to j + j), \\
\phi_A &\to u + e \qquad (\phi_A \to j + \ell^-), \\
\phi_A &\to d + \nu \qquad (\phi_A \to j + \not{E}_T).
\end{aligned} \tag{184}$$

6.2.3 $\Phi \sim (\mathbf{3}, \mathbf{1}, -\frac{4}{3})$

The Lagrangian contains the following interactions:

$$\begin{aligned}
-\mathcal{L} \supset\ & \frac{1}{2}\lambda_{\bar{u}\bar{u}}\,\Phi_A^\dagger \bar{u}_A\,\bar{u}_A + \lambda_{\bar{d}\bar{e}}\,\Phi_A\,\bar{d}_A\,\bar{e}_A + \frac{c_{QQ}}{2\Lambda^2}\,\Phi_A\,(Q_A H_A)(Q_A H_A) + \frac{c_{QL}}{\Lambda^2}\,\Phi_A^\dagger\,(H_A^\dagger Q_A)(H_A^\dagger L_A) + \text{H.c.} \\
\supset\ & \frac{1}{2}\lambda_{\bar{u}\bar{u}}\,\phi_A^\dagger \bar{u}_A\,\bar{u}_A + \lambda_{\bar{d}\bar{e}}\,\phi_A\,\bar{d}_A\,\bar{e}_A + \frac{c_{QQ} v_A^2}{4\Lambda^2}\,\phi_A\,u_A\,u_A + \frac{c_{QL} v_A^2}{2\Lambda^2}\,\phi_A^\dagger\,d_A\,e_A + \text{H.c.}
\end{aligned} \tag{185}$$

The interactions in Eq. (185) lead to the following decays of ϕ_A:

$$\begin{aligned}
\phi_A &\to \bar{u} + \bar{u} \qquad (\phi_A \to j + j), \\
\phi_A &\to d + e \qquad (\phi_A \to j + \ell^-).
\end{aligned} \tag{186}$$

6.2.4 $\Phi \sim (\mathbf{3}, \mathbf{1}, \frac{5}{3})$

The Lagrangian contains the following interactions:

$$\begin{aligned} -\mathcal{L} &\supset \frac{c_{Q\bar{e}}}{\Lambda}\,\Phi_A^\dagger (Q_A H_A)\,\bar{e}_A + \frac{c_{\bar{u}L}}{\Lambda}\,\Phi_A\,\bar{u}_A\,(H_A^\dagger L_A) + \text{H.c.} \\ &\supset \frac{c_{Q\bar{e}} v_A}{\sqrt{2}\Lambda}\,\phi_A^\dagger\,u_A\,\bar{e}_A + \frac{c_{\bar{u}L} v_A}{\sqrt{2}\Lambda}\,\phi_A\,\bar{u}_A\,e_A + \text{H.c.} \end{aligned} \tag{187}$$

The interactions in Eq. (187) lead to the following decays of ϕ_A:

$$\phi_A \;\; \to u + \bar{e} \qquad (\phi_A \to j + \ell^+). \tag{188}$$

6.2.5 $\Phi \sim (\mathbf{6}, \mathbf{1}, \frac{1}{3})$

The Lagrangian contains the following interactions:

$$\begin{aligned} -\mathcal{L} &\supset \frac{1}{2}\lambda_{QQ}\,\Phi_A^\dagger (Q_A Q_A) + \lambda_{\bar{u}\bar{d}}\,\Phi_A\,\bar{u}_A\,\bar{d}_A + \frac{c_{QQ}}{\Lambda^2}\,\Phi_A^\dagger\,(H_A^\dagger Q_A)(Q_A H_A) + \text{H.c.} \\ &\supset \lambda_{QQ}\,\phi_A^\dagger\,u_A\,d_A + \lambda_{\bar{u}\bar{d}}\,\phi_A\,\bar{u}_A\,\bar{d}_A + \frac{c_{QQ} v_A^2}{2\Lambda^2}\,\phi_A^\dagger\,u_A\,d_A + \text{H.c.} \end{aligned} \tag{189}$$

The interactions in Eq. (189) lead to the following decays of ϕ_A:

$$\phi_A \;\; \to u + d \qquad (\phi_A \to j + j). \tag{190}$$

6.2.6 $\Phi \sim (\mathbf{6}, \mathbf{1}, -\frac{2}{3})$

The Lagrangian contains the following interactions:

$$\begin{aligned} -\mathcal{L} &\supset \frac{1}{2}\lambda_{\bar{d}\bar{d}}\,\Phi_A\,\bar{d}_A\,\bar{d}_A + \frac{c_{QQ}}{2\Lambda^2}\,\Phi_A^\dagger\,(H_A^\dagger Q_A)(H_A^\dagger Q_A) + \text{H.c.} \\ &\supset \frac{1}{2}\lambda_{\bar{d}\bar{d}}\,\phi_A\,\bar{d}_A\,\bar{d}_A + \frac{c_{QQ} v_A^2}{4\Lambda^2}\,\phi_A^\dagger\,d_A\,d_A + \text{H.c.} \end{aligned} \tag{191}$$

The interactions in Eq. (191) lead to the following decays of ϕ_A:

$$\phi_A \;\; \to d + d \qquad (\phi_A \to j + j). \tag{192}$$

6.2.7 $\Phi \sim (\mathbf{6}, \mathbf{1}, \frac{4}{3})$

The Lagrangian contains the following interactions:

$$\begin{aligned} -\mathcal{L} &\supset \frac{1}{2}\lambda_{\bar{u}\bar{u}}\,\Phi_A\,\bar{u}_A\,\bar{u}_A + \frac{c_{QQ}}{2\Lambda^2}\,\Phi_A^\dagger (Q_A H_A)(Q_A H_A) + \text{H.c.} \\ &\supset \frac{1}{2}\lambda_{\bar{u}\bar{u}}\,\phi_A\,\bar{u}_A\,\bar{u}_A + \frac{c_{QQ} v_A^2}{4\Lambda^2}\,\phi_A^\dagger\,u_A\,u_A + \text{H.c.} \end{aligned} \tag{193}$$

The interactions in Eq. (193) lead to the following decays of ϕ_A:

$$\phi_A \;\to u + u \qquad (\phi_A \to j + j). \tag{194}$$

6.2.8 $\Phi \sim (\mathbf{8}, \mathbf{1}, 0)$

The Lagrangian contains the following interactions:

$$\begin{aligned} -\mathcal{L} &\supset \frac{c_{Q\bar{u}}}{\Lambda}\,\Phi_A (Q_A H_A)\,\bar{u}_A + \frac{c_{Q\bar{d}}}{\Lambda}\,\Phi_A (H_A^\dagger Q_A)\,\bar{d}_A + \text{H.c.} \\ &\supset \frac{c_{Q\bar{u}}\,v_A}{\sqrt{2}\Lambda}\,\phi_A\,u_A\,\bar{u}_A + \frac{c_{Q\bar{d}}\,v_A}{\sqrt{2}\Lambda}\,\phi_A\,d_A\,\bar{d}_A + \text{H.c.} \end{aligned} \tag{195}$$

The interactions in Eq. (240) lead to the following decays of ϕ_A:

$$\begin{aligned} \phi_A \;&\to u + \bar{u} \qquad (\phi_A \to j + j). \\ \phi_A \;&\to d + \bar{d} \qquad (\phi_A \to j + j). \end{aligned} \tag{196}$$

6.2.9 $\Phi \sim (\mathbf{8}, \mathbf{1}, 1)$

[2] The Lagrangian contains the following interactions:

$$\begin{aligned} -\mathcal{L} &\supset \frac{c_{Q\bar{u}}}{\Lambda}\,\Phi\,(H^\dagger Q)\,\bar{u} + \frac{c_{Q\bar{d}}}{\Lambda}\,\Phi^\dagger (Q H)\,\bar{d} + \text{H.c.} \\ &\supset \frac{c_{Q\bar{u}}\,v_A}{\sqrt{2}\Lambda}\,\phi_A\,d_A\,\bar{u}_A + \frac{c_{Q\bar{d}}\,v_A}{\sqrt{2}\Lambda}\,\phi_A^\dagger\,u_A\,\bar{d}_A + \text{H.c.} \end{aligned} \tag{197}$$

The interactions in Eq. (240) lead to the following decays of ϕ_A:

$$\phi_A \;\to u + \bar{d} \qquad (\phi_A \to j + j). \tag{198}$$

[2] list here for future convenience, though not really considered in our models.

6.2.10 Summary

In summary, from Table 6, the visible sector colored scalars ϕ_A can decay in a variety of ways, depending on their quantum numbers and the particular couplings allowed by gauge symmetry. Color triplets can decay to a pair of SM quarks, a quark and a neutrino, or a quark and a charged lepton. For example, the scalar $\Phi_A \sim (\mathbf{3}, \mathbf{1}, \frac{2}{3})$ decays as $\phi_A \to \bar{d}\,\bar{d}, u\,\nu, d\,\bar{e}$. On the other hand, color sextets (octets) decay strictly to pairs of quarks (quark-antiquark pairs). For instance, in the case of the sextet scalar $\Phi \sim (\mathbf{6}, \mathbf{1}, -\frac{2}{3})$ decays as $\phi_A \to dd$.

Taking into account the various flavors of quark and lepton, there are a variety of potential collider signatures of the colored scalars, which we explore in Chapter 8. Of course, the colored scalar can decay in more channels than those listed in Table 6. One possibility is that ϕ_A decays to a pair of SM bosons. For instance, the color octet may decay to a pair of gluons through the dimension five operator $\mathrm{Tr}\,\Phi_A G_A G_A$. Another interesting possibility emerges if operators that couple fields in the two sectors are present. These are typically higher dimension operators, and can naturally arise when 'singlet' fields [138], which transform by at most a sign under $\mathbb{Z}_2$, are integrated out. As an example, taking $\Phi_{A,B} \sim (\mathbf{3}, \mathbf{1}, \frac{2}{3})$, we can write the operator $(\Phi_A \bar{u}_A)(\Phi_B \bar{u}_B) \supset f_\Phi\, \phi_A \bar{u}_A \hat{\bar{u}}_{B3}$, leading to the decay of ϕ_A to one SM quark and one twin quark. The same operator could allow the twin quark to decay back into the visible sector via an off-shell ϕ_A.

6.3 Twin Fermion Mass Terms

6.3.1 Technical Note On Fermion Masses In $SU(2)$ Gauge Theory

Consider an $SU(2)$ gauge theory with two flavors of left chirality fermions in the fundamental representation. We can write these fermions as

$$\psi = \psi_{\alpha\hat{\imath}}, \qquad \chi = \chi_{\alpha\hat{\imath}} \tag{199}$$

where α is a Lorentz spinor index and $\hat{i}$ is an $SU(2)$ color index. We can write a mass term coupling the two fermions in several ways:

$$\begin{aligned} -\mathcal{L} &\supset m\,\psi\,\chi + \text{H.c.} \\ &= m\,\epsilon^{\alpha\beta}\,\epsilon^{\hat{i}\hat{j}}\,\psi_{\beta\,\hat{j}}\,\chi_{\alpha\,\hat{i}} + \text{H.c.} \\ &= -m\,\epsilon^{\alpha\beta}\,\epsilon^{\hat{i}\hat{j}}\,\chi_{\beta\,\hat{j}}\,\psi_{\alpha\,\hat{i}} + \text{H.c.} \\ &= -m\,\chi\,\psi + \text{H.c.} \\ &= \frac{1}{2}m\,\psi\,\chi - \frac{1}{2}m\,\chi\,\psi + \text{H.c.} \\ &= \frac{1}{2}\begin{bmatrix}\psi & \chi\end{bmatrix}\begin{bmatrix}0 & m \\ -m & 0\end{bmatrix}\begin{bmatrix}\psi \\ \chi\end{bmatrix} + \text{H.c.} \end{aligned} \tag{200}$$

From the equation above, we can also see that a mass term involving the same fermion vanishes identically, i.e.,

$$\psi\psi = 0. \tag{201}$$

6.3.2 Higgs Yukawa Couplings

We now examine the new twin fermion masses generated by Φ_B. These depend on the particular scalar representation and symmetry breaking pattern. For each model, there are of course the usual mass terms that arise solely from twin electroweak symmetry breaking,

$$\begin{aligned} -\mathcal{L} &\supset y_e(H_B^\dagger L_B)\,\bar{e}_B + y_u(Q_B H_B)\bar{u}_B + y_d(H_B^\dagger Q_B)\bar{d}_B + \frac{c_\nu}{\Lambda_\nu}(L_B H_B)(L_B H_B) + \text{H.c.} \\ &\supset \frac{y_\ell\,v_B}{\sqrt{2}}e_B\bar{e}_B + \frac{y_u\,v_B}{\sqrt{2}}u_B\bar{u}_B + \frac{y_d\,v_B}{\sqrt{2}}d_B\bar{d}_B + \frac{c_\nu\,v_B^2}{2\Lambda_\nu}\nu_B\nu_B + \text{H.c.} \end{aligned} \tag{202}$$

These terms generate twin fermion masses which are related to those in the SM by factors of $v_B/v_A = \cot\vartheta$.

6.3.3 $\Phi \sim (\mathbf{3}, \mathbf{1}, \frac{2}{3})$

The Lagrangian contains the following interactions:

$$\begin{aligned}
-\mathcal{L} \supset\ & \frac{1}{2}\lambda_{\bar{d}\bar{d}}\, \Phi_B^\dagger \bar{d}_B\, \bar{d}_B + \frac{c_{\bar{u}L}}{\Lambda}\, \Phi_B\, \bar{u}_B\, (L_B H_B) + \frac{c_{\bar{d}L}}{\Lambda}\, \Phi_B\, \bar{d}_B\, (H_B^\dagger L_B) + \frac{c_{Q\bar{e}}}{\Lambda}\, \Phi_B^\dagger (H_B^\dagger Q_B)\, \bar{e}_B \\
& + \frac{c_{QQ}}{2\Lambda^2}\, \Phi_B\, (H_B^\dagger Q_B)(H_B^\dagger Q_B) + \frac{c_{QL}}{\Lambda^2}\, \Phi_B^\dagger\, (Q_B H_B)(L_B H_B) + \text{H.c.} \\
\supset\ & \frac{1}{2}\lambda_{\bar{d}\bar{d}} f_\Phi\, \hat{\bar{d}}_B\, \hat{\bar{d}}_B + \frac{c_{\bar{u}L} v_B f_\Phi}{\sqrt{2}\Lambda}\, \hat{\bar{u}}^3_B\, \nu_B + \frac{c_{\bar{d}L} v_B f_\Phi}{\sqrt{2}\Lambda}\, \hat{\bar{d}}^3_B\, e_B + \frac{c_{Q\bar{e}} v_B f_\Phi}{\sqrt{2}\Lambda}\, \hat{d}^3_B\, \bar{e}_B \\
& - \frac{c_{QQ} v_B^2 f_\Phi}{4\Lambda^2}\, \hat{d}_B\, \hat{d}_B + \frac{c_{QL} v_B^2 f_\Phi}{2\Lambda^2}\, \hat{u}^3_B \nu_B + \text{H.c.}
\end{aligned} \tag{203}$$

where in the second line we have set the scalar to its VEV, $\langle \Phi_i \rangle = f_\Phi \delta_{i3}$ (Eq. (38)), effecting the spontaneous symmetry breakdown of $[SU(3)_c \times SU(2)_L \times U(1)_Y \to SU(2)_c \times U(1)'_{\text{EM}}]_B$. We have also used the quark decomposition in Eq. (112).

Interestingly, there are new mass terms in Eq. (203) beyond those generated by the Higgs VEV. In particular, we may have a "Majorana" type mass term for the down-type quark fields since they are not charged under the unbroken twin electromagnetic gauge symmetry; see Table 3[3]. There are also mass terms which marry (couple) "3rd color" ($[SU(2)_c]_B$ singlet) quark fields with neutrinos or charged leptons. From the electric charges in Table 3 it is easy to verify that the operators in the second line of Eq. (203) respect the unbroken twin electromagnetic gauge symmetry.

We have suppressed all indices in writing the Lagrangian, but it is straightforward to restore them as needed. A couple of examples from the second line in Eq. (203) are presented below:

$$\begin{aligned}
\frac{1}{2}\lambda_{\bar{d}\bar{d}} f_\Phi\, \hat{\bar{d}}_B\, \hat{\bar{d}}_B &= \frac{1}{2}(\lambda_{\bar{d}\bar{d}})_{IJ} f_\Phi\, \epsilon^{\hat{i}\hat{j}}\, \hat{\bar{d}}^{\,I}_{B\hat{j}}\, \hat{\bar{d}}^{\,J}_{B\hat{i}}, \\
\frac{c_{\bar{u}L} v_B f_\Phi}{\sqrt{2}\Lambda}\, \hat{\bar{u}}_{B3}\, \nu_B &= \frac{(c_{\bar{u}L})^J_I v_B f_\Phi}{\sqrt{2}\Lambda}\, \hat{\bar{u}}^{\,I}_{B3}\, \nu_{BJ}
\end{aligned} \tag{204}$$

where I, J are generation indices and $\hat{i}, \hat{j}$ are $[SU(2)_c]_B$ color indices. Hatted quark fields with definite $[SU(2)_c]_B$ transformation properties were defined in Eq. (112).

[3]Strictly speaking these are not Majorana mass terms, since they couple quarks of different flavor and color.

For convenience, we note here again that the couplings $\lambda_{\bar{d}\bar{d}}$, c_{QQ} in Eq. (171) are anti-symmetric in the generation space, i .e., $(\lambda_{\bar{d}\bar{d}})_{JI} = -(\lambda_{\bar{d}\bar{d}})_{IJ}$, etc.

Different physical mass hierarchies can arise depending on the size of the various couplings in Eq. (203). For instance, consider a simple case in which only $\lambda^{12}_{\bar{d}\bar{d}} = -\lambda^{21}_{\bar{d}\bar{d}} \neq 0$. Define the following mass parameters:

$$m_d = \frac{y_d v_B}{\sqrt{2}}, \qquad m_s = \frac{y_s v_B}{\sqrt{2}}, \qquad \overline{M}_d = \lambda^{12}_{\bar{d}\bar{d}} f_\Phi. \tag{205}$$

Using Eq. (112), and the convention in Eq. (200), we can then write the mass terms in the $[SU(2)_c]_B$ doublet down and strange sectors. We have from the Higgs Yukawa coupling (202)

$$\begin{aligned} -\mathcal{L} &\supset m_d \, d_{B\,i} \, \bar{d}^i_B + \text{H.c.} \\ &\supset m_d \, \epsilon^{\alpha\beta} \, \hat{d}_{B\,\beta\,\hat{i}} \, \epsilon^{\hat{i}\hat{j}} \, \hat{\bar{d}}_{B\alpha\hat{j}} + \text{H.c.} \\ &\supset m_d \, \epsilon^{\alpha\beta} \, \epsilon^{\hat{i}\hat{j}} \, \hat{\bar{d}}_{B\,\beta\,\hat{j}} \, \hat{d}_{B\alpha\hat{i}} + \text{H.c.} \\ &\supset m_d \, \hat{\bar{d}}_B \, \hat{d}_B + \text{H.c.} \end{aligned} \tag{206}$$

and similarly for the strange quark. From Eq. (203) we also get a term

$$\begin{aligned} -\mathcal{L} &\supset \frac{1}{2} \, \lambda^{IJ}_{\bar{d}\bar{d}} \, \epsilon_{\ell m n} \Phi^{\dagger\,\ell}_B \, \bar{d}^{m\,I}_B \, \bar{d}^{n\,J}_B + \text{H.c.} \\ &\supset \frac{1}{2} \, \lambda^{IJ}_{\bar{d}\bar{d}} f_\Phi \, \epsilon_{\hat{m}\hat{n}} \, \epsilon^{\hat{m}\hat{j}} \, \epsilon^{\hat{n}\hat{i}} \, \epsilon^{\alpha\beta} \, \hat{\bar{d}}^I_{B\,\beta\,\hat{j}} \, \hat{\bar{d}}^J_{B\,\alpha\,\hat{i}} + \text{H.c.} \\ &\supset \frac{1}{2} \, \lambda^{IJ}_{\bar{d}\bar{d}} f_\Phi \, \epsilon^{\alpha\beta} \, \epsilon^{\hat{i}\hat{j}} \, \hat{\bar{d}}^I_{B\,\beta\,\hat{j}} \, \hat{\bar{d}}^J_{B\,\alpha\,\hat{i}} + \text{H.c.} \\ &\supset \lambda^{12}_{\bar{d}\bar{d}} f_\Phi \, \epsilon^{\alpha\beta} \, \epsilon^{\hat{i}\hat{j}} \, \hat{\bar{d}}_{B\,\beta\,\hat{j}} \, \hat{\bar{s}}_{B\,\alpha\,\hat{i}} + \text{H.c.} \\ &\supset \overline{M}_d \, \hat{\bar{d}}_B \, \hat{\bar{s}}_B + \text{H.c.} \end{aligned} \tag{207}$$

Putting everything together, we have

$$\begin{aligned} -\mathcal{L} &\supset \overline{M}_d \, \hat{\bar{d}}_B \, \hat{\bar{s}}_B \, + m_d \, \hat{\bar{d}}_B \, \hat{d}_B + m_s \, \hat{\bar{s}}_B \, \hat{s}_B + \text{H.c.} \\ &= \frac{1}{2} \Big[\begin{array}{cccc} \hat{\bar{d}}_B & \hat{\bar{s}}_B & \hat{d}_B & \hat{s}_B \end{array} \Big] \begin{bmatrix} 0 & \overline{M}_d & m_d & 0 \\ -\overline{M}_d & 0 & 0 & m_s \\ -m_d & 0 & 0 & 0 \\ 0 & -m_s & 0 & 0 \end{bmatrix} \begin{bmatrix} \hat{\bar{d}}_B \\ \hat{\bar{s}}_B \\ \hat{d}_B \\ \hat{s}_B \end{bmatrix} + \text{H.c.} \end{aligned} \tag{208}$$

In the limit $\overline{M}_d \gg m_s, m_d$, a seesaw mechanism operates, and there are two mass eigenstates fermions with approximate mass eigenvalues $\overline{M}_d$ and $m_s m_d/\overline{M}_d$. Taking $f_\Phi \sim \Lambda \sim 5$ TeV, $\sin\vartheta \simeq 1/3$, and $\lambda^{12}_{\bar{d}\bar{d}}$ order one, we find $\overline{M}_d \sim 5$ TeV, and $m_s m_d/\overline{M}_d \sim 100$ eV.

On the other hand, if both $\lambda^{12}_{\bar{d}\bar{d}} = -\lambda^{21}_{\bar{d}\bar{d}} \neq 0$ and $c^{12}_{QQ} = -c^{21}_{QQ} \neq 0$ both give large contributions to the quark masses relative to those from the Higgs Yukawa couplings. Define the following mass parameters:

$$m_d = \frac{y_d v_B}{\sqrt{2}}, \qquad m_s = \frac{y_s v_B}{\sqrt{2}}, \qquad \overline{M}_d = \lambda^{12}_{\bar{d}\bar{d}} f_\Phi. \qquad M_d = -\frac{c^{12}_{QQ} v_B^2 f_\Phi}{2\Lambda^2}, \tag{209}$$

The mass terms for the $[SU(2)_c]_B$ doublet down type quarks are in this case given by

$$\begin{aligned} -\mathcal{L} \;&\supset\; \overline{M}_d\, \hat{\bar{d}}_B\, \hat{\bar{s}}_B + M_d\, \hat{d}_B\, \hat{s}_B + m_d\, \hat{\bar{d}}_B\, \hat{d}_B + m_s\, \hat{\bar{s}}_B\, \hat{s}_B + \text{H.c.} \\ &= \frac{1}{2}\begin{bmatrix} \hat{\bar{d}}_B & \hat{\bar{s}}_B & \hat{d}_B & \hat{s}_B \end{bmatrix} \begin{bmatrix} 0 & \overline{M}_d & m_d & 0 \\ -\overline{M}_d & 0 & 0 & m_s \\ -m_d & 0 & 0 & M_d \\ 0 & -m_s & -M_d & 0 \end{bmatrix} \begin{bmatrix} \hat{\bar{d}}_B \\ \hat{\bar{s}}_B \\ \hat{d}_B \\ \hat{s}_B \end{bmatrix} + \text{H.c.} \end{aligned} \tag{210}$$

In the limit $\overline{M}_d, M_d \gg m_s, m_d$, there are two mass eigenstates with approximate masses equal to $\overline{M}_d$ and M_d. Taking $f_\Phi \sim \Lambda \sim 5$ TeV, $\sin\vartheta \simeq 1/3$, and order one values for $\lambda^{12}_{\bar{d}\bar{d}}$ and c^{12}_{QQ}, we find $\overline{M}_d \sim 5$ TeV, and $M_d \sim 50$ GeV.

6.3.4 $\Phi \sim (\mathbf{3}, \mathbf{1}, -\frac{1}{3})$

The Lagrangian contains the following interactions:

$$\begin{aligned} -\mathcal{L} \supset\; & \frac{1}{2}\lambda_{QQ}\, \Phi_B (Q_B Q_B) + \lambda_{QL}\, \Phi_B^\dagger (Q_B L_B) + \lambda_{\bar{u}\bar{d}}\, \Phi_B^\dagger\, \bar{u}_B\, \bar{d}_B + \lambda_{\bar{u}\bar{e}}\, \Phi_B\, \bar{u}_B\, \bar{e}_B + \frac{c_{\bar{d}L}}{\Lambda}\, \Phi_B\, \bar{d}_B\, (L_B H_B) \\ & + \frac{c_{QQ}}{\Lambda^2}\, \Phi_B\, (Q_B H_B)\, (H_B^\dagger Q_B) + \frac{c_{QL1}}{\Lambda^2}\, \Phi_B^\dagger\, (H_B^\dagger Q_B)(L_B H_B) + \frac{c_{QL2}}{\Lambda^2}\, \Phi_B^\dagger\, (Q_B H_B)(H_B^\dagger L_B) + \text{H.c.} \\ \supset\; & -\lambda_{QQ}\, f_\Phi\, \hat{u}_B\, \hat{d}_B + \lambda_{QL}\, f_\Phi\, \hat{u}_{B3}\, e_B - \lambda_{QL}\, f_\Phi\, \hat{d}_{B3}\, \nu_B + \lambda_{\bar{u}\bar{d}}\, f_\Phi\, \hat{\bar{u}}_B\, \hat{\bar{d}}_B + \lambda_{\bar{u}\bar{e}}\, f_\Phi\, \hat{\bar{u}}_{B3}\, \bar{e}_B \\ & + \frac{c_{\bar{d}L} v_B f_\Phi}{\sqrt{2}\Lambda}\, \hat{\bar{d}}^3_B\, \nu_B - \frac{c_{QQ} v_B^2 f_\Phi}{2\Lambda^2}\, \hat{u}_B \hat{d}_B + \frac{c_{QL1} v_B^2 f_\Phi}{2\Lambda^2}\, \hat{d}_{B3}\, \nu_B + \frac{c_{QL2} v_B^2 f_\Phi}{2\Lambda^2}\, \hat{u}_{B3}\, e_B + \text{H.c.} \end{aligned} \tag{211}$$

There are new mass terms in Eq. (211) beyond those generated by the Higgs VEV. There are mass terms which marry (couple) $[SU(2)_c]_B$ doublet up with doublet down type quarks, as well as "3rd color" ($[SU(2)_c]_B$ singlet) quark fields with neutrinos or charged leptons.

From the electric charges in Table 3 it is easy to verify that the operators in the second line of Eq. (211) respect the unbroken twin electromagnetic gauge symmetry.

Note again the coupling λ_{QQ} in Eq. (173) is symmetric in the generation space, $(\lambda_{QQ})^{JI} = (\lambda_{QQ})^{IJ}$.

In principle, a Majorana type mass term for $\hat{d}_{B3}$ and $\hat{\bar{d}}^3_B$ is also possible since it has zero electric charge, see Table 3. It is only generated in dimension six operators involving two triplet scalars as $\Phi^\dagger_B(H^\dagger_B Q_B)\ \Phi_B \bar{d}_B \to \hat{\bar{d}}_{B3}\hat{d}_{B3}$.

6.3.5 $\Phi \sim (\mathbf{3}, \mathbf{1}, -\frac{4}{3})$

The Lagrangian contains the following interactions:

$$\begin{aligned} -\mathcal{L} \supset\ & \frac{1}{2}\lambda_{\bar{u}\bar{u}}\, \Phi^\dagger_B \bar{u}_B\, \bar{u}_B + \lambda_{\bar{d}\bar{e}}\, \Phi_B\, \bar{d}_B\, \bar{e}_B + \frac{c_{QQ}}{2\Lambda^2}\, \Phi_B\, (Q_B H_B)(Q_B H_B) \\ & + \frac{c_{QL}}{\Lambda^2}\, \Phi^\dagger_B\, (H^\dagger_B Q_B)(H^\dagger_B L_B) + \text{H.c.} \\ \supset\ & \frac{1}{2}\lambda_{\bar{u}\bar{u}}\, f_\Phi\, \hat{\bar{u}}_B\, \hat{\bar{u}}_B + \lambda_{\bar{d}\bar{e}}\, f_\Phi\, \hat{\bar{d}}^3_B\, \bar{e}_B - \frac{c_{QQ} v_B^2 f_\Phi}{4\Lambda^2}\, \hat{u}_B\, \hat{u}_B + \frac{c_{QL} v_B^2 f_\Phi}{2\Lambda^2}\, \hat{d}_{B3}\, e_B + \text{H.c.} \end{aligned} \tag{212}$$

There are new mass terms in Eq. (212) beyond those generated by the Higgs VEV. In particular, we may have a "Majorana" type mass term for the up-type quark fields since they are not charged under the unbroken twin electromagnetic gauge symmetry; see Table 3. There are mass terms which marry "3rd color" ($[SU(2)_c]_B$ singlet) down quark fields with charged leptons. From the electric charges in Table 3 it is easy to verify that the operators in the second line of Eq. (212) respect the unbroken twin electromagnetic gauge symmetry.

6.3.6 $\Phi \sim (\mathbf{3}, \mathbf{1}, \frac{5}{3})$

The Lagrangian contains the following interactions:

$$\begin{aligned} -\mathcal{L} \supset\ & \frac{c_{Q\bar{e}}}{\Lambda}\, \Phi^\dagger_B (Q_B H_B)\, \bar{e}_B + \frac{c_{\bar{u}L}}{\Lambda}\, \Phi\, \bar{u}_B\, (H^\dagger_B L_B) + \text{H.c.} \\ \supset\ & \frac{c_{Q\bar{e}}\, v_B f_\Phi}{\sqrt{2}\Lambda}\, \hat{u}_{B3}\, \bar{e}_B + \frac{c_{\bar{u}L}\, v_B f_\Phi}{\sqrt{2}\Lambda}\, \hat{\bar{u}}^3_B\, e_B + \text{H.c.} \end{aligned} \tag{213}$$

We see that for this model there are mass terms which marry "3rd color" ($[SU(2)_c]_B$ singlet) up quark fields with charged leptons. From the electric charges in Table 3 it is easy to verify that the operators in the second line of Eq. (213) respect the unbroken twin electromagnetic gauge symmetry, for it carries the same charge as electron.

6.3.7 Discussion of Triplet

Twin fermion masses can be distorted away from the MTH expectation in a variety of ways, but there are correlated effects in the visible sector due to the $\mathbb{Z}_2$ related interactions. For example, if both $\lambda_{\bar{d}\bar{d}}$ and $c_{\bar{u}L}$ in Eq. (203) are nonzero, both baryon number and lepton number are violated by one unit, leading to nucleon decay in the visible sector. These and other indirect constraints on scalar-fermion couplings are outlined in Chapter. 7.

6.3.8 $\Phi \sim (\mathbf{6}, \mathbf{1}, \frac{1}{3})$

Next for color sextet, we examine each of the two possible gauge symmetry breaking patterns in turn.

$[SU(3)_c \to SU(2)_c]_B$

In this case the sextet scalar obtains a VEV, $\langle \Phi_{B\,ij} \rangle = f_\Phi \delta_{i3} \delta_{j3}$. The Lagrangian contains the following interactions which generate the twin quark masses:

$$\begin{aligned} -\mathcal{L} &\supset \frac{1}{2}\lambda_{QQ}\, \Phi_B^\dagger (Q_B Q_B) + \lambda_{\bar{u}\bar{d}}\, \Phi_B\, \bar{u}_B\, \bar{d}_B + \frac{c_{QQ}}{\Lambda^2}\, \Phi_B^\dagger\, (Q_B H_B)(H_B^\dagger Q_B) + \text{H.c.} \\ &\supset \lambda_{QQ} f_\Phi\, \hat{u}_{B3}\, \hat{d}_{B3} + \lambda_{\bar{u}\bar{d}} f_\Phi\, \hat{\bar{u}}^3_B\, \hat{\bar{d}}^3_B + \frac{c_{QQ} v_B^2 f_\Phi}{2\Lambda^2}\, \hat{u}_{B3}\, \hat{d}_{B3} + \text{H.c.} \end{aligned} \tag{214}$$

We see that for this model there are mass terms which marry "3rd color" ($[SU(2)_c]_B$ singlet) up and down quark fields. From the electric charges in Table 4 it is easy to verify that the operators in the second line of Eq. (214) respect the unbroken twin electromagnetic gauge symmetry, for they are charged 1/2 and opposite.

$[SU(3)_c \to SO(3)_c]_B$

In this case $\langle \Phi_{B\,ij} \rangle = \frac{f_\Phi}{\sqrt{3}} \delta_{ij}$. The Lagrangian contains the following interactions:

$$\begin{aligned} -\mathcal{L} &\supset \frac{1}{2} \lambda_{QQ}\, \Phi_B^\dagger (Q_B Q_B) + \lambda_{\bar{u}\bar{d}}\, \Phi_B\, \bar{u}_B\, \bar{d}_B + \frac{c_{QQ}}{\Lambda^2}\, \Phi_B^\dagger\, (Q_B H_B)(H_B^\dagger Q_B) + \text{H.c.} \\ &\supset \frac{\lambda_{QQ} f_\Phi}{\sqrt{3}}\, u_B\, d_B + \frac{\lambda_{\bar{u}\bar{d}}\, f_\Phi}{\sqrt{3}}\, \bar{u}_B\, \bar{d}_B + \frac{c_{QQ} v_B^2 f_\Phi}{2\sqrt{3}\Lambda^2}\, u_B\, d_B + \text{H.c.} \end{aligned} \tag{215}$$

In this case there are new mass terms that marry the up and down type quarks, which transform as vectors under the unbroken $[SO(3)_c]_B$ gauge symmetry. The presence of such mass terms is consistent with the fact that there are no unbroken $U(1)$ gauge symmetries in the low energy theory. We have suppressed the $[SO(3)_c]_B$ color and generation indices in (215). To demonstrate how the indices are contracted, we provide an example:

$$\frac{\lambda_{QQ} f_\Phi}{\sqrt{3}}\, u_B\, d_B = \frac{(\lambda_{QQ})^{IJ} f_\Phi}{\sqrt{3}}\, u_{BiI}\, d_{BiJ}, \tag{216}$$

where $i = 1, 2, 3$ is an $[SO(3)_c]_B$ color index and $I, J = 1, 2, 3$ are generation indices.

6.3.9 $\Phi \sim (\mathbf{6}, \mathbf{1}, -\frac{2}{3})$

$[SU(3)_c \to SU(2)_c]_B$

In this case $\langle \Phi_{B\,ij} \rangle = f_\Phi \delta_{i3} \delta_{j3}$. The Lagrangian contains the following interactions:

$$\begin{aligned} -\mathcal{L} &\supset \frac{1}{2} \lambda_{\bar{d}\bar{d}}\, \Phi_B\, \bar{d}_B\, \bar{d}_B + \frac{c_{QQ}}{2\Lambda^2}\, \Phi_B^\dagger\, (H_B^\dagger Q_B)(H_B^\dagger Q_B) + \text{H.c.} \\ &\supset \frac{1}{2} \lambda_{\bar{d}\bar{d}}\, f_\Phi\, \hat{\bar{d}}_B^3\, \hat{\bar{d}}_B^3 + \frac{c_{QQ} v_B^2 f_\Phi}{4\Lambda^2}\, \hat{d}_{B3}\, \hat{d}_{B3} + \text{H.c.} \end{aligned} \tag{217}$$

We see that Majorana mass terms for the "3rd color" ($[SU(2)_c]_B$ singlet) down quark fields are generated. This is consistent with the fact that these quark fields are not charged under the unbroken twin electromagnetic gauge symmetry; see Table 4.

$[SU(3)_c \to SO(3)_c]_B$

In this case $\langle \Phi_{B\,ij} \rangle = \frac{f_\Phi}{\sqrt{3}} \delta_{ij}$. The Lagrangian contains the following interactions:

$$\begin{aligned} -\mathcal{L} &\supset \frac{1}{2} \lambda_{\bar{d}\bar{d}}\, \Phi_B\, \bar{d}_B\, \bar{d}_B + \frac{c_{QQ}}{2\Lambda^2}\, \Phi_B^\dagger\, (H_B^\dagger Q_B)(H_B^\dagger Q_B) + \text{H.c.} \\ &\supset \frac{\lambda_{\bar{d}\bar{d}}\, f_\Phi}{2\sqrt{3}}\, \bar{d}_B\, \bar{d}_B + \frac{c_{QQ}\, v_B^2 f_\Phi}{4\sqrt{3}\,\Lambda^2}\, d_B\, d_B + \text{H.c.} \end{aligned} \tag{218}$$

We see that Majorana mass terms for the $[SO(3)_c]_B$ down quark fields are generated. The presence of such mass terms is consistent with the fact that there are no unbroken $U(1)$ gauge symmetries in the low energy theory.

6.3.10 $\Phi \sim (\mathbf{6}, \mathbf{1}, \frac{4}{3})$

$[SU(3)_c \to SU(2)_c]_B$

In this case $\langle \Phi_{B\,ij} \rangle = f_\Phi \delta_{i3} \delta_{j3}$. The Lagrangian contains the following interactions:

$$\begin{aligned} -\mathcal{L} &\supset \frac{1}{2} \lambda_{\bar{u}\bar{u}}\, \Phi_B\, \bar{u}_B\, \bar{u}_B + \frac{c_{QQ}}{2\Lambda^2}\, \Phi_B^\dagger (Q_B H_B)(Q_B H_B) + \text{H.c.} \\ &\supset \frac{1}{2} \lambda_{\bar{u}\bar{u}}\, f_\Phi\, \hat{\bar{u}}_B^3\, \hat{\bar{u}}_B^3 + \frac{c_{QQ} v_B^2 f_\Phi}{4\Lambda^2}\, \hat{u}_{B3}\, \hat{u}_{B3} + \text{H.c.} \end{aligned} \tag{219}$$

We see that Majorana mass terms for the "3rd color" ($[SU(2)_c]_B$ singlet) up quark fields are generated. This is consistent with the fact that these quark fields are not charged under the unbroken twin electromagnetic gauge symmetry; see Table 4.

$[SU(3)_c \to SO(3)_c]_B$

In this case $\langle \Phi_{B\,ij} \rangle = \frac{f_\Phi}{\sqrt{3}} \delta_{ij}$. The Lagrangian contains the following interactions:

$$\begin{aligned} -\mathcal{L} &\supset \frac{1}{2} \lambda_{\bar{u}\bar{u}}\, \Phi_B\, \bar{u}_B\, \bar{u}_B + \frac{c_{QQ}}{2\Lambda^2}\, \Phi_B^\dagger (Q_B H_B)(Q_B H_B) + \text{H.c.} \\ &\supset \frac{\lambda_{\bar{u}\bar{u}}\, f_\Phi}{2\sqrt{3}}\, \bar{u}_B\, \bar{u}_B + \frac{c_{QQ} v_B^2 f_\Phi}{4\sqrt{3}\Lambda^2}\, u_B\, u_B + \text{H.c.} \end{aligned} \tag{220}$$

We see that Majorana mass terms for the $[SO(3)_c]_B$ up quark fields are generated. The presence of such mass terms is consistent with the fact that there are no unbroken $U(1)$ gauge symmetries in the low energy theory.

6.3.11 Summary of Sextet

In contrast to the triplet case, no lepton mass terms are generated from those couplings. There are, however, new type of mass terms generated for quarks. The new mass terms can dominate over the usual EW ones for large enough couplings, and may or may not feature a seesaw behavior in analogy with the color triplet example discussed above. In the case of first symmetry breaking pattern, only the '3rd color', $[SU(2)_c]_B$ singlet quark obtains a mass. Conversely, in the second case of symmetry breaking pattern to $[SO(3)_c]_B$, all quark colors can be lifted.

6.3.12 $\Phi \sim (\mathbf{8}, \mathbf{1}, 0)$

Likely for color octet, we examine each of the two possible gauge symmetry breaking patterns in turn.

$[SU(3)_c \to SU(2)_c \times U(1)_c]_B$

In this case, the octet scalar obtains a VEV, $\Phi_B = \sqrt{2} f_\Phi T^8$. The Lagrangian contains the following interactions:

$$\begin{aligned} -\mathcal{L} &\supset \frac{c_{Q\bar{u}}}{\Lambda}\,\Phi_B(Q_B H_B)\,\bar{u}_B + \frac{c_{Q\bar{d}}}{\Lambda}\,\Phi_B(H_B^\dagger Q_B)\,\bar{d}_B + \text{H.c.} \\ &\supset \frac{c_{Q\bar{u}}\,v_B\,f_\Phi}{2\sqrt{3}\,\Lambda}\,\left(\hat{\bar{u}}_B\,\hat{u}_B - 2\,\hat{u}_{B3}\,\hat{\bar{u}}^3_B\right) + \frac{c_{Q\bar{d}}\,v_B\,f_\Phi}{2\sqrt{3}\,\Lambda}\,\left(\hat{\bar{d}}_B\,\hat{d}_B - 2\,\hat{d}_{B3}\,\hat{\bar{d}}^3_B\right) + \text{H.c.} \end{aligned} \tag{221}$$

We note that the mass terms in (221) respect the unbroken $[SU(2)_c \times U(1)_c \times U(1)_{\rm EM}]_B$ gauge symmetry. Interestingly, all quark colors obtain a mass from a single interaction.[4]

$[SU(3)_c \to U(1)_c \times U(1)'_c]_B$

In this case, the octet scalar obtains a VEV, $\Phi_B = \sqrt{2} f_\Phi T^3$. The Lagrangian contains the following interactions:

$$\begin{aligned} -\mathcal{L} &\supset \frac{c_{Q\bar{u}}}{\Lambda}\,\Phi_B(Q_B H_B)\,\bar{u}_B + \frac{c_{Q\bar{d}}}{\Lambda}\,\Phi_B(H_B^\dagger Q_B)\,\bar{d}_B + \text{H.c.} \\ &\supset \frac{c_{Q\bar{u}} v_B f_\Phi}{2\Lambda}\,\left(u_{B1}\,\bar{u}^1_B - u_{B2}\,\bar{u}^2_B\right) + \frac{c_{Q\bar{d}} v_B f_\Phi}{2\Lambda}\,\left(d_{B1}\,\bar{d}^1_B - d_{B2}\,\bar{d}^2_B\right) + \text{H.c.} \end{aligned} \tag{222}$$

[4] also note that the generation indices of the first term in the parenthesis should be switched compared to the second term.

Only the first and second quark colors are lifted, while there is no mass term generated for the 3rd color quarks with a single scalar. The mass terms are consistent with the unbroken $[U(1)_c \times U(1)'_c \times U(1)_{\rm EM}]_B$ gauge symmetry.

6.3.13 $\Phi \sim (\mathbf{8}, \mathbf{1}, 1)$

[5] For the color octet with charge, the hypercharge boson gets a mass, but there is no mixing with gluons. Thus the $U(1)_{EM}$ is completely broken.

$[SU(3)_c \to SU(2)_c \times U(1)_c]_B$

Note that here the cubic coupling Eq. 80 is not allowed, though we can still use other couplings like Eq. 81 to align the VEV. The Lagrangian contains the following interactions:

$$\begin{aligned} -\mathcal{L} &\supset \frac{c_{Q\bar{u}}}{\Lambda}\,\Phi\,(H^\dagger Q)\,\bar{u} + \frac{c_{Q\bar{d}}}{\Lambda}\,\Phi^\dagger (QH)\,\bar{d} + \text{H.c.} \\ &\supset \frac{c_{Q\bar{u}}\,v_B\,f_\Phi}{2\sqrt{3}\,\Lambda}\,\left(\hat{\bar{u}}_B\,\hat{d}_B - 2\,\hat{d}_{B3}\,\hat{\bar{u}}^3_B\right) + \frac{c_{Q\bar{d}}\,v_B\,f_\Phi}{2\sqrt{3}\,\Lambda}\,\left(\hat{\bar{d}}_B\,\hat{u}_B - 2\,\hat{u}_{B3}\,\hat{\bar{d}}^3_B\right) + \text{H.c.} \end{aligned} \tag{223}$$

We note that the mass terms in (223) respect the unbroken $[SU(2)_c \times U(1)_c]_B$ gauge symmetry.[6]

$[SU(3)_c \to U(1)_c \times U(1)'_c]_B$

The Lagrangian contains the following interactions:

$$\begin{aligned} -\mathcal{L} &\supset \frac{c_{Q\bar{u}}}{\Lambda}\,\Phi\,(H^\dagger Q)\,\bar{u} + \frac{c_{Q\bar{d}}}{\Lambda}\,\Phi^\dagger (QH)\,\bar{d} + \text{H.c.} \\ &\supset \frac{c_{Q\bar{u}} v_B f_\Phi}{2\Lambda}\,\left(d_{B1}\,\bar{u}^1_B - d_{B2}\,\bar{u}^2_B\right) + \frac{c_{Q\bar{d}} v_B f_\Phi}{2\Lambda}\,\left(u_{B1}\,\bar{d}^1_B - u_{B2}\,\bar{d}^2_B\right) + \text{H.c.} \end{aligned} \tag{224}$$

The mass terms in (224) respect the unbroken $[U(1)_c \times U(1)'_c]_B$ gauge symmetry.

In both cases, the presence of such mass terms is consistent with the fact that there is no unbroken $U(1)_{EM}$ gauge symmetry in the low energy theory.

[5] list here for future convenience, though not considered in our models

[6] also note that the generation indices of the first term in the parenthesis should be switched compared to the second term.

6.3.14 Summary of Octet

As with the sextet, no lepton mass terms are generated from those couplings, while the resulting quark mass terms are similar to the standard ones arising from the Higgs Yukawa couplings (202) in that they marry $SU(2)_L$ singlet and doublet quarks. The precise form of the quark masses depend on the pattern of gauge symmetry breaking. The mass terms can be as large as $\mathcal{O}(100\,\mathrm{GeV})$ for order one Wilson coefficients and $f_\Phi \sim \Lambda$.

6.3.15 Other Sources of Twin Fermion Masses

Thus far we have considered twin fermion masses involving a single colored scalar field, and all such possibilities of this type are shown in Table 6. Additional options arise from couplings involving two colored scalars. First, there is always the possibility of coupling the gauge singlet operator $|\Phi_B|^2$ to the usual Higgs Yukawa operators, e.g., $|\Phi_B|^2(H^\dagger L_B)\bar{e}_B$. After Φ_B obtains a VEV, effective Yukawa couplings are generated in the twin sector, which can exceed the SM ones by a factor of 10 for the light generations without spoiling naturalness, considering the scalar coupling terms $\lambda_\Phi|\Phi_A|^2|\Phi_B|^2$ in the effective potential and a loop suppression factor, see the discussion in Ref. [82] for further details. Furthermore, we can couple two color triplet scalars to pairs of quark fields in nontrivial ways to generate new twin quark masses. As an illustration consider $\Phi \sim (\mathbf{3}, \mathbf{1}, \frac{2}{3})$, with operator $\Phi_{B\,i}\,\Phi_{B\,j}\,\bar{u}_B^i\,\bar{u}_B^j \supset f_\Phi^2\,\hat{\bar{u}}_{B3}\,\hat{\bar{u}}_{B3}$, which provides an additional mass term beyond those presented in Eq. (203).

7.0 Indirect Constraints

The previous section showed that the spontaneous breakdown of twin color and $\mathbb{Z}_2$ can also dynamically generate new twin fermion mass terms, when there are sizable couplings between the colored scalar fields and matter fields. The exact $\mathbb{Z}_2$ symmetry correlates these new masses to visible sector phenomena, including baryon and lepton number violation, quark and lepton flavor changing processes, CP-violation, and deviations in electroweak probes. Indirect tests in the visible sector can limit the size and structure of the new twin fermion mass terms. Given the range of models and possible new couplings (see Table 6), a complete vetting of these constraints is beyond our scope. Instead, we provide illustrative examples of the characteristic phenomena that can occur. Many of the phenomena we consider here occur in the context of R-parity violating supersymmetry; for a review see Ref. [139].

7.1 Baryon and Lepton Number Violation

The couplings of the new colored scalars to fermions lead to the possibility of baryon and lepton number violating phenomena. In particular, the models with color triplet scalars generically lead to the violation of these symmetries. On the other hand, in the simplest setup the color sextet and octet scalars do not cause B or L violation.

Let us consider this in more detail before examining specific tests of these symmetries. We will examine the model Lagrangians presented in Section 6.1. For any given model Lagrangian, if only one coupling is nonzero and all others are zero, B and L are good symmetries since the scalar Φ can be assigned definite charge under B and L. However, if two or more of these couplings do not vanish, these symmetries can be violated. Let us consider in particular pairs of nonvanishing couplings in each model.

$\Phi \sim (\mathbf{3}, \mathbf{1}, \frac{2}{3})$:

We have the following cases:

- Pairs that conserve both B and L:

$$(\lambda_{\bar{d}\bar{d}}, c_{QQ}), \quad (c_{\bar{u}L}, c_{\bar{d}L}), \quad (c_{\bar{u}L}, c_{Q\bar{e}}), \quad (c_{\bar{d}L}, c_{Q\bar{e}}). \tag{225}$$

- Pairs that conserve B but violate L by two units:

$$(c_{\bar{u}L}, c_{QL}), \quad (c_{\bar{d}L}, c_{QL}), \quad (c_{Q\bar{e}}, c_{QL}). \tag{226}$$

- Pairs that violate both B by one unit and L by one unit:

$$\begin{aligned}&(\lambda_{\bar{d}\bar{d}}, c_{\bar{u}L}), \quad (\lambda_{\bar{d}\bar{d}}, c_{\bar{d}L}), \quad (\lambda_{\bar{d}\bar{d}}, c_{Q\bar{e}}), \quad (\lambda_{\bar{d}\bar{d}}, c_{QL}),\\ &(c_{\bar{u}L}, c_{QQ}), \quad (c_{\bar{d}L}, c_{QQ}), \quad (c_{Q\bar{e}}, c_{QQ}), \quad (c_{QQ}, c_{QL}).\end{aligned} \tag{227}$$

$\Phi \sim (\mathbf{3}, \mathbf{1}, -\frac{1}{3})$:

We have the following cases:

- Pairs that conserve both B and L:

$$\begin{aligned}&(\lambda_{QQ}, \lambda_{\bar{u}\bar{d}}), \quad (\lambda_{QQ}, c_{QQ}), \quad (\lambda_{QL}, \lambda_{\bar{u}\bar{e}}), \quad (\lambda_{QL}, c_{QL1}), \quad (\lambda_{QL}, c_{QL2}),\\ &(\lambda_{\bar{u}\bar{d}}, c_{QQ}), \quad (\lambda_{\bar{u}\bar{e}}, c_{QL1}), \quad (\lambda_{\bar{u}\bar{e}}, c_{QL2}), \quad (c_{QL1}, c_{QL2}).\end{aligned} \tag{228}$$

- Pairs that conserve B but violate L by two units:

$$(\lambda_{QL}, c_{\bar{d}L}), \quad (\lambda_{\bar{u}\bar{e}}, c_{\bar{d}L}), \quad (c_{\bar{d}L}, c_{QL1}), \quad (c_{\bar{d}L}, c_{QL2}). \tag{229}$$

- Pairs that violate both B by one unit and L by one unit:

$$\begin{aligned}&(\lambda_{QQ}, \lambda_{QL}), \quad (\lambda_{QQ}, \lambda_{\bar{u}\bar{e}}), \quad (\lambda_{QQ}, c_{\bar{d}L}), \quad (\lambda_{QQ}, c_{QL1}), \quad (\lambda_{QQ}, c_{QL2}),\\ &(\lambda_{QL}, \lambda_{\bar{u}\bar{d}}), \quad (\lambda_{QL}, c_{QQ}), \quad (\lambda_{\bar{u}\bar{d}}, \lambda_{\bar{u}\bar{e}}), \quad (\lambda_{\bar{u}\bar{d}}, c_{\bar{d}L}), \quad (\lambda_{\bar{u}\bar{d}}, c_{QL1}),\\ &(\lambda_{\bar{u}\bar{d}}, c_{QL2}), \quad (\lambda_{\bar{u}\bar{e}}, c_{QQ}), \quad (c_{\bar{d}L}, c_{QQ}), \quad (c_{QQ}, c_{QL1}), \quad (c_{QQ}, c_{QL2}).\end{aligned} \tag{230}$$

$\Phi \sim (\mathbf{3}, \mathbf{1}, -\frac{4}{3})$:

We have the following cases:

- Pairs that conserve both B and L:

$$(\lambda_{\bar{u}\bar{u}}, c_{QQ}), \quad (\lambda_{\bar{d}\bar{e}}, c_{QL}), \tag{231}$$

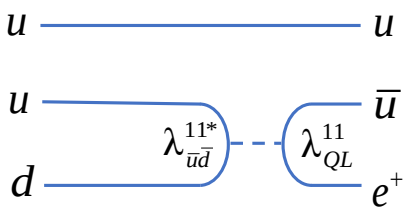

Figure 12: Tree level contribution to proton decay.

- Pairs that violate both B by one unit and L by one unit:

$$(\lambda_{\bar{u}\bar{u}}, \lambda_{\bar{d}\bar{e}}), \quad (\lambda_{\bar{u}\bar{u}}, c_{QL}), \quad (\lambda_{\bar{d}\bar{e}}, c_{QQ}), \quad (c_{QQ}, c_{QL}). \tag{232}$$

  $\Phi \sim (\mathbf{3}, \mathbf{1}, \frac{5}{3})$:

  There is just one pair, $(c_{Q\bar{e}}, c_{\bar{u}L})$, and in this case both B and L are conserved.

  For models with sextet or octet scalars: One can easily see that B and L are conserved in these models.

7.1.1 B Violation

In triplet models with hypercharge $Y_\Phi = \frac{2}{3}, -\frac{1}{3}, -\frac{4}{3}$ the proton may decay, which leads to strong constraints on certain combinations of couplings. For a comprehensive review on proton decay see Ref. [140]. For example, consider $\Phi \sim (\mathbf{3}, \mathbf{1}, -\frac{1}{3})$ with non-vanishing couplings to the first generation,

$$\begin{aligned} \mathcal{L} &\supset \lambda^{11}_{QL}\, \Phi^\dagger_A\, (Q^1_A L^1_A) + \lambda^{11}_{\bar{u}\bar{d}}\, \Phi^\dagger_A\, \bar{u}^1_A\, \bar{d}^1_A + \text{H.c.} \\ &\supset \lambda^{11}_{QL}\, \phi^\dagger_A\, u_A\, e_A + \lambda^{11}_{\bar{u}\bar{d}}\, \phi^\dagger_A\, \bar{u}_A\, \bar{d}_A + \text{H.c.}\ . \end{aligned} \tag{233}$$

In this case, tree level exchange of ϕ_A allows the proton to decay into a pion and positron, $p^+ \to e^+\pi^0$, with decay width

$$\begin{aligned}\Gamma(p^+ \to e^+\pi^0) &= \frac{|\lambda^{11}_{QL}\,\lambda^{11*}_{\bar{u}\bar{d}}\,|^2}{m^4_{\phi_A}}\frac{|\alpha|^2(1+F+D)^2 m_p}{64\pi f^2}\left(1-\frac{m_\pi^2}{m_p^2}\right)^2 \\ &\simeq (10^{34}\,\mathrm{yr})^{-1}\left(\frac{\sqrt{|\lambda^{11}_{QL}\,\lambda^{11*}_{\bar{u}\bar{d}}\,|}}{4\times 10^{-13}}\right)^4\left(\frac{\mathrm{TeV}}{m_{\phi_A}}\right)^4\end{aligned} \tag{234}$$

where $|\alpha| = 0.0090\,\mathrm{GeV}^3$ [141] is the nucleon decay hadronic matrix element, $F + D \simeq 1.267$ [142] is a baryon chiral Lagrangian parameter, and $f = 131$ MeV. The current limits from Ref. [143] for this channel are $\tau_p/\mathrm{Br}(p^+ \to e^+\pi^0) > 1.6 \times 10^{34}$ yrs at 90% C.L. The non-observation of proton decay generally places strong limits on pairs of couplings that violate B in triplet scalars models. Depending on the flavor structure of the couplings, there may be other proton decay modes and other nucleon/baryon decays allowed.

In scenarios with a single colored scalar in the visible sector, nucleon decays with $\Delta B = 1$ are usually the most sensitive probes of B violating couplings. Processes like neutron-antineutron oscillations and dinucleon decays with $\Delta B = 2$ are expected to be less sensitive. However, if there are additional colored scalar fields of different hypercharge present and suitable coupling between scalars in the potential then such $\Delta B = 2$ processes can be observable; see e.g., Ref. [144] for a recent study.

7.1.2 L Number Violation

In triplet models with $Y_\Phi = \frac{2}{3}, -\frac{1}{3}$, certain combinations of scalar-fermion couplings can violate lepton number by two units while conserving baryon number. In such cases we generally expect that neutrino masses are generated radiatively. For instance, consider again $\Phi \sim (\mathbf{3}, \mathbf{1}, -\frac{1}{3})$, but with the following interactions:

$$\begin{aligned}-\mathcal{L} &\supset \lambda_{QL}\,\Phi^\dagger_A(Q_A L_A) + \frac{c_{\bar{d}L}}{\Lambda}\,\Phi_A\,\bar{d}_A\,(L_A H_A) + \mathrm{H.c.} \\ &\supset -\lambda_{QL}\,\phi^\dagger_A\,d_A\,\nu_A + \frac{c_{\bar{d}L}v_A}{\sqrt{2}\Lambda}\,\phi_A\,\bar{d}_A\,\nu_A + \mathrm{H.c.}\,.\end{aligned} \tag{235}$$

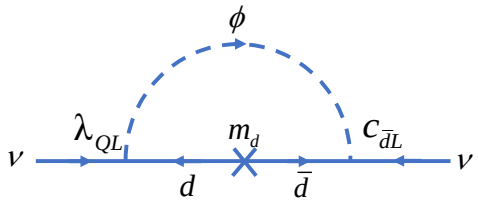

Figure 13: One-loop contributions to neutrino masses.

These interactions break lepton number by two units. Neutrino masses will be generated at one loop, with characteristic size

$$m_\nu \sim \frac{\lambda_{QL}\, c_{\bar{d}L}\, m_d\, v_A}{16\sqrt{2}\pi^2\Lambda} \log\left(\frac{\Lambda}{m_{\phi_A}}\right) \approx 0.1\,\text{eV}\,\left(\frac{\lambda_{QL}\, c_{\bar{d}L}}{10^{-7}}\right)\left(\frac{5\,\text{TeV}}{\Lambda}\right). \tag{236}$$

Here we have fixed $m_{\phi_A} = 1\,\text{TeV}$ and used the bottom mass for m_d, which leads to the strongest constraint.

7.2 Quark and Lepton FCNC

The interactions of the colored scalars with matter in Table 6 can also lead to new tree level or radiative flavor changing neutral currents (FCNCs) in the quark and lepton sectors. A variety of rare FCNC processes are possible, many of which impose strong constraints on the new scalar-fermion couplings.

For instance, sextet and octet models can mediate new tree level contributions to $\Delta F = 2$ transitions in the kaon system. Taking $\Phi \sim (\mathbf{6}, \mathbf{1}, -\frac{2}{3})$ as an example, we write the interaction

$$\mathcal{L} \supset \frac{1}{2}\,\lambda_{\bar{d}\bar{d}}\,\phi_A\,\bar{d}_A\,\bar{d}_A + \text{H.c.}\,. \tag{237}$$

If the diagonal couplings $\lambda^{11}_{\bar{d}\bar{d}}$ and $\lambda^{22}_{\bar{d}\bar{d}}$ are nonvanishing, then tree level sextet scalar exchange generates the effective interaction

$$\mathcal{L} \supset C^{sd}_{V,RR}\,(\bar{s}_A\gamma^\mu P_R d_A)(\bar{s}_A\gamma^\mu P_R d_A) + \text{H.c.}\,, \tag{238}$$

with Wilson coefficient

$$C^{sd}_{V,RR} = \frac{\lambda^{11^*}_{\bar{d}\bar{d}}\;\lambda^{22}_{\bar{d}\bar{d}}}{8m^2_{\phi_A}} \approx \left(\frac{1}{10^4\,\text{TeV}}\right)^2\left(\frac{\text{TeV}}{m_{\phi_A}}\right)^2\left(\frac{\lambda^{11^*}_{\bar{d}\bar{d}}\;\lambda^{22}_{\bar{d}\bar{d}}}{10^{-7}}\right). \tag{239}$$

Current constraints from Kaon mixing $K^0 - \bar{K}^0$ on such operators probe new physics scales of order 10^4 TeV [145][1], which, noting Eq. (239), limits the typical size of these couplings to be at the level of 10^{-3} or smaller.

Octet scalars, $\Phi \sim (\mathbf{8}, \mathbf{1}, 0)$, can also induce neutral meson mixing at tree level. After electroweak symmetry breaking, the scalar-quark coupling is

$$-\mathcal{L} \supset \frac{c_{Q\bar{d}}\,v_A}{\sqrt{2}\Lambda}\,\phi_A\,d_A\,\bar{d}_A + \text{H.c.}\,. \tag{240}$$

If, for instance, $c^{12}_{Q\bar{d}}$ is nonzero, exchange of ϕ_A generates the effective interaction

$$\mathcal{L} \supset C^{sd}_{S,LL}\,(\bar{s}^i_A P_L d_{Aj})(\bar{s}^j_A P_L d_{Ai}) + \text{H.c.}\,, \tag{241}$$

where i, j denote color indices. The Wilson coefficient is given by

$$C^{sd}_{S,LL} = \frac{(c^{12}_{Q\bar{d}})^2\,v_A^2}{8m^2_{\phi_A}\Lambda^2} \approx \left(\frac{1}{10^4\,\text{TeV}}\right)^2\left(\frac{\text{TeV}}{m_{\phi_A}}\right)^2\left(\frac{5\,\text{TeV}}{\Lambda}\right)^2\left(\frac{c^{12}_{Q\bar{d}}}{6\times10^{-3}}\right)^2. \tag{242}$$

While color triplet scalars do not mediate tree level $\Delta F = 2$ transitions, sizable loop contributions to these operators can arise. As an example consider $\Phi \sim (\mathbf{3}, \mathbf{1}, -\frac{1}{3})$ with interaction

$$-\mathcal{L} = \lambda_{\bar{u}\bar{d}}\,\phi^\dagger_A\,\bar{u}_A\,\bar{d}_A + \text{H.c.}\,. \tag{243}$$

[1]See e.g., Table IV in Ref. [145] for the bounds on $\text{Re}\,C^1_K$ and $\text{Im}\,C^1_K$. The Kaon mass difference $\Delta m_K < 5\times10^{-19}$ GeV was measured by KTeV experiment at Fermilab [146], the CP violating parameter $\epsilon_K \sim 2\times10^{-3}$ was first established in 1964 [147],

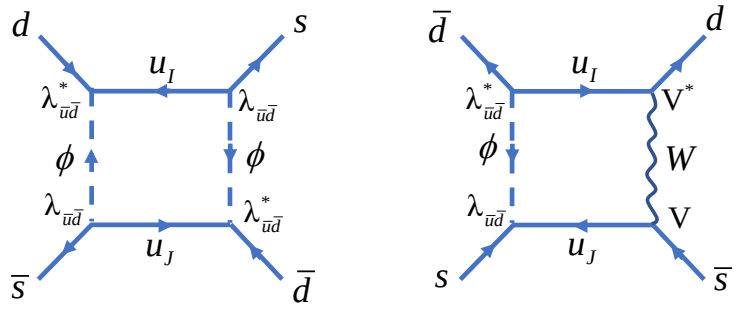

Figure 14: One-loop box diagrams contributing to kaon mixing, for the first type: left, and second type: right, respectively.

There are two types of one-loop box diagrams that generate contributions to kaon mixing [148, 149]. The first involves the exchange of two colored scalars and leads to the effective Lagrangian (238). In the limit $m_{\phi_A} \gg m_t$, the Wilson coefficient is

$$-C^{sd}_{V,RR} = \frac{\left(\sum_I \lambda^{I2}_{\bar{u}\bar{d}} \lambda^{I1*}_{\bar{u}\bar{d}}\right)^2}{64\pi^2 m^2_{\phi_A}} \approx \left(\frac{1}{10^4\,\text{TeV}}\right)^2 \left(\frac{\text{TeV}}{m_{\phi_A}}\right)^2 \left(\frac{\sum_I \lambda^{I2}_{\bar{u}\bar{d}} \lambda^{I1*}_{\bar{u}\bar{d}}}{3\times 10^{-3}}\right)^2 . \tag{244}$$

The second type of diagram involves the exchange of one W boson and one colored scalar, leading to the effective Lagrangian

$$\mathcal{L} \supset C^{sd}_{S,RL} \left[(\bar{s}^i_A P_R d_{Ai})(\bar{s}^j_A P_L d_{Aj}) - (\bar{s}^i_A P_R d_{Aj})(\bar{s}^j_A P_L d_{Ai})\right] + \text{H.c.} . \tag{245}$$

For anarchic couplings[2] $\lambda_{\bar{u}\bar{d}}$ and heavy scalar mass $m_{\phi_A} \gg m_t$, the leading contribution is

$$C^{sd}_{S,RL} = \frac{G_F}{8\sqrt{2}\pi^2} V_{td} V^*_{ts} \lambda^{32}_{\bar{u}\bar{d}} \lambda^{31*}_{\bar{u}\bar{d}} \frac{m_t^2}{m_\phi^2} \log\left(\frac{m_\phi^2}{m_W^2}\right) \approx \left(\frac{1}{10^4\,\text{TeV}}\right)^2 \left(\frac{\text{TeV}}{m_{\phi_A}}\right)^2 \left(\frac{\lambda^{32}_{\bar{u}\bar{d}} \lambda^{31*}_{\bar{u}\bar{d}}}{2\times 10^{-3}}\right), \tag{246}$$

where V_{IJ} are the CKM matrix elements between up-type quark I and down-type quark J.

Thus, the typical constraints on the couplings in this case are at the 10^{-2}–10^{-1} level.

[2] couplings of the same order, without hierarchy in strength for different flavors.

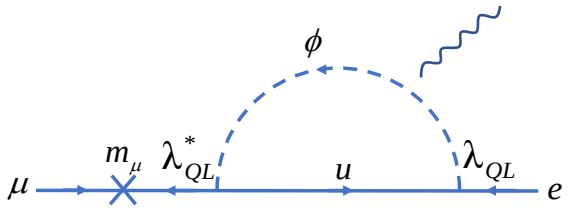

Figure 15: One-loop contributions to rare muon decay $\mu \to e\gamma$.

Color triplets can also facilitate lepton flavor violation, such as the decay $\mu \to e\gamma$. If $\Phi \sim (\mathbf{3}, \mathbf{1}, -\frac{1}{3})$, for example, the coupling λ_{QL} in Eq. (233) is

$$-\mathcal{L} \supset \lambda_{QL}\, \Phi^\dagger_A (Q_A L_A) + \text{H.c.} \,. \tag{247}$$

The $\mu \to e\gamma$ branching ratio is found to be

$$\begin{aligned} \text{Br}(\mu \to e\gamma) &= \tau_\mu \frac{\alpha\, |\sum_I \lambda^{I1*}_{QL} \lambda^{I2}_{QL}|^2\, m_\mu^5}{2^{14}\, \pi^4\, m_\phi^4} \\ &\simeq 4 \times 10^{-13} \left(\frac{1\,\text{TeV}}{m_\phi}\right)^4 \left(\frac{|\sum_I \lambda^{I1*}_{QL} \lambda^{I2}_{QL}|^2}{2 \times 10^{-6}}\right), \end{aligned} \tag{248}$$

where $\tau_\mu \simeq 2.2 \times 10^{-6}$ s is the muon lifetime. The MEG experiment has placed a 90% CL upper bound on the branching ratio, $\text{Br}(\mu \to e\gamma)_{\text{MEG}} < 4.2 \times 10^{-13}$ [150]. So, for a colored triplet with mass of order 1 TeV, the couplings are typically constrained to be smaller than about 0.04.

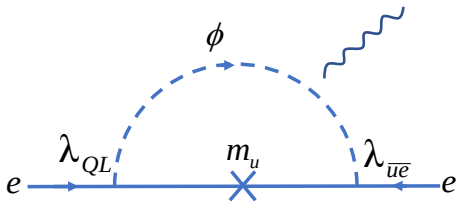

Figure 16: One-loop contributions to electron EDM.

7.3 Electric Dipole Moments

When multiple scalar-fermion couplings are present in the theory new physical complex phases appear. These can source (cause) new flavor-diagonal CP violation in the form of fermion electric dipole moments (EDMs). To illustrate, we investigate the contribution to electron electric dipole moment coming from a triplet $\Phi \sim (\mathbf{3}, \mathbf{1}, -\frac{1}{3})$ with interactions

$$-\mathcal{L} \supset \lambda_{QL} \Phi_A^\dagger \, (Q_A L_A) + \lambda_{\bar{u}\bar{e}} \, \Phi_A \, \bar{u}_A \, \bar{e}_A + \text{H.c.} \, . \tag{249}$$

Exchange of up-type quarks leads to an electron EDM at one loop, described by the effective Lagrangian

$$\mathcal{L} \supset -\frac{i}{2} \, d_e \, \bar{e}_A \, \sigma_{\mu\nu} \gamma^5 e_A \, F_A^{\mu\nu}. \tag{250}$$

In the case of flavor anarchic couplings, the top loop dominates and leads to the prediction

$$d_e \simeq \frac{e \, m_t}{32\pi^2 m_\phi^2} \left[7 + 4 \log \left(\frac{m_t^2}{m_\phi^2} \right) \right] \text{Im}[\lambda_{QL}^{31} \, \lambda_{\bar{u}\bar{e}}^{31}] \approx 10^{-29} \, e \, \text{cm} \left(\frac{1 \, \text{TeV}}{m_{\phi_A}} \right)^2 \left(\frac{\text{Im}[\lambda_{QL}^{31} \, \lambda_{\bar{u}\bar{e}}^{31}]}{10^{-10}} \right). \tag{251}$$

The best constraint on the electron EDM comes from the ACME collaboration: $|d_e| < 1.1 \times 10^{-29} e$ cm [151]. We see that for generic complex phases the constraints on the couplings are quite severe for this scenario. We expect that the neutron EDM can also provide a promising probe of certain combinations of couplings.

7.4 Charged Current Processes

The new interactions of fermions with colored scalars can also lead to new charged current processes. To illustrate, we consider here the decays of charged pions that occur for $\Phi \sim (\mathbf{3}, \mathbf{1}, -\frac{1}{3})$ with interaction

$$\mathcal{L} \supset \lambda_{QL}\, \Phi_A^\dagger\, (Q_A\, L_A) + \text{H.c.} \tag{252}$$

Nonvanishing $(\lambda_{QL})_{11}$ or $(\lambda_{QL})_{12}$ lead to a modification to the lepton universality ratio,

$$R_\pi \equiv \frac{\Gamma(\pi^- \to e^- \bar{\nu}_e)}{\Gamma(\pi^- \to \mu^- \bar{\nu}_\mu)} \simeq R_\pi^{\text{SM}} \left(1 + \frac{|\lambda_{QL}^{11}|^2 - |\lambda_{QL}^{12}|^2}{2\sqrt{2}\, G_F\, |V_{ud}|\, m_{\phi_A}^2} \right). \tag{253}$$

We have neglected the effects of decays such as $\pi^- \to e^- \bar{\nu}_\mu$, etc., which do not interfere with the SM weak contribution, retaining only the dominant coherent contributions. The SM prediction [152] and measured value [153] are

$$R_\pi^{\text{SM}} = 1.2352(2) \times 10^{-4}, \qquad R_\pi^{\text{exp}} = 1.2344(30) \times 10^{-4}, \tag{254}$$

where the experimental uncertainty dominates the theoretical uncertainty. We apply a 2σ C.L. bound by demanding the new physics correction in Eq. (253) is less than twice the experimental uncertainty. This leads to the constraint

$$\sqrt{|\lambda_{QL}^{11}|^2 - |\lambda_{QL}^{12}|^2} < 0.4 \left(\frac{m_{\phi_A}}{1\,\text{TeV}} \right). \tag{255}$$

In addition to pion decays, such couplings may be probed in hadronic tau decays as well as tests of charged current universality in the quark sector.

7.5 Discussion

Evidently, interactions between the colored scalar and matter can manifest in a host of precision tests. The exact $\mathbb{Z}_2$ symmetry in our scenario ties any constraints coming from these measurements to the possible form and maximum size of the new twin fermion mass terms generated by those couplings (see Sec. 6). We have seen that some of these constraints can be quite stringent (e.g., from baryon number violation, EDM, or tree level FCNCs), although it is clear that they hinge, in many cases, on a particular coupling combination or flavor structure. Though it is beyond the scope of this work, it would be interesting to explore more broadly how the various patterns of new twin fermion mass terms arising from twin gauge symmetry breaking intersect with experimental constraints.

8.0 Collider Phenomenology

8.1 Higgs Coupling Modifications

A coupling between the colored scalar and the Higgs fields is an essential ingredient in our scenario. This couplings allows for viable electroweak vacuum alignment, following spontaneous $\mathbb{Z}_2$ breaking by the Φ_B VEV. Consequently, the physical Higgs scalar and the colored scalars are coupled, $V \supset A_{h\phi_A^\dagger\phi_A} h\,|\phi_A|^2$, where $A_{h\phi_A^\dagger\phi_A}$ is given in Eq. (67). Through this coupling the new colored, charged scalars generate one loop contributions to the $h\gamma\gamma$ and hgg effective couplings, which can modify the decay of the Higgs to two photons or the production of the Higgs in gluon fusion. These modifications can be expressed in terms of modifications of the Higgs partial widths. Assuming $2m_\phi \gg m_h$, we find (see e.g., Ref. [154]):

$$\frac{\Gamma(h\to\gamma\gamma)}{\Gamma(h\to\gamma\gamma)_{\rm SM}} \simeq \left|\cos\vartheta - c_\Phi\, d_\Phi\, Y_\Phi^2\, \frac{A_{h\phi_A\phi_A^*}\, v_A}{6\, m_\phi^2\, A_{\gamma\gamma}^{\rm SM}}\right|^2, \tag{256}$$

$$\frac{\Gamma(h\to gg)}{\Gamma(h\to gg)_{\rm SM}} \simeq \left|\cos\vartheta + c_\Phi\, T_\Phi\, \frac{A_{h\phi_A\phi_A^*}\, v_A}{3\, m_\phi^2\, A_{gg}^{\rm SM}}\right|^2, \tag{257}$$

where $A_{\gamma\gamma}^{\rm SM} \approx 6.5$, $A_{gg}^{\rm SM} \approx 1.4$, d_Φ is the dimension of the scalar representation, T_Φ is its Dynkin index, and $c_\Phi = 1$ ($\frac{1}{2}$) for complex (real) scalars. As mentioned in the introduction, the LHC has measured the $h\gamma\gamma$ and hgg couplings with 10% precision [31, 155]. For $\sin\vartheta \lesssim 1/3$, we find that current measurements can only probe relatively light scalars and low symmetry breaking scales f_Φ, typically below about 300 (500 GeV) for color triplet (sextet and octet) scalars. In most cases direct searches for pair produced colored scalars yield stronger limits. However, as these searches depend on the assumed decay mode, Higgs coupling measurements still offer a complementary test of light colored and charged scalars. Looking forward, the Higgs coupling measurements at the HL-LHC and at future colliders may be able to achieve percent level precision, probing smaller values of $\sin\vartheta$ and/or heavy colored scalar masses. The radial modes of the color symmetry breaking will also have a small effect upon the Higgs couplings, but as shown for the analogous hypercharge case the effect is typically negligible [82].

8.2 Direct Searches for Colored Scalars

The colored scalar field ϕ_A in the visible sector can naturally have a mass near the TeV scale and could therefore be produced in large numbers at hadron colliders like the LHC. We concentrate on pair production, $p\,p \to \phi_A\,\phi_A^*$, since as an inevitable consequence of the strong interaction it provides the most robust probe of the colored scalars. There can also be single ϕ_A production channels provided the scalar-fermion couplings discussed in Sec. 6 are sizeable, e.g., $qq' \to \phi_A$, $qg \to \phi_A \ell$, etc, but we focus on the various signatures expected from colored scalar pair production.

For the color triplet, we use the pair production cross sections for the lightest scalar top quark in the Minimal Supersymmetric Standard Model in the decoupling limit (heavy squarks and gluinos) from Ref. [156], based on resummed results at the next-to-leading logarithmic (NLL) accuracy matched to next-to-leading order (NLO) predictions. For the color sextet scalars, we use the leading order calculatiuon from Ref. [157]. NLO results exist in the literature for color octet scalar production [158, 159], and we use the results for real octet scalars from Ref. [159]. In Figure 17 we show the cross sections for pair production, $\sigma(pp \to \phi_A \phi_A^*)$ as a function of the scalar mass.

8.2.1 Signatures

- *Squark searches*: Color triplet scalars with quantum numbers $(\mathbf{3}, \mathbf{1}, -\frac{1}{3})$, $(\mathbf{3}, \mathbf{1}, \frac{2}{3})$ can decay to any quark flavor and a neutrino, $\phi_A \to q\,\nu$, where the q can be either a top, bottom, or light quark. The resulting collider signatures are identical to those of squark pair production in the Minimal Supersymmetric Standard Model, in which the squark decays to a quark and a massless stable neutralino. Therefore, searches for first and second generation squarks, sbottoms, and stops can be directly applied to these scenarios. A CMS search based on 137 fb^{-1} at $\sqrt{s} = 13$ TeV rules out a single squark decaying to a light jet and massless neutralino for squark masses below about 1.2 TeV [51], while comparable limits have been obtained by an ATLAS search [160]. Final states containing a bottom or top quark along with a neutrino resemble sbottom or stop searches, which

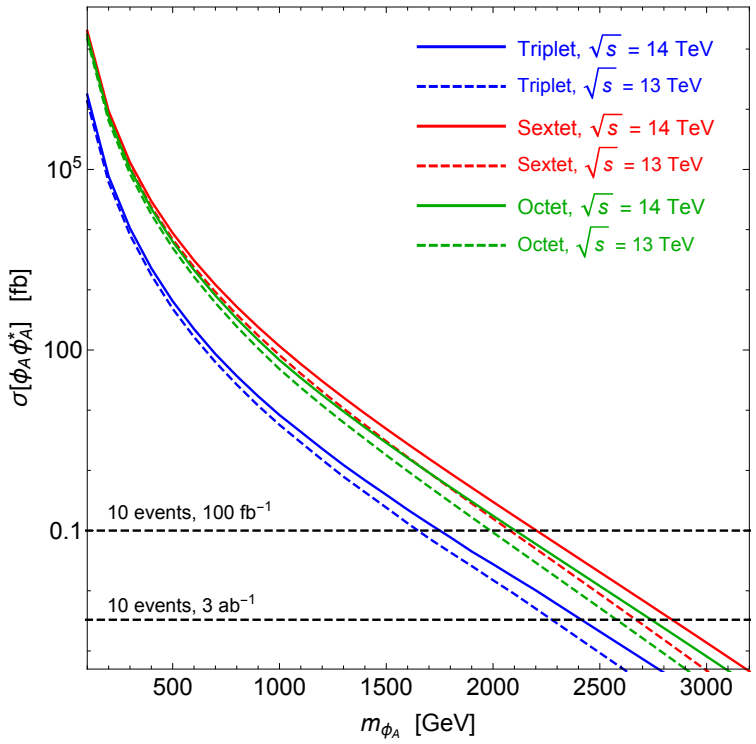

Figure 17: Pair production cross sections at the LHC for electroweak singlet, color triplet, sextet, and octet scalars ϕ_A.

constrain the triplet scalars to be heavier than about 1.2 TeV [51, 52]. The HL-LHC and, especially, a future 100 TeV hadron collider will be able to significantly extend the mass reach for such scalars. Taking stops as an example, the HL-LHC (3 ab^{-1}, $\sqrt{s} = 14$ TeV) will be able to constrain scalar masses up to about 1.6 TeV [161], while a future 100 TeV collider can probe scalars as heavy as 10 TeV [162].

- *Leptoquark Searches*: The color triplet models may also feature 'leptoquark' signals if the scalar decays to a quark and a charged lepton. A number of searches have been carried out targeting various leptoquark signals, depending on the flavor of the quark and charged lepton in the decay. Searches for first- and second-generation leptoquarks focus on the signature $\ell\ell jj$, with ℓ being an electron or muon. The best limits to date exclude scalar masses in the 1.4–1.6 TeV range and below [163, 164, 165]. The scalar may also have a significant branching ratio into a light jet and a neutrino. To cover these scenarios experiments have searched for the $\ell\nu jj$ final state, though these tend to give somewhat weaker constraints in comparison to the $\ell\ell jj$ channel. In the future, the HL-LHC will be able to probe first and second generation leptoquarks in the 2–3 TeV range, while a future 100 TeV hadron collider will be able to extend the reach to the 10 TeV range and beyond; see, e.g., Ref. [166] for a phenomenological study of the prospects in the $\mu\mu jj$ channel.

  Various searches for third generation leptoquarks exist in which the scalar decays involve one or more of τ, b, t. For example, scalars decaying to $t\tau$ ($b\tau$) are constrained to be heavier than about 900 GeV (1 TeV) by ATLAS and CMS searches [167, 168, 169]. There is also a CMS search in the $t\mu$ channel that constrains scalar masses below 1.4 TeV [170]. Bounds on scalar leptoquarks decaying to te have been obtained from a recast of a CMS SUSY multipleptons analysis [171, 172] and probe scalar masses below about 900 GeV. Finally, ATLAS searches [173] for scalar leptoquarks decaying to be and $b\mu$ place mass limits in the 1.5 TeV range. See Refs. [171, 174] for a comprehensive guide to leptoquark searches.

- *Diquark Searches*: Colored triplets, sextets, and octets may also decay to pairs of quarks or quark-antiquark pairs, $\phi_A \to qq$ or $\phi_A \to q\bar{q}$. Pair produced colored scalars then form four quark final states. Both ATLAS [53] and CMS [54] have searched for such

paired dijet resonances using a portion of the Run 2 dataset, and constrain color triplet scalars below about 500 GeV (600 GeV) when the scalar decays to light jets (one bottom jet and one light jet). The ATLAS study also gives an interpretation in the context of color octet scalars decaying to a pair of jets, limiting octet scalars below about 800 GeV. Because the pair production cross section for sextet scalars is comparable to that of octets [157, 158, 159], we expect similar limits for sextets decaying to pairs of light jets. In the long term, we expect the full HL-LHC dataset to improve the mass reach by a factor of two or more. Decays to $t\bar{t}$ are another interesting channel though a dedicated study for pair produced scalars decaying in this manner has not yet been undertaken by the collaborations. However, a recast of a CMS analysis of SM four top production has been performed [175] and constrains color octets with masses below about 1 TeV. By scaling up to the full HL-LHC 3ab^{-1} dataset at $\sqrt{s} = 14$ TeV this limit can be extended to octet masses of about 1.3 TeV [176] .

- *Long-lived Particle Signatures*: The signatures discussed above assume prompt scalar decays. However, if the couplings of the scalar to fermions discussed in Sec. 6 are suppressed, the scalar may be long-lived on collider scales. A variety of potential signatures exist in this case, many of which are quite striking and have small SM backgrounds. Examples include heavy stable R-hadrons, displaced vertices and kinked tracks. There is an active program at the LHC to search for signatures of this kind, and we refer the readers to the recent review articles [177, 178] for an in-depth survey.

9.0 Conclusions

The Mirror Twin Higgs provides an elegant symmetry-based understanding of the apparent little hierarchy between the EW scale and the dynamics at the 5–10 TeV scale posited to address the big hierarchy problem. Arguments related to vacuum alignment and cosmology suggest that the mirror symmetry protecting the light Higgs must be broken, and an attractive possibility is that this $\mathbb{Z}_2$ breaking is spontaneous in nature. In this work, we have investigated the simultaneous spontaneous breakdown of the twin color gauge symmetry and $\mathbb{Z}_2$. Remarkably, despite being related by an exact mirror symmetry in the UV, vast differences between the two sectors are exhibited in the low energy effective theory below the TeV scale as a result of spontaneous symmetry breaking. These differences manifest in the residual unbroken gauge symmetries, color confinement scale, and particle spectrum.

The richness of these effects is tied to the variety of possible colored scalar representations and associated symmetry breaking patterns. We have outlined five minimal possibilities for models with a single color triplet, sextet, or octet, and explored how the twin sector departs from the mirror onset. In particular, we have shown how new dynamical mass terms may be generated for the twin fermions. These effects are tied by the discrete $\mathbb{Z}_2$ symmetry to precision tests in the visible sector, allowing additional handles on uncovering the twin structure without direct access to many of the states. Furthermore, the new colored states may be probed at the LHC and at future high energy colliders. This richness is mostly confined to the twin sector, because only this sector experiences the color breaking. Except for qualitative difference in precision tests between the triplet and others, the visible sector phenomenology is largely the same, illustrating the variety possible in a twin sector that is identical to the SM at high energies.

There are a number of open questions worthy of further consideration. Seeing as departures from MTH scenarios are often motivated by cosmology it would be very interesting to examine the possible cosmological histories within our models. For instance, the addition of a new colored field could play a role in baryogenesis. Moreover, the twin baryons and other bound states of the various residual color symmetries may provide interesting dark matter

candidates or manifest as a new form of dark radiation. In many cases these dark sectors may exhibit novel gauge interactions, including new long range forces and/or very low confinement scales. Another direction concerns the possible UV completions of our models. In particular, we expect that the new colored scalars utilized in this work may find a natural home in supersymmetric completions as a superpartner of a quark, or in composite Higgs models as a colored pNGB.

Bibliography

[1] F. Englert and R. Brout. Broken Symmetry and the Mass of Gauge Vector Mesons. *Phys. Rev. Lett.*, 13:321–323, 1964. doi:10.1103/PhysRevLett.13.321.

[2] Peter W. Higgs. Broken symmetries, massless particles and gauge fields. *Phys. Lett.*, 12:132–133, 1964. doi:10.1016/0031-9163(64)91136-9.

[3] Peter W. Higgs. Broken Symmetries and the Masses of Gauge Bosons. *Phys. Rev. Lett.*, 13:508–509, 1964. doi:10.1103/PhysRevLett.13.508.

[4] G.S. Guralnik, C.R. Hagen, and T.W.B. Kibble. Global Conservation Laws and Massless Particles. *Phys. Rev. Lett.*, 13:585–587, 1964. doi:10.1103/PhysRevLett.13.585.

[5] Peter W. Higgs. Spontaneous Symmetry Breakdown without Massless Bosons. *Phys. Rev.*, 145:1156–1163, 1966. doi:10.1103/PhysRev.145.1156.

[6] T.W.B. Kibble. Symmetry breaking in nonAbelian gauge theories. *Phys. Rev.*, 155:1554–1561, 1967. doi:10.1103/PhysRev.155.1554.

[7] S.L. Glashow. Partial Symmetries of Weak Interactions. *Nucl. Phys.*, 22:579–588, 1961. doi:10.1016/0029-5582(61)90469-2.

[8] Steven Weinberg. A Model of Leptons. *Phys. Rev. Lett.*, 19:1264–1266, 1967. doi:10.1103/PhysRevLett.19.1264.

[9] Abdus Salam. Weak and Electromagnetic Interactions. *Conf. Proc. C*, 680519:367–377, 1968. doi:10.1142/9789812795915_0034.

[10] Paul A.M. Dirac. Quantum theory of emission and absorption of radiation. *Proc. Roy. Soc. Lond. A*, A114:243, 1927. doi:10.1098/rspa.1927.0039.

[11] Enrico Fermi. Quantum Theory of Radiation. *Rev. Mod. Phys.*, 4(1):87–132, 1932. doi:10.1103/RevModPhys.4.87.

[12] R.P. Feynman. *QED: The Strange Theory of Light and Matter*. 1986.

[13] C. N. Yang and R. L. Mills. Conservation of isotopic spin and isotopic gauge invariance. *Phys. Rev.*, 96:191–195, Oct 1954. URL: https://link.aps.org/doi/10.1103/PhysRev.96.191, doi:10.1103/PhysRev.96.191.

[14] Murray Gell-Mann. The Eightfold Way: A Theory of strong interaction symmetry. 3 1961. doi:10.2172/4008239.

[15] G. Zweig. An SU(3) model for strong interaction symmetry and its breaking. Version 1. 1 1964.

[16] H. Fritzsch, Murray Gell-Mann, and H. Leutwyler. Advantages of the Color Octet Gluon Picture. *Phys. Lett. B*, 47:365–368, 1973. doi:10.1016/0370-2693(73)90625-4.

[17] H.David Politzer. Reliable Perturbative Results for Strong Interactions? *Phys. Rev. Lett.*, 30:1346–1349, 1973. doi:10.1103/PhysRevLett.30.1346.

[18] David J. Gross and Frank Wilczek. Ultraviolet Behavior of Nonabelian Gauge Theories. *Phys. Rev. Lett.*, 30:1343–1346, 1973. doi:10.1103/PhysRevLett.30.1343.

[19] M. Tanabashi et al. Review of Particle Physics. *Phys. Rev.*, D98(3):030001, 2018. doi:10.1103/PhysRevD.98.030001.

[20] Nicola Cabibbo. Unitary Symmetry and Leptonic Decays. *Phys. Rev. Lett.*, 10:531–533, 1963. doi:10.1103/PhysRevLett.10.531.

[21] Makoto Kobayashi and Toshihide Maskawa. CP Violation in the Renormalizable Theory of Weak Interaction. *Prog. Theor. Phys.*, 49:652–657, 1973. doi:10.1143/PTP.49.652.

[22] B. Pontecorvo. Neutrino Experiments and the Problem of Conservation of Leptonic Charge. *Sov. Phys. JETP*, 26:984–988, 1968.

[23] Ziro Maki, Masami Nakagawa, and Shoichi Sakata. Remarks on the unified model of elementary particles. *Prog. Theor. Phys.*, 28:870–880, 1962. doi:10.1143/PTP.28.870.

[24] Combined Higgs boson production and decay measurements with up to 137 fb-1 of proton-proton collision data at sqrts = 13 TeV. Technical Report CMS-PAS-HIG-19-005, CERN, Geneva, 2020. URL: https://cds.cern.ch/record/2706103.

[25] Georges Aad et al. Observation of a new particle in the search for the Standard Model Higgs boson with the ATLAS detector at the LHC. *Phys. Lett. B*, 716:1–29, 2012. arXiv:1207.7214, doi:10.1016/j.physletb.2012.08.020.

[26] Serguei Chatrchyan et al. Observation of a New Boson at a Mass of 125 GeV with the CMS Experiment at the LHC. *Phys. Lett. B*, 716:30–61, 2012. arXiv:1207.7235, doi:10.1016/j.physletb.2012.08.021.

[27] John F. Gunion, Howard E. Haber, Gordon L. Kane, and Sally Dawson. *The Higgs Hunter's Guide*, volume 80. 2000.

[28] LHC Higgs Cross Section Working Group. . https://twiki.cern.ch/twiki/bin/view/LHCPhysics/CERNHLHE2019/, 2019. [Online; and PDG: http://pdg.lbl.gov.

[29] J R Andersen et al. Handbook of LHC Higgs Cross Sections: 3. Higgs Properties. 7 2013. arXiv:1307.1347, doi:10.5170/CERN-2013-004.

[30] D. de Florian et al. Handbook of LHC Higgs Cross Sections: 4. Deciphering the Nature of the Higgs Sector. 2/2017, 10 2016. arXiv:1610.07922, doi:10.23731/CYRM-2017-002.

[31] Georges Aad et al. Combined measurements of Higgs boson production and decay using up to 80 fb^{-1} of proton-proton collision data at $\sqrt{s} = 13$ TeV collected with the ATLAS experiment. *Phys. Rev. D*, 101(1):012002, 2020. arXiv:1909.02845, doi:10.1103/PhysRevD.101.012002.

[32] M. Cepeda et al. *Report from Working Group 2: Higgs Physics at the HL-LHC and HE-LHC*, volume 7, pages 221–584. 12 2019. arXiv:1902.00134, doi:10.23731/CYRM-2019-007.221.

[33] The International Linear Collider Technical Design Report - Volume 1: Executive Summary. 6 2013. arXiv:1306.6327.

[34] Keisuke Fujii et al. Physics Case for the 250 GeV Stage of the International Linear Collider. 10 2017. arXiv:1710.07621.

[35] Tim Barklow, Keisuke Fujii, Sunghoon Jung, Robert Karl, Jenny List, Tomohisa Ogawa, Michael E. Peskin, and Junping Tian. Improved Formalism for Precision Higgs Coupling Fits. *Phys. Rev.*, D97(5):053003, 2018. arXiv:1708.08912, doi:10.1103/PhysRevD.97.053003.

[36] T.K. Charles et al. The Compact Linear Collider (CLIC) - 2018 Summary Report. 2/2018, 12 2018. arXiv:1812.06018, doi:10.23731/CYRM-2018-002.

[37] A. Abada et al. FCC Physics Opportunities: Future Circular Collider Conceptual Design Report Volume 1. *Eur. Phys. J. C*, 79(6):474, 2019. doi:10.1140/epjc/s10052-019-6904-3.

[38] Mingyi Dong et al. CEPC Conceptual Design Report: Volume 2 - Physics & Detector. 11 2018. arXiv:1811.10545.

[39] Chen-Ning Yang. Selection Rules for the Dematerialization of a Particle Into Two Photons. *Phys. Rev.*, 77:242–245, 1950. doi:10.1103/PhysRev.77.242.

[40] Vardan Khachatryan et al. Constraints on the spin-parity and anomalous HVV couplings of the Higgs boson in proton collisions at 7 and 8 TeV. *Phys. Rev. D*, 92(1):012004, 2015. arXiv:1411.3441, doi:10.1103/PhysRevD.92.012004.

[41] Georges Aad et al. Study of the spin and parity of the Higgs boson in diboson decays with the ATLAS detector. *Eur. Phys. J. C*, 75(10):476, 2015. [Erratum: Eur.Phys.J.C 76, 152 (2016)]. arXiv:1506.05669, doi:10.1140/epjc/s10052-015-3685-1.

[42] Georges Aad et al. Test of CP Invariance in vector-boson fusion production of the Higgs boson using the Optimal Observable method in the ditau decay channel with the ATLAS detector. *Eur. Phys. J. C*, 76(12):658, 2016. arXiv:1602.04516, doi:10.1140/epjc/s10052-016-4499-5.

[43] Stephen P. Martin. *A Supersymmetry primer*, volume 21, pages 1–153. 2010. arXiv:hep-ph/9709356, doi:10.1142/9789812839657_0001.

[44] Savas Dimopoulos and Howard Georgi. Softly Broken Supersymmetry and SU(5). *Nucl. Phys. B*, 193:150–162, 1981. doi:10.1016/0550-3213(81)90522-8.

[45] Christopher T. Hill and Elizabeth H. Simmons. Strong Dynamics and Electroweak Symmetry Breaking. *Phys. Rept.*, 381:235–402, 2003. [Erratum: Phys.Rept. 390, 553–554 (2004)]. arXiv:hep-ph/0203079, doi:10.1016/S0370-1573(03)00140-6.

[46] Giuliano Panico and Andrea Wulzer. *The Composite Nambu-Goldstone Higgs*, volume 913. Springer, 2016. arXiv:1506.01961, doi:10.1007/978-3-319-22617-0.

[47] Nima Arkani-Hamed, Savas Dimopoulos, and G.R. Dvali. The Hierarchy problem and new dimensions at a millimeter. *Phys. Lett. B*, 429:263–272, 1998. arXiv:hep-ph/9803315, doi:10.1016/S0370-2693(98)00466-3.

[48] Lisa Randall and Raman Sundrum. A Large mass hierarchy from a small extra dimension. *Phys. Rev. Lett.*, 83:3370–3373, 1999. arXiv:hep-ph/9905221, doi:10.1103/PhysRevLett.83.3370.

[49] V. Agrawal, Stephen M. Barr, John F. Donoghue, and D. Seckel. Viable range of the mass scale of the standard model. *Phys. Rev. D*, 57:5480–5492, 1998. arXiv:hep-ph/9707380, doi:10.1103/PhysRevD.57.5480.

[50] Michele Papucci, Joshua T. Ruderman, and Andreas Weiler. Natural SUSY Endures. *JHEP*, 09:035, 2012. arXiv:1110.6926, doi:10.1007/JHEP09(2012)035.

[51] Albert M Sirunyan et al. Search for supersymmetry in proton-proton collisions at 13 TeV in final states with jets and missing transverse momentum. *JHEP*, 10:244, 2019. arXiv:1908.04722, doi:10.1007/JHEP10(2019)244.

[52] Search for new phenomena with top quark pairs in final states with one lepton, jets, and missing transverse momentum in pp collisions at $\sqrt{s} = 13$ TeV with the ATLAS detector. Technical Report ATLAS-CONF-2020-003, CERN, Geneva, Feb 2020. URL: https://cds.cern.ch/record/2711489.

[53] Morad Aaboud et al. A search for pair-produced resonances in four-jet final states at $\sqrt{s} = 13$ TeV with the ATLAS detector. *Eur. Phys. J.*, C78(3):250, 2018. arXiv:1710.07171, doi:10.1140/epjc/s10052-018-5693-4.

[54] Albert M Sirunyan et al. Search for pair-produced resonances decaying to quark pairs in proton-proton collisions at $\sqrt{s} = 13$ TeV. *Phys. Rev.*, D98(11):112014, 2018. arXiv:1808.03124, doi:10.1103/PhysRevD.98.112014.

[55] Riccardo Barbieri and Alessandro Strumia. What is the limit on the Higgs mass? *Phys. Lett. B*, 462:144–149, 1999. arXiv:hep-ph/9905281, doi:10.1016/S0370-2693(99)00882-5.

[56] Nathaniel Craig, Simon Knapen, and Pietro Longhi. Neutral Naturalness from Orbifold Higgs Models. *Phys. Rev. Lett.*, 114(6):061803, 2015. arXiv:1410.6808, doi:10.1103/PhysRevLett.114.061803.

[57] Z. Chacko, Hock-Seng Goh, and Roni Harnik. The Twin Higgs: Natural electroweak breaking from mirror symmetry. *Phys. Rev. Lett.*, 96:231802, 2006. arXiv:hep-ph/0506256, doi:10.1103/PhysRevLett.96.231802.

[58] Z. Chacko, Yasunori Nomura, Michele Papucci, and Gilad Perez. Natural little hierarchy from a partially goldstone twin Higgs. *JHEP*, 01:126, 2006. arXiv:hep-ph/0510273, doi:10.1088/1126-6708/2006/01/126.

[59] Riccardo Barbieri, Thomas Gregoire, and Lawrence J. Hall. Mirror world at the large hadron collider. 2005. arXiv:hep-ph/0509242.

[60] Gustavo Burdman, Z. Chacko, Hock-Seng Goh, and Roni Harnik. Folded supersymmetry and the LEP paradox. *JHEP*, 02:009, 2007. arXiv:hep-ph/0609152, doi:10.1088/1126-6708/2007/02/009.

[61] Haiying Cai, Hsin-Chia Cheng, and John Terning. A Quirky Little Higgs Model. *JHEP*, 05:045, 2009. arXiv:0812.0843, doi:10.1088/1126-6708/2009/05/045.

[62] David Poland and Jesse Thaler. The Dark Top. *JHEP*, 11:083, 2008. arXiv:0808.1290, doi:10.1088/1126-6708/2008/11/083.

[63] Brian Batell and Matthew McCullough. Neutrino Masses from Neutral Top Partners. *Phys. Rev.*, D92(7):073018, 2015. arXiv:1504.04016, doi:10.1103/PhysRevD.92.073018.

[64] Csaba Csáki, Teng Ma, and Jing Shu. Trigonometric Parity for the Composite Higgs. *Phys. Rev. Lett.*, 121(23):231801, 2018. arXiv:1709.08636, doi:10.1103/PhysRevLett.121.231801.

[65] Javi Serra and Riccardo Torre. Neutral naturalness from the brother-Higgs model. *Phys. Rev.*, D97(3):035017, 2018. arXiv:1709.05399, doi:10.1103/PhysRevD.97.035017.

[66] Timothy Cohen, Nathaniel Craig, Gian F. Giudice, and Matthew Mccullough. The Hyperbolic Higgs. *JHEP*, 05:091, 2018. arXiv:1803.03647, doi:10.1007/JHEP05(2018)091.

[67] Hsin-Chia Cheng, Lingfeng Li, Ennio Salvioni, and Christopher B. Verhaaren. Singlet Scalar Top Partners from Accidental Supersymmetry. *JHEP*, 05:057, 2018. arXiv:1803.03651, doi:10.1007/JHEP05(2018)057.

[68] Barry M. Dillon. Neutral-naturalness from a holographic $SO(6)/SO(5)$ composite Higgs model. *Phys. Rev. D*, 99(11):115008, 2019. arXiv:1806.10702, doi:10.1103/PhysRevD.99.115008.

[69] Ling-Xiao Xu, Jiang-Hao Yu, and Shou-Hua Zhu. Minimal Neutral Naturalness Model. 2018. arXiv:1810.01882.

[70] Javi Serra, Stefan Stelzl, Riccardo Torre, and Andreas Weiler. Hypercharged Naturalness. *JHEP*, 10:060, 2019. arXiv:1905.02203, doi:10.1007/JHEP10(2019)060.

[71] Aqeel Ahmed, Saereh Najjari, and Christopher B. Verhaaren. A Minimal Model for Neutral Naturalness and pseudo-Nambu-Goldstone Dark Matter. 3 2020. arXiv:2003.08947.

[72] Adam Falkowski, Stefan Pokorski, and Martin Schmaltz. Twin SUSY. *Phys. Rev.*, D74:035003, 2006. arXiv:hep-ph/0604066, doi:10.1103/PhysRevD.74.035003.

[73] Spencer Chang, Lawrence J. Hall, and Neal Weiner. A Supersymmetric twin Higgs. *Phys. Rev.*, D75:035009, 2007. arXiv:hep-ph/0604076, doi:10.1103/PhysRevD.75.035009.

[74] Puneet Batra and Z. Chacko. A Composite Twin Higgs Model. *Phys. Rev.*, D79:095012, 2009. arXiv:0811.0394, doi:10.1103/PhysRevD.79.095012.

[75] Nathaniel Craig and Kiel Howe. Doubling down on naturalness with a supersymmetric twin Higgs. *JHEP*, 03:140, 2014. arXiv:1312.1341, doi:10.1007/JHEP03(2014)140.

[76] Michael Geller and Ofri Telem. Holographic Twin Higgs Model. *Phys. Rev. Lett.*, 114:191801, 2015. arXiv:1411.2974, doi:10.1103/PhysRevLett.114.191801.

[77] Riccardo Barbieri, Davide Greco, Riccardo Rattazzi, and Andrea Wulzer. The Composite Twin Higgs scenario. *JHEP*, 08:161, 2015. arXiv:1501.07803, doi:10.1007/JHEP08(2015)161.

[78] Matthew Low, Andrea Tesi, and Lian-Tao Wang. Twin Higgs mechanism and a composite Higgs boson. *Phys. Rev.*, D91:095012, 2015. arXiv:1501.07890, doi:10.1103/PhysRevD.91.095012.

[79] Andrey Katz, Alberto Mariotti, Stefan Pokorski, Diego Redigolo, and Robert Ziegler. SUSY Meets Her Twin. *JHEP*, 01:142, 2017. arXiv:1611.08615, doi:10.1007/JHEP01(2017)142.

[80] Pouya Asadi, Nathaniel Craig, and Ying-Ying Li. Twin Turtles. *JHEP*, 02:138, 2019. arXiv:1810.09467, doi:10.1007/JHEP02(2019)138.

[81] Gustavo Burdman, Zackaria Chacko, Roni Harnik, Leonardo de Lima, and Christopher B. Verhaaren. Colorless Top Partners, a 125 GeV Higgs, and the Limits on Naturalness. *Phys. Rev.*, D91(5):055007, 2015. arXiv:1411.3310, doi:10.1103/PhysRevD.91.055007.

[82] Brian Batell and Christopher B. Verhaaren. Breaking Mirror Twin Hypercharge. *JHEP*, 12:010, 2019. arXiv:1904.10468, doi:10.1007/JHEP12(2019)010.

[83] Albert M Sirunyan et al. Search for invisible decays of a Higgs boson produced through vector boson fusion in proton-proton collisions at $\sqrt{s} = 13$ TeV. *Phys. Lett. B*, 793:520–551, 2019. arXiv:1809.05937, doi:10.1016/j.physletb.2019.04.025.

[84] Search for invisible Higgs boson decays with vector boson fusion signatures with the ATLAS detector using an integrated luminosity of 139 fb^{-1}. 4 2020.

[85] Nathaniel Craig, Andrey Katz, Matt Strassler, and Raman Sundrum. Naturalness in the Dark at the LHC. *JHEP*, 07:105, 2015. arXiv:1501.05310, doi:10.1007/JHEP07(2015)105.

[86] Hugues Beauchesne, Kevin Earl, and Thomas Gregoire. The spontaneous $\mathbb{Z}_2$ breaking Twin Higgs. *JHEP*, 01:130, 2016. arXiv:1510.06069, doi:10.1007/JHEP01(2016)130.

[87] Roni Harnik, Kiel Howe, and John Kearney. Tadpole-Induced Electroweak Symmetry Breaking and pNGB Higgs Models. *JHEP*, 03:111, 2017. arXiv:1603.03772, doi:10.1007/JHEP03(2017)111.

[88] Jiang-Hao Yu. Radiative-$\mathbb{Z}_2$-breaking twin Higgs model. *Phys. Rev.*, D94(11):111704, 2016. arXiv:1608.01314, doi:10.1103/PhysRevD.94.111704.

[89] Jiang-Hao Yu. A tale of twin Higgs: natural twin two Higgs doublet models. *JHEP*, 12:143, 2016. arXiv:1608.05713, doi:10.1007/JHEP12(2016)143.

[90] Tae Hyun Jung. Spontaneous Twin Symmetry Breaking. 2019. arXiv:1902.10978.

[91] Zackaria Chacko, Nathaniel Craig, Patrick J. Fox, and Roni Harnik. Cosmology in Mirror Twin Higgs and Neutrino Masses. *JHEP*, 07:023, 2017. arXiv:1611.07975, doi:10.1007/JHEP07(2017)023.

[92] P.A.R. Ade et al. Planck 2015 results. XIII. Cosmological parameters. *Astron. Astrophys.*, 594:A13, 2016. arXiv:1502.01589, doi:10.1051/0004-6361/201525830.

[93] Nathaniel Craig and Andrey Katz. The Fraternal WIMP Miracle. *JCAP*, 1510(10):054, 2015. arXiv:1505.07113, doi:10.1088/1475-7516/2015/10/054.

[94] Nathaniel Craig, Simon Knapen, Pietro Longhi, and Matthew Strassler. The Vector-like Twin Higgs. *JHEP*, 07:002, 2016. arXiv:1601.07181, doi:10.1007/JHEP07(2016)002.

[95] Marco Farina. Asymmetric Twin Dark Matter. *JCAP*, 1511(11):017, 2015. arXiv:1506.03520, doi:10.1088/1475-7516/2015/11/017.

[96] Nathaniel Craig, Seth Koren, and Timothy Trott. Cosmological Signals of a Mirror Twin Higgs. *JHEP*, 05:038, 2017. arXiv:1611.07977, doi:10.1007/JHEP05(2017)038.

[97] Riccardo Barbieri, Lawrence J. Hall, and Keisuke Harigaya. Minimal Mirror Twin Higgs. *JHEP*, 11:172, 2016. arXiv:1609.05589, doi:10.1007/JHEP11(2016)172.

[98] Csaba Csaki, Eric Kuflik, and Salvator Lombardo. Viable Twin Cosmology from Neutrino Mixing. *Phys. Rev.*, D96(5):055013, 2017. arXiv:1703.06884, doi:10.1103/PhysRevD.96.055013.

[99] Keisuke Harigaya, Robert Mcgehee, Hitoshi Murayama, and Katelin Schutz. A Predictive Mirror Twin Higgs with Small $\mathbf{Z}_2$ Breaking. 5 2019. arXiv:1905.08798.

[100] Isabel Garcia Garcia, Robert Lasenby, and John March-Russell. Twin Higgs WIMP Dark Matter. *Phys. Rev.*, D92(5):055034, 2015. arXiv:1505.07109, doi:10.1103/PhysRevD.92.055034.

[101] Isabel Garcia Garcia, Robert Lasenby, and John March-Russell. Twin Higgs Asymmetric Dark Matter. *Phys. Rev. Lett.*, 115(12):121801, 2015. arXiv:1505.07410, doi:10.1103/PhysRevLett.115.121801.

[102] Marat Freytsis, Simon Knapen, Dean J. Robinson, and Yuhsin Tsai. Gamma-rays from Dark Showers with Twin Higgs Models. *JHEP*, 05:018, 2016. arXiv:1601.07556, doi:10.1007/JHEP05(2016)018.

[103] Marco Farina, Angelo Monteux, and Chang Sub Shin. Twin mechanism for baryon and dark matter asymmetries. *Phys. Rev.*, D94(3):035017, 2016. arXiv:1604.08211, doi:10.1103/PhysRevD.94.035017.

[104] Riccardo Barbieri, Lawrence J. Hall, and Keisuke Harigaya. Effective Theory of Flavor for Minimal Mirror Twin Higgs. *JHEP*, 10:015, 2017. arXiv:1706.05548, doi:10.1007/JHEP10(2017)015.

[105] Yonit Hochberg, Eric Kuflik, and Hitoshi Murayama. Twin Higgs model with strongly interacting massive particle dark matter. *Phys. Rev.*, D99(1):015005, 2019. arXiv:1805.09345, doi:10.1103/PhysRevD.99.015005.

[106] Hsin-Chia Cheng, Lingfeng Li, and Rui Zheng. Coscattering/Coannihilation Dark Matter in a Fraternal Twin Higgs Model. *JHEP*, 09:098, 2018. arXiv:1805.12139, doi:10.1007/JHEP09(2018)098.

[107] John Terning, Christopher B. Verhaaren, and Kyle Zora. Composite Twin Dark Matter. 2019. arXiv:1902.08211.

[108] Seth Koren and Robert McGehee. Freezing-in twin dark matter. *Phys. Rev. D*, 101(5):055024, 2020. arXiv:1908.03559, doi:10.1103/PhysRevD.101.055024.

[109] Marcin Badziak, Giovanni Grilli Di Cortona, and Keisuke Harigaya. Natural Twin Neutralino Dark Matter. *Phys. Rev. Lett.*, 124(12):121803, 2020. arXiv:1911.03481, doi:10.1103/PhysRevLett.124.121803.

[110] Kohei Fujikura, Kohei Kamada, Yuichiro Nakai, and Masahide Yamaguchi. Phase Transitions in Twin Higgs Models. *JHEP*, 12:018, 2018. arXiv:1810.00574, doi:10.1007/JHEP12(2018)018.

[111] Kevin Earl, Chee Sheng Fong, Thomas Gregoire, and Alberto Tonero. Mirror Dirac leptogenesis. *JCAP*, 03:036, 2020. arXiv:1903.12192, doi:10.1088/1475-7516/2020/03/036.

[112] Valentina Prilepina and Yuhsin Tsai. Reconciling Large And Small-Scale Structure In Twin Higgs Models. *JHEP*, 09:033, 2017. arXiv:1611.05879, doi:10.1007/JHEP09(2017)033.

[113] Zackaria Chacko, David Curtin, Michael Geller, and Yuhsin Tsai. Cosmological Signatures of a Mirror Twin Higgs. *JHEP*, 09:163, 2018. arXiv:1803.03263, doi:10.1007/JHEP09(2018)163.

[114] Csaba Csaki, Michael Geller, Ofri Telem, and Andreas Weiler. The Flavor of the Composite Twin Higgs. *JHEP*, 09:146, 2016. arXiv:1512.03427, doi:10.1007/JHEP09(2016)146.

[115] Wolfgang Altmannshofer and Brian Maddock. Flavorful Two Higgs Doublet Model with a Twin. 3 2020. arXiv:2003.01320.

[116] Di Liu and Neal Weiner. A Portalino to the Twin Sector. 5 2019. arXiv:1905.00861.

[117] Brian Batell, Wei Hu, and Christopher B. Verhaaren. Breaking Mirror Twin Color. *JHEP*, 08:009, 2020. arXiv:2004.10761, doi:10.1007/JHEP08(2020)009.

[118] Ling-Fong Li. Group Theory of the Spontaneously Broken Gauge Symmetries. *Phys. Rev.*, D9:1723–1739, 1974. doi:10.1103/PhysRevD.9.1723.

[119] Simon Hands, John B. Kogut, Maria-Paola Lombardo, and Susan E. Morrison. Symmetries and spectrum of SU(2) lattice gauge theory at finite chemical potential. *Nucl. Phys. B*, 558:327–346, 1999. arXiv:hep-lat/9902034, doi:10.1016/S0550-3213(99)00364-8.

[120] J.B. Kogut, Misha A. Stephanov, and D. Toublan. On two color QCD with baryon chemical potential. *Phys. Lett. B*, 464:183–191, 1999. arXiv:hep-ph/9906346, doi:10.1016/S0370-2693(99)00971-5.

[121] R. Aloisio, V. Azcoiti, G. Di Carlo, A. Galante, and A.F. Grillo. Fermion condensates in two colors finite density QCD at strong coupling. *Phys. Lett. B*, 493:189–196, 2000. arXiv:hep-lat/0009034, doi:10.1016/S0370-2693(00)01108-4.

[122] J.B. Kogut, D.K. Sinclair, S.J. Hands, and S.E. Morrison. Two color QCD at nonzero quark number density. *Phys. Rev. D*, 64:094505, 2001. arXiv:hep-lat/0105026, doi:10.1103/PhysRevD.64.094505.

[123] John B. Kogut, Dominique Toublan, and D.K. Sinclair. The Phase diagram of four flavor SU(2) lattice gauge theory at nonzero chemical potential and temperature. *Nucl. Phys. B*, 642:181–209, 2002. arXiv:hep-lat/0205019, doi:10.1016/S0550-3213(02)00678-8.

[124] J.B. Kogut, D. Toublan, and D.K. Sinclair. The PseudoGoldstone spectrum of two color QCD at finite density. *Phys. Rev. D*, 68:054507, 2003. arXiv:hep-lat/0305003, doi:10.1103/PhysRevD.68.054507.

[125] Y. Nishida, K. Fukushima, and T. Hatsuda. Thermodynamics of strong coupling two color QCD with chiral and diquark condensates. *Phys. Rept.*, 398:281–300, 2004. arXiv:hep-ph/0306066, doi:10.1016/j.physrep.2004.05.005.

[126] Maria-Paola Lombardo, Maria Luigia Paciello, Silvano Petrarca, and Bruno Taglienti. Glueballs and the superfluid phase of Two-Color QCD. *Eur. Phys. J. C*, 58:69–81, 2008. arXiv:0804.4863, doi:10.1140/epjc/s10052-008-0718-z.

[127] Matthew R. Buckley and Ethan T. Neil. Thermal dark matter from a confining sector. *Phys. Rev. D*, 87(4):043510, 2013. arXiv:1209.6054, doi:10.1103/PhysRevD.87.043510.

[128] William Detmold, Matthew McCullough, and Andrew Pochinsky. Dark Nuclei I: Cosmology and Indirect Detection. *Phys. Rev. D*, 90(11):115013, 2014. arXiv:1406.2276, doi:10.1103/PhysRevD.90.115013.

[129] Lindsay Forestell, David E. Morrissey, and Kris Sigurdson. Non-Abelian Dark Forces and the Relic Densities of Dark Glueballs. *Phys. Rev. D*, 95(1):015032, 2017. arXiv:1605.08048, doi:10.1103/PhysRevD.95.015032.

[130] Thomas DeGrand and Ethan T. Neil. Repurposing lattice QCD results for composite phenomenology. *Phys. Rev. D*, 101(3):034504, 2020. arXiv:1910.08561, doi:10.1103/PhysRevD.101.034504.

[131] Michael J. Teper. Glueball masses and other physical properties of SU(N) gauge theories in D = (3+1): A Review of lattice results for theorists. 12 1998. arXiv:hep-th/9812187.

[132] Biagio Lucini and Gregory Moraitis. The Running of the coupling in SU(N) pure gauge theories. *Phys. Lett. B*, 668:226–232, 2008. arXiv:0805.2913, doi:10.1016/j.physletb.2008.08.047.

[133] Heisenberg W. and Euler H. Folgerungen aus der Diracschen Theorie des Positrons. *Zeitschrift für Physik*, 98:714–732, 1936. doi:https://doi.org/10.1007/BF01343663.

[134] V.A. Novikov, L.V. Okun, M.A. Shifman, A.I. Vainshtein, M.B. Voloshin, and V.I. Zakharov. Quantum chromodynamics and charm. An excursion into theory. *ITEP–83*, 10, 1977. URL: https://inis.iaea.org/search/search.aspx?orig_q=RN:10422528.

[135] Jose E. Juknevich, Dmitry Melnikov, and Matthew J. Strassler. A Pure-Glue Hidden Valley I. States and Decays. *JHEP*, 07:055, 2009. arXiv:0903.0883, doi:10.1088/1126-6708/2009/07/055.

[136] Y. Chen et al. Glueball spectrum and matrix elements on anisotropic lattices. *Phys. Rev. D*, 73:014516, 2006. arXiv:hep-lat/0510074, doi:10.1103/PhysRevD.73.014516.

[137] Junhai Kang and Markus A. Luty. Macroscopic Strings and 'Quirks' at Colliders. *JHEP*, 11:065, 2009. arXiv:0805.4642, doi:10.1088/1126-6708/2009/11/065.

[138] Fady Bishara and Christopher B. Verhaaren. Singleton Portals to the Twin Sector. 2018. arXiv:1811.05977.

[139] R. Barbier et al. R-parity violating supersymmetry. *Phys. Rept.*, 420:1–202, 2005. arXiv:hep-ph/0406039, doi:10.1016/j.physrep.2005.08.006.

[140] Pran Nath and Pavel Fileviez Perez. Proton stability in grand unified theories, in strings and in branes. *Phys. Rept.*, 441:191–317, 2007. arXiv:hep-ph/0601023, doi:10.1016/j.physrep.2007.02.010.

[141] N. Tsutsui et al. Lattice QCD calculation of the proton decay matrix element in the continuum limit. *Phys. Rev.*, D70:111501, 2004. arXiv:hep-lat/0402026, doi:10.1103/PhysRevD.70.111501.

[142] Nicola Cabibbo, Earl C. Swallow, and Roland Winston. Semileptonic hyperon decays. *Ann. Rev. Nucl. Part. Sci.*, 53:39–75, 2003. arXiv:hep-ph/0307298, doi:10.1146/annurev.nucl.53.013103.155258.

[143] K. Abe et al. Search for proton decay via $p \to e^+\pi^0$ and $p \to \mu^+\pi^0$ in 0.31 megaton·years exposure of the Super-Kamiokande water Cherenkov detector. *Phys. Rev.*, D95(1):012004, 2017. arXiv:1610.03597, doi:10.1103/PhysRevD.95.012004.

[144] Jonathan M. Arnold, Bartosz Fornal, and Mark B. Wise. Simplified models with baryon number violation but no proton decay. *Phys. Rev.*, D87:075004, 2013. arXiv:1212.4556, doi:10.1103/PhysRevD.87.075004.

[145] M. Bona et al. Model-independent constraints on $\Delta F = 2$ operators and the scale of new physics. *JHEP*, 03:049, 2008. arXiv:0707.0636, doi:10.1088/1126-6708/2008/03/049.

[146] E. Abouzaid et al. Precise Measurements of Direct CP Violation, CPT Symmetry, and Other Parameters in the Neutral Kaon System. *Phys. Rev. D*, 83:092001, 2011. arXiv:1011.0127, doi:10.1103/PhysRevD.83.092001.

[147] J.H. Christenson, J.W. Cronin, V.L. Fitch, and R. Turlay. Evidence for the 2π Decay of the K_2^0 Meson. *Phys. Rev. Lett.*, 13:138–140, 1964. doi:10.1103/PhysRevLett.13.138.

[148] Riccardo Barbieri and A. Masiero. Supersymmetric Models with Low-Energy Baryon Number Violation. *Nucl. Phys. B*, 267:679–689, 1986. doi:10.1016/0550-3213(86)90136-7.

[149] Pietro Slavich. Constraints on R-parity violating stop couplings from flavor physics. *Nucl. Phys. B*, 595:33–43, 2001. arXiv:hep-ph/0008270, doi:10.1016/S0550-3213(00)00700-8.

[150] A. M. Baldini et al. Search for the lepton flavour violating decay $\mu^+ \to e^+\gamma$ with the full dataset of the MEG experiment. *Eur. Phys. J.*, C76(8):434, 2016. arXiv:1605.05081, doi:10.1140/epjc/s10052-016-4271-x.

[151] V. Andreev et al. Improved limit on the electric dipole moment of the electron. *Nature*, 562(7727):355–360, 2018. doi:10.1038/s41586-018-0599-8.

[152] Douglas Bryman, William J. Marciano, Robert Tschirhart, and Taku Yamanaka. Rare kaon and pion decays: Incisive probes for new physics beyond the standard model. *Ann. Rev. Nucl. Part. Sci.*, 61:331–354, 2011. doi:10.1146/annurev-nucl-102010-130431.

[153] A. Aguilar-Arevalo et al. Improved Measurement of the $\pi \to e\nu$ Branching Ratio. *Phys. Rev. Lett.*, 115(7):071801, 2015. arXiv:1506.05845, doi:10.1103/PhysRevLett.115.071801.

[154] Brian Batell, Stefania Gori, and Lian-Tao Wang. Exploring the Higgs Portal with 10/fb at the LHC. *JHEP*, 06:172, 2012. arXiv:1112.5180, doi:10.1007/JHEP06(2012)172.

[155] Albert M Sirunyan et al. Combined measurements of Higgs boson couplings in proton–proton collisions at $\sqrt{s} = 13\,\text{TeV}$. *Eur. Phys. J. C*, 79(5):421, 2019. arXiv:1809.10733, doi:10.1140/epjc/s10052-019-6909-y.

[156] Christoph Borschensky, Michael Krämer, Anna Kulesza, Michelangelo Mangano, Sanjay Padhi, Tilman Plehn, and Xavier Portell. Squark and gluino production cross sections in pp collisions at $\sqrt{s} = 13$, 14, 33 and 100 TeV. *Eur. Phys. J.*, C74(12):3174, 2014. arXiv:1407.5066, doi:10.1140/epjc/s10052-014-3174-y.

[157] Chuan-Ren Chen, William Klemm, Vikram Rentala, and Kai Wang. Color Sextet Scalars at the CERN Large Hadron Collider. *Phys. Rev.*, D79:054002, 2009. arXiv:0811.2105, doi:10.1103/PhysRevD.79.054002.

[158] Dorival Goncalves-Netto, David Lopez-Val, Kentarou Mawatari, Tilman Plehn, and Ioan Wigmore. Sgluon Pair Production to Next-to-Leading Order. *Phys. Rev.*, D85:114024, 2012. arXiv:1203.6358, doi:10.1103/PhysRevD.85.114024.

[159] Céline Degrande, Benjamin Fuks, Valentin Hirschi, Josselin Proudom, and Hua-Sheng Shao. Automated next-to-leading order predictions for new physics at the LHC: the case of colored scalar pair production. *Phys. Rev.*, D91(9):094005, 2015. arXiv:1412.5589, doi:10.1103/PhysRevD.91.094005.

[160] Search for squarks and gluinos in final states with jets and missing transverse momentum using 139 fb^{-1} of $\sqrt{s}$ =13 TeV *pp* collision data with the ATLAS detector. Technical Report ATLAS-CONF-2019-040, CERN, Geneva, Aug 2019. URL: https://cds.cern.ch/record/2686254.

[161] Xabier Cid Vidal et al. Report from Working Group 3. *CERN Yellow Rep. Monogr.*, 7:585–865, 2019. arXiv:1812.07831, doi:10.23731/CYRM-2019-007.585.

[162] A. Abada et al. FCC-hh: The Hadron Collider. *Eur. Phys. J. ST*, 228(4):755–1107, 2019. doi:10.1140/epjst/e2019-900087-0.

[163] Morad Aaboud et al. Searches for scalar leptoquarks and differential cross-section measurements in dilepton-dijet events in proton-proton collisions at a centre-of-mass energy of $\sqrt{s} = 13$ TeV with the ATLAS experiment. *Eur. Phys. J.*, C79(9):733, 2019. arXiv:1902.00377, doi:10.1140/epjc/s10052-019-7181-x.

[164] Albert M Sirunyan et al. Search for pair production of first-generation scalar leptoquarks at $\sqrt{s} = 13$ TeV. *Phys. Rev.*, D99(5):052002, 2019. arXiv:1811.01197, doi:10.1103/PhysRevD.99.052002.

[165] Albert M Sirunyan et al. Search for pair production of second-generation leptoquarks at $\sqrt{s} = 13$ TeV. *Phys. Rev.*, D99(3):032014, 2019. arXiv:1808.05082, doi:10.1103/PhysRevD.99.032014.

[166] B. C. Allanach, Tyler Corbett, and Maeve Madigan. Sensitivity of Future Hadron Colliders to Leptoquark Pair Production in the Di-Muon Di-Jets Channel. *Eur. Phys. J.*, C80(2):170, 2020. arXiv:1911.04455, doi:10.1140/epjc/s10052-020-7722-3.

[167] Morad Aaboud et al. Searches for third-generation scalar leptoquarks in $\sqrt{s} = 13$ TeV pp collisions with the ATLAS detector. *JHEP*, 06:144, 2019. arXiv:1902.08103, doi:10.1007/JHEP06(2019)144.

[168] Albert M Sirunyan et al. Search for heavy neutrinos and third-generation leptoquarks in hadronic states of two τ leptons and two jets in proton-proton collisions at $\sqrt{s} = 13$ TeV. *JHEP*, 03:170, 2019. arXiv:1811.00806, doi:10.1007/JHEP03(2019)170.

[169] Albert M Sirunyan et al. Search for third-generation scalar leptoquarks decaying to a top quark and a τ lepton at $\sqrt{s} = 13$ TeV. *Eur. Phys. J.*, C78:707, 2018. arXiv:1803.02864, doi:10.1140/epjc/s10052-018-6143-z.

[170] Albert M Sirunyan et al. Search for leptoquarks coupled to third-generation quarks in proton-proton collisions at $\sqrt{s} = 13$ TeV. *Phys. Rev. Lett.*, 121(24):241802, 2018. arXiv:1809.05558, doi:10.1103/PhysRevLett.121.241802.

[171] Bastian Diaz, Martin Schmaltz, and Yi-Ming Zhong. The leptoquark Hunter's guide: Pair production. *JHEP*, 10:097, 2017. arXiv:1706.05033, doi:10.1007/JHEP10(2017)097.

[172] CMS Collaboration. Search for new physics with multileptons and jets in 35.9 fb^{-1} of pp collision data at $\sqrt{s} = 13$ TeV. 3 2017.

[173] Morad Aaboud et al. Search for B-L R -parity-violating top squarks in $\sqrt{s}$ =13 TeV pp collisions with the ATLAS experiment. *Phys. Rev.*, D97(3):032003, 2018. arXiv:1710.05544, doi:10.1103/PhysRevD.97.032003.

[174] Martin Schmaltz and Yi-Ming Zhong. The leptoquark Hunter's guide: large coupling. *JHEP*, 01:132, 2019. arXiv:1810.10017, doi:10.1007/JHEP01(2019)132.

[175] Luc Darmé, Benjamin Fuks, and Mark Goodsell. Cornering sgluons with four-top-quark events. *Phys. Lett.*, B784:223–228, 2018. arXiv:1805.10835, doi:10.1016/j.physletb.2018.08.001.

[176] P. Azzi et al. Report from Working Group 1. *CERN Yellow Rep. Monogr.*, 7:1–220, 2019. arXiv:1902.04070, doi:10.23731/CYRM-2019-007.1.

[177] Lawrence Lee, Christian Ohm, Abner Soffer, and Tien-Tien Yu. Collider Searches for Long-Lived Particles Beyond the Standard Model. *Prog. Part. Nucl. Phys.*, 106:210–255, 2019. arXiv:1810.12602, doi:10.1016/j.ppnp.2019.02.006.

[178] Juliette Alimena et al. Searching for long-lived particles beyond the Standard Model at the Large Hadron Collider. 2019. arXiv:1903.04497.